COMPLEXITY AS AGING NON-POISSON RENEWAL PROCESSES

Simone Bianco, B.S., M.S.

Dissertation Prepared for the Degree of

DOCTOR OF PHILOSOPHY

UNIVERSITY OF NORTH TEXAS

May 2007

APPROVED:

Paolo Grigolini, Major Professor
William D. Deering, Committee Member
Arkadii Krokhin, Committee Member
James A. Roberts, Committee Member
Duncan Weathers, Program Coordinator
Floyd D. McDaniel, Chair of the Department of Physics
Sandra L. Terrell, Dean of the Robert B. Toulouse School of Graduate Studies

Bianco, Simone, Complexity as Aging Non-Poisson Renewal Processes. Doctor of Philosophy (Physics), May 2007, 110 pp., 1 table, 37 illustrations, references, 103 titles.

The search for a satisfactory model for complexity, meant as an intermediate condition between total order and total disorder, is still subject of debate in the scientific community. In this dissertation the emergence of non-Poisson renewal processes in several complex systems is investigated. After reviewing the basics of renewal theory, another popular approach to complexity, called modulation, is introduced. I show how these two different approaches, given a suitable choice of the parameter involved, can generate the same macroscopic outcome, namely an inverse power law distribution density of events occurrence.

To solve this ambiguity, a numerical instrument, based on the theoretical analysis of the aging properties of renewal systems, is introduced. The application of this method, called renewal aging experiment, allows us to distinguish if a time series has been generated by a renewal or a modulation process. This method of analysis is then applied to several physical systems, from blinking quantum dots, to the human brain activity, to seismic fluctuations.

Theoretical conclusions about the underlying nature of the considered complex systems are drawn.

ACKNOWLEDGMENTS

I would like to thank Prof. Grigolini, for supporting me for the entire period of the PhD, and, above all, for sharing with me his view of Physics. A very special thank goes to my wife, Nanza, without whom it would have been impossible to work on this dissertation, and to my parents and parents-in-law.

I would like to thank all the faculties and staff at the Department of Physics. Especially, I wish to thank Dr. Krokhin for his support and friendship in these years. A special thank goes to the faculties at the Center for Nonlinear Science of the University of North Texas, Dr. Deering and Dr. Roberts, director of the center, for their help and their support through these years. I am deeply grateful to Mrs. Bowden for her help in all the situations, ordinary and non-ordinary, that have occurred during the time I spent at the Department of Physics. A special thank goes also to Mrs. Deacon, without whom it would have been very difficult for me to achieve this important objective. A very special thank goes to Mrs. Bourns and the staff of the UNT grant office for guiding me through the very delicate process of a human subject application.

The invaluable help of Dr. Paradisi, ISAC-CNR of Lecce, Italy, is warmly acknowledged, as well as the collaboration of Dr. Ignaccolo, at the Center for Nonlinear Science at the University of North Texas. Also, the research assistance of Mr. Nagaraj and Mr. Geneston is thankfully acknowledged.

Dr. Simpkins and all the members of the Institutional Review Board, are thankfully acknowledged for approving the use of human subjects data for this dissertation, through application No. 07-103. I very warmly acknowledge the Welch foundation for basic research in Chemistry for financial support through grant No. B-1577, and the Army Research Office for financial support through grant No. W911NF-5-00059.

CONTENTS

LIST OF TABLES

LIST OF ILLUSTRATIONS

CHAPTER 1

INTRODUCTION

1.1. Towards a Proper Model for Complexity

The search for a proper model for complexity, meant as an intermediate condition between total order and total disorder, is a very active topic in recent physics literature [96]. Recent advances in experimental and theoretical physics have proved the necessity to abandon the paradigms of ordinary statistical physics to describe many complex processes. Single molecule spectroscopy [64, 65, 66, 50] is a striking example of a case where no recourse can be made to the Gibbs ensemble approach to describe such systems: The Gibbs ensemble view is strongly violated by systems where the signal is obtained from the action of a field on a single molecule. On the other hand, theoretical advances in these fields may be useful to investigate phenomena whose origin is still strongly debated, as the famous $1/f$ noise [79, 38].

Complexity challenges today the classical role of physicists in science. New disciplines are attracting more and more physicists, mainly for their problem-solving and models-building abilities, so as to make possible predictions. Today it is not strange anymore to find physicists working with financial data, or discussing about DNA, or again trying to model the growth on Internet, all tasks before limited to scientists working in specific fields. Today physicists are probably the first to understand the complex world around them, and they are the first to adapt their knowledge to study it in all its aspects. In this view complexity is the science for the physicist of the new millennium, their role being central to describe today's world.

Clearly, no unified approach to complexity is available today. Among the most famous theoretical approaches, it is possible to quote Superstatistics [23, 24], self-organized criticality [14], non-extensive thermodynamics [91], and non-Poisson renewal theory [41]. The first

three quoted theories are actually closely connected, according to the authors of Refs. [13, 58], as it is possible to derive one from the other. On the contrary, non-Poisson renewal theory is very different from the others: Its main tenet is the presence of *critical events*, recurrent events in the pattern of a variable of the system. These events are sometimes manifestations of a physical property of the system, as the jump from the *light on* to the *light off* state in blinking quantum dots, or they are sometimes hidden by a cloud of other non significant events, or *pseudo-events*, as in the case of earthquakes. However, their presence is very important. A generalization of the stochastic resonance [51], called *complexity matching* was studied for the first time in Refs. [7, 8]. Its main tenet rests on the assumption that a complex system is characterized by critical events. On top of that, the perturbing signal must be also complex. The maximum amount of information is transmitted when both the perturbing signal and the system have the same "complexity", as indicated by suitably chosen parameters. Thus, the name complexity matching. If this condition is not realized, then the response of the system to the perturbation decays in time [19].

Complex networks are indeed one of the most important instruments available today to theoretical physicists [2]. Using complex networks it is possible to explain the how cancer spreads in an organism [94], how the internet grows [17], and how the human brain behaves [26]. Moreover, perturbing a complex network is not easy. A complex network is an incredibly robust object, this fact being mainly due to the cooperation among the single constituents of the network. Recently, the authors of Ref. [26] have proved that, in particular conditions, the cooperation of many interacting units generates a non-Poisson renewal process. This important result, while on one hand suggests an explanation for the robustness of the network to external perturbations, on the other hand opens the way to the complexity matching effect.

In this dissertation the first step towards the recognition of a proper model for complexity is made. A numerical algorithm, called *renewal aging experiment* is introduced for the first time in this work to answer the questions on how is it possible to assess if a process

is non-Poisson and renewal. Moreover, new data analysis techniques to process raw data are introduced in this dissertation. In several of the situations analyzed in this work new theoretical models are introduces to take into account the results of the statistical analysis of the data sets. All of the models have in common the presence of critical events, whose importance is still not fully recognized by the mainstream statistical physics. From this work it will appear evident that a proper model for complexity must take into account their important role. Our hope is that this dissertation, through the investigation of several complex systems, will serve the purpose to properly acknowledge this importance, towards a proper model for complexity.

This dissertation is divided as follows: chapters 2 and 3 serve the purpose of introducing two approaches to complexity, namely non-Poisson renewal theory and modulation, of which superstatistics is a limiting case; I prove that, in particular conditions, using the ordinary methods of statistical physics, is not possible to distinguish if a process has been generated by one approach or the other; in chapter 4, the renewal aging experiment is introduced to solve this problem; chapter 5 is devoted to the discussion of renewal and modulation in single molecule spectroscopy; in chapter 6 is discussed how non-Poisson renewal theory can be used to model human brain signals, afforded by a suitable statistical data analysis of the ElectroEncephaloGrams; in chapter 7 the global properties of a particular complex network are studied in order to build an effective model for both blinking quantum dots and human brain; chapter 8 contains further examples of systems analyzed through the statistical methods introduced in this dissertation, namely the financial time series and seismic fluctuations; chapter 9 concludes.

CHAPTER 2

RENEWAL THEORY

In this chapter an approach to complexity based on non-Poisson renewal theory will be discussed.

2.1. Preliminaries

Renewal processes are stochastic processes characterized by the following properties:

- stochastic (*critical*) events are associated with the pattern of a variable of the system;
- the occurrence of an event erases completely the memory of the past, either deterministic or stochastic.

According to the given definition, a Poisson process is a renewal process, being the occurrence of an event a stochastic process with no memory. The distribution of times between two subsequent events (*waiting times*) is, in this case, exponential.

A more interesting case is the presence of non-exponential tails in the probability distribution functions. In this case we talk about *non-Poisson renewal process*. From the definition it also stems another general property of renewal processes: The correlation function of waiting times is $\delta-$peaked in 0.

An important perspective naturally fulfilling the renewal assumptions is the *subordination* theory. According to the seminal work of Montroll and Weiss [78] it is possible to generate, from an ordinary diffusive process, processes with anomalous diffusion, *subordinated* to the original one. This effect is attained by assuming that the distance between two events is extracted randomly from a suitably chosen distribution. The same generalization con be made for the intensity of the jump of the walker. Subordination is also the key ingredient of

the generation of non ordinary fluctuation-dissipation processes, see, for instance, Ref. [47].

In the next section I discuss a simple example of non-Poisson renewal process.

2.2. A Paradigmatic Case

In this section a simple dynamical way of realizing the non-Poisson renewal condition [3] is introduced. Consider a particle moving in the interval $I = [0, 1]$ according to the following equation of motion:

$$\frac{dy}{dt} = \alpha y^z, \tag{1}$$

with $0 < \alpha \ll 1$ and $z > 1$. The particle moves from the initial condition $y(0) = y_0$, $0 < y_0 < 1$. When the particle reaches the value 1 it is injected back to a totally random initial condition between 0 and 1 with uniform probability. The back injection is an example of what has been called *critical event*.

To solve the equation of motion (1), let us rewrite it as

$$\frac{dy}{y^z} = \alpha dt. \tag{2}$$

Thus, integrating both terms, we get

$$\frac{y^{1-z}(t)}{(1-z)} = \alpha t + \frac{y_0^{1-z}}{(1-z)}, \tag{3}$$

and therefore

$$y(t) = \left[y_0^{1-z} - (z-1)\alpha t\right]^{-\frac{1}{(z-1)}}. \tag{4}$$

Note that

$$\ddot{y} = \alpha z y^{2z-1} > 0, \tag{5}$$

and that the quantity in the square brackets of Eq. (4) vanishes at

$$t_\infty = \frac{1}{y_0^{z-1}} \frac{1}{\alpha(z-1)}. \tag{6}$$

This means that the particle reaches the border at $t < t_\infty$ and therefore there is no upper limit to the time distribution that we are building, because $t_\infty \to \infty$ when $y_0 \to 0$.

Let us now evaluate the time τ_i that it takes for the particle to reach the border after the $(i-1)$th back injection. To this purpose, let us notice that, at the moment of the critical event, $y(t) = 1$. Therefore, inverting Eq. (4),

$$\tau_i = \frac{1}{\alpha(1-z)} \left(1 - y_{i-1}^{z-1}\right), \tag{7}$$

where y_{i-1} is the $(i-1)$th random initial position after the back injection. Since the initial positions are randomly chosen, also the waiting times will be independent variables.

To characterize the dynamics of the process, let us introduce the *waiting time probability density function* (WT-PDF), indicated with the symbol $\psi(\tau)$. The quantity $\psi(\tau)d\tau$ represents the probability of events occurrence in the interval $[\tau, \tau + d\tau]$.

Let us now introduce the *Survival Probability* (SP) associated with the process, defined as

$$\Psi(t) = 1 - \int_0^t \psi(t')dt'. \tag{8}$$

The SP represents the probability that no event occurs up to the time t.

The WT-PDF of critical events can be obtained from the principle of conservation of the probability. In fact the probability of having an event in the interval $[\tau, \tau + d\tau]$ is identical to the probability of having a back injection to a random position in the interval $[y_0, y_0 + dy_0]$, namely

$$\psi(\tau)d\tau = p(y_0)dy_0. \tag{9}$$

Since the back injection is uniform in I, $p(y_0) = 1$. Inverting Eq. (9) one obtains

$$\psi(\tau) = \left|\frac{dy_0}{dt}\right|. \tag{10}$$

Thus, the solution of the Jacobian transformation gives the form of the waiting time distribution for the process, namely

$$\psi(\tau) = \frac{\alpha}{[1 + \alpha(z-1)\tau]^{\frac{z}{z-1}}}. \tag{11}$$

If we pose

$$\mu \equiv \frac{z}{z-1} \tag{12}$$

and

$$T \equiv \frac{\mu - 1}{\alpha}, \tag{13}$$

$\psi(\tau)$ assumes the following form

$$\psi(t) = (\mu - 1)\frac{T^{\mu-1}}{(t+T)^{\mu}}, \tag{14}$$

i.e., an (asymptotic) inverse power law. In Fig. 2.1 we can see an example of the SP generated through the procedure described in this section, for parameters $\mu = 1.8$ and $\alpha = 0.01$.

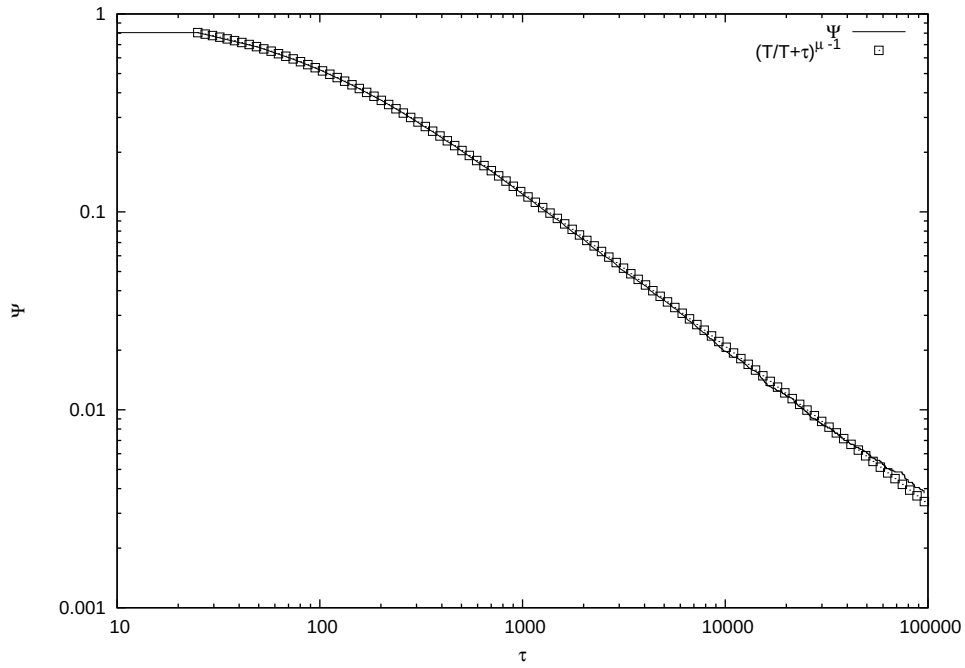

FIGURE 2.1. The SP generated through the dynamical model of Eq. (1) (full line). The fitting function (squares) is the theoretical SP corresponding to the inverse power law form of Eq. (14), for $\mu = 1.8$.

Let us now write the equation of motion for the evolution of the probability $p(y,t)$ for the map. To this purpose, let us write the general expression for the differential equation

involving $p(y,t)$ [46], namely

$$\frac{\partial}{\partial t}p(y,t) = \mathscr{L}p(y_t). \tag{15}$$

The equation of motion for $y(t)$ consists of two terms: a deterministic part within the interval I, and the random back injection. From the theory of Liouvillian [46], the operator $\mathscr{L}$ represents the time evolution operator in the Schrödinger-like picture [46]. In the Heisenberg-like picture, the time evolution operator acts on $y(t)$ such that

$$\dot{y}(t) = \mathscr{L}^{\dagger}y(t). \tag{16}$$

This implies the following form for the operator $\mathscr{L}$

$$\mathscr{L} = \alpha\frac{\partial}{\partial y}y^z + \alpha p(1,t). \tag{17}$$

The first term of Eq. (17) corresponds to the deterministic evolution of the variable y, while the second term takes care of the random back injection process. The meaning of the second term of Eq. (17) is the following: The particle is moving in time towards 1, implying that the population density within the interval decreases. This effect is compensated by the back injection. In conclusion

$$\frac{\partial}{\partial t}p(y,t) = \alpha\left[-\frac{\partial}{\partial y}y^z p(y,t) + p(1,t)\right]. \tag{18}$$

It is easy to prove that the normalization condition for $p(y,t)$ is fulfilled. In fact

$$\frac{d}{dt}\int_0^1 p(y,t)dy = \tag{19}$$

$$= \int_0^1 \left(\frac{d}{dt}p(y,t)\right)dy = \tag{20}$$

$$= -\int_0^1 \alpha\frac{d}{dy}\left(y^z p(y,t)\right)dy + \alpha p(1,t) = \tag{21}$$

$$= -\alpha\left[y^z p(y,t)\right]_0^1 + \alpha p(1,t) = \tag{22}$$

$$= -\alpha p(1,t) + \alpha p(1,t) = 0, \tag{23}$$

which proves the normalization condition.

Let us find the equilibrium condition for the equation of motion Eq. (17). This distribution is given by the (normalized) expression

$$p_{eq}(y) = \frac{2-z}{y^{z-1}}, \tag{24}$$

as it is easily proved by direct calculation

$$\mathscr{L} p_{eq}(y) = -\alpha(2-z) + \alpha(2-z) = 0. \tag{25}$$

The equilibrium distribution imposes the condition $z > 2$, as it must be normalizable.

2.3. Homogenous Non-Poisson Processes

In the previous section a simple non-Poisson renewal process was introduced. In this section a renewal process driven by a time-dependent rate $q(t)$ is described [41]. The waiting time distribution is found to coincide with Eq. (14), with a suitable choice of the parameters, and with a resetting prescription.

Consider the following quantity

$$q(t) = \frac{q_0}{(1+q_1 t)}. \tag{26}$$

Let us now imagine to divide the interval $I = [0,1]$ into two parts, $I_1 = [0, 1-q_i]$ and $I_2 = [1-q_1, 1]$, with $q_i \equiv q(i)$, $i = 1, \ldots, n$, and $q_i \ll 1$. Let us now draw a number from the interval I. The probability of drawing a number from the interval I_2 is very small and decreases with time. The function $q(t)$ represents a time-dependent rate of events.

By definition, the SP of the (discrete) drawing process, assuming independent drawings, is

$$\Psi(n) = \prod_{i=1}^{n} (1-q_i). \tag{27}$$

Evaluating the logarithms of both terms and using the condition $q_i \ll 1$, we get

$$\log(\Psi(t)) = -\sum_{i=1}^{n} q_i. \tag{28}$$

Every time a number is drawn from the interval I_2, the physical time is reset, that is, if the event happens at the time t_i, the rate evolves from the moment of the event on according to the following expression

$$q(t) = \frac{q_0}{1 + q_1(t - t_i)}. \tag{29}$$

This implies that the process is homogenous in time, i.e. the rules do not change with time. Thus, this process is called *Homogeneous Non-Poisson Process* (HNPP).

Solving Eq. (28) and assuming large values of n so as to go to the continuous limit, we get

$$\Psi(t) = \exp\left(-\int_0^\tau q(t)dt\right) = \tag{30}$$

$$= \exp\left(-\frac{q_0}{q_1}\log(1 + q_1\tau)\right) = \tag{31}$$

$$= \exp\left(\log(1 + q_1\tau)^{-(q_0/q_1)}\right) = \tag{32}$$

$$= \left(\frac{1}{1 + q_1\tau}\right)^{q_0/q_1} = \tag{33}$$

$$= \left(\frac{T}{T + t}\right)^{\mu - 1}, \tag{34}$$

the last step obtained by posing

$$T = \frac{1}{q_1} \qquad \mu = \frac{q_0}{q_1} + 1. \tag{35}$$

Eq. (34) yields a waiting time distribution of the form of Eq. (14).

Let us stress again the meaning of this section: A non-Poisson renewal Process is also compatible with a dynamical prescription of a time-dependent rate decreasing in time. This process is compatible with the simple model of Eq. (1): In facts, also in this case the density of events is changing (decreasing) in time, until an event occurs. At that moment the process starts from the beginning, realizing in this way the renewal condition, and implying the homogeneity of time.

The model of this section can be used to describe a two-state renewal process, namely a process where a critical event is the passage from a state 1 (or on) to a state 2 (or off) and vice-versa, and the time at which an event occurs is completely uncorrelated from the previous. As we shall see in section 3.2, a different resetting condition generates a completely different physical situation. We shall consider the HNPP again in section 3.2.

2.4. Conclusions

In this chapter the general properties of non-Poisson renewal theory were outlined. In particular, two different ways of generating the inverse power law WT-PDF of Eq. (14) were discussed. In the next chapter I discuss another approach to complexity, namely the modulation theory. I prove that, in particular conditions, also modulation can generate a WT-PDF compatible with Eq. (14).

CHAPTER 3

MODULATION

In this chapter we illustrate an approach to complexity, based on the modulation of a Poisson process.

3.1. Modulation Theory

To illustrate the modulation theory, let us consider a particle moving in a double-well potential under the action of a white noise. The distribution density of passage times between one well and the other is an exponential [9]

$$\psi(\tau) = qe^{-q\tau}, \tag{36}$$

where the q is an Arrhenius-like rate of the form

$$q = Ae^{-\frac{Q}{D}}. \tag{37}$$

The quantities Q and D represent, respectively, the intensity of the potential barrier and the thermal noise, proportional to the temperature. If we allow both Q and D to fluctuate, the process may become a modulated Poisson process. The condition for this to happen is the following: Choose a rate of events production q_i, and extract a number N_m of waiting times from the exponential distribution associated to the Poisson process of Eq. (36). Then, change the rate to, e.g., q_{i+1} and extract again N_m waiting times: If $N_m \gg 1$, then the process is a modulation. Moreover, the author of Ref. [39] stresses that, in order for a process to be considered a modulation, the time it takes for the system to select a different rate must be much slower than the time scale of the selected exponential process. This condition is implicitly realized by setting $N_m \gg 1$.

What happens in the case $N_m \simeq 1$? Imagine to extract only one waiting time τ_i from

an exponential distribution with rate q_i. Then change the rate to q_{i+1}, independent on q_i, and extract a waiting time, τ_{I+1}. Since q_i and q_{i+1} are independent, τ_i and τ_{i+1} will be uncorrelated. Thus, the process is indistinguishable from a renewal process.

A recent proposal [23, 24, 39], called *superstatistics* considers the case of infinitely slow modulation, namely the situation $N_m \to \infty$.

A major point of interest of this approach is that it is virtually possible to obtain distribution densities of any form. The author of Ref. [23] adopts the following general formula for slow modulation processes

$$\psi(t) = \int_0^\infty \Pi(q)\psi_q(t)dq, \tag{38}$$

where $\Pi(q)$ is a suitable weight function and $\psi_q(t) = qe^{-qt}$ is the exponential waiting time distribution density associated with the Poisson process. By choosing as weight function

$$\Pi(q) = \frac{T^{\mu-1}}{\Gamma(\mu-1)} q^{\mu-2} e^{-qT}, \tag{39}$$

a waiting time distribution density of the form of Eq. (14) is obtained. It seems therefore that both renewal and modulation processes, even though significantly different at microscopic level, given a suitable choice of the parameters, can lead to the same macroscopic outcome, namely an inverse power law waiting times distribution density. The problem will be dealt with in chapter 4, with the introduction of the concept of renewal aging.

Let us now prove explicitely how to get Eq. (14) with the stochastic prescription of Eq. (39). Let us plug Eq. (39) into Eq. (38) and write

$$\psi(\tau) = \frac{T^{\mu-1}}{\Gamma(\mu-1)} \int_0^\infty dq q^{\mu-1} e^{-q(t+T)}. \tag{40}$$

Using the following change of integration variables

$$y = q(t+T) \tag{41}$$

$$dy = dq(t+T), \tag{42}$$

one has

$$\psi(t) = \frac{T^{\mu-1}}{\Gamma(\mu-1)}\frac{1}{(t+T)^{\mu}}\int_0^{\infty} dy y^{\mu-1}e^{-y} = \tag{43}$$

$$= \frac{T^{\mu-1}}{\Gamma(\mu-1)}\frac{1}{(t+T)^{\mu}}\Gamma(\mu-1) = \tag{44}$$

$$= (\mu-1)\frac{T^{\mu-1}}{(t+T)^{\mu}}, \tag{45}$$

that coincides with Eq. (14). In Ref. [23] this result was used to lay the dynamical foundations of another attractive approach to complexity, called *non-extensive statistical mechanics* [91]. For this reason the latter approach is not discussed here. The interest reader can consult the book of Ref. [52] for a review of the subject.

3.2. Homogenous Non-Poisson Processes vs. Non-Homogenous Poisson Processes

It is now important to discuss the physical meaning of Eq. (38). In order for the process to be slow modulation, the system's rate must change very slowly with time, and this means that the system produces many random exponential events with the same rate, until q gets a new value. Let us make the assumption that the rate changes in time according to a deterministic prescription, namely

$$\Pi(q) = \frac{1}{T_s}\left|\frac{1}{dq/dt}\right|. \tag{46}$$

The previous equation affords an analytical way of find the expression for the time dependent rate in the case of deterministic motion. The parameter T_s is a time scale which can be properly adjusted to fit the experimental results. Physically, from Eq. (46) it stems that its value rules the speed of the modulation. The larger the value of T_s, the slower the modulation, and vice-versa.

As an example of this physical picture, let us consider the case

$$\dot{q}(t) \propto -\frac{1}{\Pi(q)}, \tag{47}$$

i.e. , $q(t)$ is a monotonically decreasing function of time. In the previous the implicit assumption to be in the slow modulation condition has been made. Using Eq. (39), one

obtains

$$\dot{q}(t) = -A_\mu q^{2-\mu} \exp(qT), \tag{48}$$

where A_μ is suitable constant, and let us assume that $q(t)T \ll 1, \forall t$. The previous expression is a consequence of the slow modulation conditions. Thus

$$\exp(q(t)T) \sim 1, \tag{49}$$

that implies

$$\frac{dq}{dt} = -A_\mu q^{2-\mu}. \tag{50}$$

The solution of the previous differential equation is given by

$$q(t) = \left(q(0)^{\mu-1} - (\mu-1)A_\mu t\right)^{\frac{1}{(\mu-1)}}. \tag{51}$$

It is therefore possible to evaluate, from the basic equations of slow modulation, and in the case of deterministic time evolution of the rate, the dynamical conditions under which the distribution of event times is created. Note that Eq. (51) is valid only in the case $\mu < 2$. In fact, if we pose $\mu > 2$, $\dot{q} \to \infty$ for $t \to \infty$. This would break the condition of infinitely slow modulation.

Note also that this process is not homogeneous in time, as the rate keeps changing forever, and the dynamical rules depend on the distance from the preparation time. For this reason this process is called *Non-Homogeneous Poisson Process* (NHPP). An application of this class of processes will be discussed in chapter 5, to model the fluorescence intermittency emitted by a single lipase molecule.

The observation of a deterministic time evolution for the system is also compatible with the renewal assumption. This point implies a very subtle, but important, difference between non-Poisson renewal and slow modulation processes. Let us address this issue by considering the following deterministic evolution for the rate

$$q(t) = \frac{q_0}{(1+q_1 t)} \qquad q(t) \ll 1. \tag{52}$$

In order to build the time series a probabilistic prescription is adopted. Consider the interval $I \equiv [0,1]$. Let us divide this interval into two parts, $I_1 \equiv [0, 1-q(t)] = I_1(t)$ and $I_2 \equiv [1-q(t), 1] = I_2(t)$. The size of both I_1 and I_2 depends on time, since q is time dependent. Let us now draw random numbers from I with uniform probability, and let us consider as event the drawing of a number from I_2. The probability of this events to occur is just $q(t)$, while the probability that no event occurs is $h(t) \equiv 1 - q(t)$. The SP for this process, after $t \gg 1$ drawings, is given by

$$\Psi(t) = h(1) \cdot h(2) \ldots h(t) \tag{53}$$

$$\log \Psi(t) = \sum_{i=1}^{t} \log h(i) = \tag{54}$$

$$= \sum_{i=1}^{t} \log(1 - q(i)) \simeq -\sum_{i=1}^{t} q(i). \tag{55}$$

Let us now consider the following dynamical rule: Every time an event occurs, the rate is reset to its initial value, q_0, and the process starts again. If the first event occurs at $t = t_1$, then the time evolution of the rate will be given by

$$q(t) = \frac{q_0}{(1 + q_1(t - t_1))}, \tag{56}$$

and so forth for the successive events. With this resetting rule the process becomes identical to the HNPP already introduced in Sec. 2.3.

Also in this case, with a suitable choice of the parameters, the waiting time distribution density generated by this process can take the Nutting law form of Eq. (14). Formally, the proof of this statement is equivalent to the one proposed in section 2.3.

How can the rate of Eq. (52) be associated with a modulation prescription? We need to choose a different resetting rule: Every time that a drawing from the interval I_2 occurs we do not reset the rate at its initial value, and keep going ahead with the same expression. Again, this is an example of how to build a NHPP. As it will shown in chapter 5, a deterministic and quasi-periodic evolution of the rate will be adopted in order to build a model to explain

the fluorescence intermittency of a single lipase molecule under the stimulation of a laser field, while in chapter 8 a stochastic procedure will be suitably chosen in order to mimic the characteristics of seismic fluctuation time series.

3.3. Conclusions

This chapter shows a way to derive a NHPP that has some benefits compared to Eq. (26). In fact in both cases we realize Eq. (45). However, thanks to T_s we can make the modulation as slow as we wish, whereas with Eq. (26) the modulation fastness or slowness is fixed. I will devote the next chapter to the derivation of a numerical procedure useful to distinguish a HNPP from a NHPP. This procedure, called *Aging Experiment* (AE) is based on a property of renewal system, called renewal aging.

CHAPTER 4

AGING

4.1. Introduction

Aging properties are found in many physical systems, such as spin glasses, systems with a large number of interacting units, but also low dimensional dynamical maps [20].

Imagine to prepare the system at the time $t = 0$, and to begin the observation at a later time $t_a > 0$. The dependence of the dynamical properties of the system on both the preparation time $t = 0$ and the observation time t_a is called *aging*. In this chapter the aging properties of both renewal and modulation processes are discussed.

4.2. Renewal Aging

To explain how a renewal process depends on the observation time let us imagine a Gibbs ensemble of trajectories created by a two-states non Poisson renewal process, for instance, a particle at the bottom of a double-well potential. For semplicty's sake, let us also imagine that the two states, to which I refer here as *on* and *off*, are statistically equivalent, i.e. they are described by the same waiting time distribution density $\psi(\tau)$. Moreover, let us prepare the systems such that all of them are, at time $t = 0$ in the state *on*. Let now the system evolve and monitor at which time the first transition occurs, a transition being a jump from one well to the other. We call the distribution density of this times $\psi_{obs}(\tau)$. The relation between $\psi_{obs}(\tau)$ and $\psi(\tau)$ will be made clear later in this chapter. For now, let us just say that they share the same renewal and time asymptotic properties.

Let us now imagine that, even though the systems were prepared at $t = 0$, the observation of the process started at a time $t_a > 0$. Which is the probability of observing a time $t > t_a$

in this case? The answer is given by the following expression [54]

$$\psi(t, t_a) = \sum_{n=0}^{\infty} \int_0^{t_a} d\tau \psi_n(\tau)\psi(t-\tau)d\tau. \tag{57}$$

The meaning of Eq. (57) is the following: The system has been prepared at $t = 0$, but the observation started at $t_a > 0$; therefore we have to consider that, for every trajectory of the ensemble, a number n of jumps could have occurred between 0 and t_a, the last of which exactly at $\tau < t_a$. The summation takes care of the fact that an arbitrary number of events might have occurred before the last. We shall apply in the next section the expression of Eq. (57) to a Poisson process.

4.2.1. *Poisson Process: No Aging*

As an example, let us consider the renewal process introduced in section 2.2, with $z = 1$, namely

$$\dot{y} = \alpha y. \tag{58}$$

The solution of this equation, with the proper choice for the initial conditions, is

$$y(t) = y_0 e^{\alpha t} \tag{59}$$

and the time necessary to reach the border is given by

$$t = \frac{1}{\alpha} \log y_0. \tag{60}$$

Applying the conservation of probability (Eq. (9)), we obtain as waiting times distribution density

$$\psi(t) = \alpha e^{-\alpha t}. \tag{61}$$

To find $\psi_n(t)$, let us prove the following fundamental relation, valid for renewal processes

$$\hat{\psi_n}(u) = \left[\hat{\psi}(u)\right]^n. \tag{62}$$

Let us call $\psi_1(t) \equiv \psi(t)$ the probability that one collision occurs between 0 and t. The probability of having two collisions occurring between 0 and t will be the product of the probabilities, as the collisions are statistically independent events, namely

$$\psi_2(t) = \int_0^t d\tau \psi_1(\tau)\psi_1(t-\tau). \tag{63}$$

The probability of having n collisions is given by

$$\psi_n(t) = \int_0^t d\tau \psi_{n-1}(\tau)\psi_1(t-\tau). \tag{64}$$

The Laplace transform of Eq. (64) is obtained by the convolution theorem for Laplace transforms [48]

$$\hat{\psi}_n(u) = \hat{\psi}_{n-1}(u)\hat{\psi}_1(u). \tag{65}$$

On the other hand

$$\hat{\psi}_{n-1}(u) = \hat{\psi}_{n-2}(u)\hat{\psi}_1(u), \tag{66}$$

and therefore

$$\hat{\psi}_n(u) = \hat{\psi}_{n-2}(u)\left[\hat{\psi}_1(u)\right]^2. \tag{67}$$

By iterating the procedure, and assuming $\psi_0 \equiv 2\delta(t)$

$$\hat{\psi}_n(u) = \left[\hat{\psi}_1(u)\right]^n. \tag{68}$$

If $\psi(\tau)$ is exponential, then

$$\hat{\psi}_n(u) = \left(\frac{\alpha}{\alpha+\tau}\right)^n, \tag{69}$$

that implies

$$\psi_n(t) = \frac{\alpha(\alpha t)^{n-1}}{(n-1)!}e^{-\alpha t}, \tag{70}$$

as can be easily proved by direct calculation.

We are now in a position to evaluate the aging of a Poisson process. Let us rewrite Eq. (57) in the following way

$$\psi(t,t_a) = \psi(t) + \sum_{n=1}^{\infty} \int_0^{t_a} d\tau \psi_n(\tau)\psi(t-\tau) = \tag{71}$$

$$= \alpha e^{-\alpha t} + \alpha^2 \sum_{n=1}^{\infty} \int_0^{t_a} d\tau \frac{(\alpha t)^{n-1}}{(n-1)!} e^{-\alpha\tau} e^{-\alpha(t-\tau)} = \tag{72}$$

$$= \alpha e^{-\alpha t} + \alpha^2 \sum_{n=1}^{\infty} \int_0^{t_a} d\tau \frac{(\alpha t)^{n-1}}{(n-1)!} e^{-\alpha t} = \tag{73}$$

$$= \alpha e^{-\alpha t} + \alpha^2 e^{-\alpha t} \int_0^{t_a} d\tau \sum_{n=0}^{\infty} \frac{(\alpha\tau)^n}{n!} = \tag{74}$$

$$= \alpha e^{-\alpha t} + \alpha^2 e^{-\alpha t} \int_0^{t_a} d\tau e^{\alpha\tau} = \tag{75}$$

$$= \alpha e^{-\alpha t} + \alpha e^{-\alpha(t-t_a)} - \alpha e^{-\alpha t} = \alpha e^{-\alpha(t-t_a)}, \tag{76}$$

i.e., statistically, the waiting time distribution density does not change with delayed observation time, thereby implying no aging effects.

4.2.2. *Observed vs. Theoretical WT-PDF*

Before analyzing the aging properties of a non-Poisson renewal process, let us consider the following case: Let us imagine a two-states stochastic process, schematized as a particle in a double well potential, but described now by a waiting time distribution density of the inverse power law form of Eq. (14). Let us discuss the relation between $\psi_{obs}(t)$ and $\psi(t)$.

Imagine that, anytime that the particle reaches the top of the barrier, a coin is tossed to decide if the particle should cross the barrier or go back to the bottom of the well it came from. The probability of either of these two events to occur is, of course, 1/2, and the occurrence of an event is ruled by the quantity $\psi(t)$. Let us imagine that the particle goes back to the bottom of the well it came from. In this case, no change in the spectrum is observed, since, if the particle was in the *on* state, it remains in the *on* state. The observed waiting times will be different from that predicted by the theoretical WT-PDF. We name

the WT-PDF of observed events with the name $\psi_{obs}(t)$.

The connection between the two distributions is given by the formula

$$\psi_{obs}(t) = \sum_{n=1}^{\infty} \left(\frac{1}{2}\right)^n \psi_n(t), \tag{77}$$

with the condition $\psi_0(t) = \delta(t)$. If there is no collision, the probability of observing a transition vanishes. If a collision occurs, then

$$\psi_{obs}(t) = \frac{1}{2}\psi(t). \tag{78}$$

This is so because the probability of observing a transition is the product of the probability that a transition occurs, given by $\psi(t)$, times the coin tossing prescription. Consequently, the probability of observing two collisions will be

$$\psi_{obs}(t) = \frac{1}{4}\psi_2(t). \tag{79}$$

Again, the previous comes from tossing the coin twice. The probability for an arbitrary large number of collisions will be the product of the probabilities of the single events, thereby obtaining Eq. (77).

It is straightforward to prove also the following important relation linking ψ_{obs} to ψ in the Laplace space

$$\hat{\psi}_{obs}(u) = \sum_{n=1}^{\infty} \left[\frac{1}{2}\hat{\psi}(u)\right]^n = \tag{80}$$

$$= \sum_{n=0}^{\infty} \left[\frac{1}{2}\hat{\psi}(u)\right]^n - 1 = \tag{81}$$

$$= \frac{1}{1 - \frac{1}{2}\hat{\psi}(u)} - 1 = \tag{82}$$

$$= \frac{\hat{\psi}(u)}{2 - \hat{\psi}(u)}, \tag{83}$$

and, inverting,

$$\hat{\psi}(u) = \frac{2\hat{\psi}_{obs}(u)}{1 + \hat{\psi}_{obs}(u)}. \tag{84}$$

From the previous it stems that the asymptotic properties of $\psi_{obs}(t)$ are the same as $\psi(t)$. Also, note that, if $\psi(t)$ is renewal, also $\psi_{obs}(t)$ is renewal. Different physical situations might require the adoption of either $\psi_{obs}(t)$ or $\psi(t)$. Since in the majority of the cases we are interested in the asymptotic properties of the processes, adopting one or the other implies no change in the Physics of the system. Let us now focus on the investigation of the aging of a non-Poisson renewal process.

4.2.3. *Aging of a Non-Poisson Renewal Process*

We are now in a condition to evaluate the expression of the aged waiting time distribution density of Eq. (14). It is important to distinguish the ergodic condition $\mu > 2$ from the non-ergodic condition $\mu < 2$. Let us now find the explicit form of Eq. (57) in the case of inverse power law WT-PDF, with $\mu < 2$ and $\mu > 2$. To find this expression, we need to evaluate first the quantity $\psi_n(t)$ in the case of Eq. (14). The Laplace transform of Eq. (14) is given by [34]

$$\hat{\psi}(u) = \frac{(\mu-1)\Gamma(1-\mu)}{(uT)^{1-\mu}} \left[e^{uT} - E_{\mu-1}^{uT}\right] \tag{85}$$

where

$$E_{\mu-1}^{uT} \equiv \sum_{n=0}^{\infty} \frac{(uT)^{n+1-\mu}}{\Gamma(n+2-\mu)} \tag{86}$$

is a generalized exponential function [95]. Expanding in Taylor series we obtain the following asymptotic expressions

$$\lim_{u\to 0} \hat{\psi}(u) = 1 - \Gamma(2-\mu)(uT)^{\mu-1} \qquad 1 < \mu < 2 \tag{87}$$

$$\lim_{u\to 0} \hat{\psi}(u) = 1 - < \tau > u - \Gamma(2-\mu)(uT)^{\mu-1} \quad 2 < \mu < 3 \tag{88}$$

with $< \tau >= \tau/(\mu-2)$ the average waiting time.

Let us evaluate now the Laplace transform of $P(t) \equiv \psi_n(t)$. $P(t)$ represents the probability of event occurrence at time t [48]. In the case $2 < \mu < 3$ we obtain

$$\hat{P}(u) = \frac{1}{< \tau > u + \Gamma(2-\mu)(uT)^{\mu-1}} = \tag{89}$$

$$= \frac{1}{<\tau> u} \frac{1}{1+\Gamma(2-\mu)\frac{(uT)^{\mu-1}}{<\tau>u}} = \tag{90}$$

$$\simeq \frac{1}{<\tau> u}\left(1-\Gamma(2-\mu)\frac{(uT)^{\mu-1}}{<\tau> u}\right) = \tag{91}$$

$$= \frac{1}{<\tau> u} - \frac{\Gamma(2-\mu)T^{\mu-1}}{<\tau>^2}\frac{1}{u^{3-\mu}}. \tag{92}$$

Using the Tauberian theorem [48], it is possible to invert the Laplace transform, thus obtaining

$$P(t) = \frac{1}{<\tau>} - \frac{\Gamma(2-\mu)T^{\mu-1}}{<\tau>^2\,\Gamma(4-\mu)}\frac{1}{t^{\mu-2}} = \tag{93}$$

$$= \frac{1}{<\tau>} - \frac{T^{\mu-1}}{<\tau>^2\,(3-\mu)(2-\mu)}\frac{1}{t^{\mu-2}} = \tag{94}$$

$$= \frac{1}{<\tau>} + \frac{T^{\mu-2}}{(3-\mu)<\tau>}\frac{1}{t^{\mu-2}} \tag{95}$$

In the case of $\mu < 2$ we get

$$\hat{P}(u) = \frac{1}{\Gamma(2-\mu)T^{\mu-1}}\frac{1}{u^{\mu-1}}, \tag{96}$$

that yields

$$P(t) = \frac{1}{\Gamma(2-\mu)T^{\mu-1}}\frac{1}{\Gamma(\mu-1)}\frac{1}{t^{2-\mu}}. \tag{97}$$

Plugging the previous equations into Eq. (57) it is possible to find the exact expression for the aged WT-PDF in case of inverse power law distribution density.

For numerical purposes it is more convenient to adopt the following approximated expression

$$\psi(t,t_a) \approx \frac{\int_0^{t_a} dx\psi(t+y)}{K_{t_a}}, \tag{98}$$

which means that a flat distribution of events occurrence $P(t)$ is assumed. The quantity K_{t_a} is a suitable normalization factor. The agreement between this formula and the exact expression has been numerically proved to be very good, in the conditions $t_a \to 0$ and $t_a \to \infty$, for both $\mu > 2$ [11] and $\mu < 2$ [28]. Particular care should be taken when

considering the condition $\mu < 2$, being it strongly non-ergodic. In this case, going too closer to $\mu = 1$ should produce larger numerical inaccuracy. Thus, in all the numerical simulations to come, we decide to use the previous instead of the exact expression. The authors of Ref. [3] have evaluated the asymptotic behavior of $\psi(t, t_a)$ of Eq. (98) in the case of $\mu < 2$ and $\mu > 2$. Particularly, they found that the following holds:

- In the case $\mu > 2$

  $$\psi(t, t_a) \sim \frac{1}{t^{\mu-1}}$$

  for $t_a \gg t$, and

  $$\psi(t, t_a) \sim \frac{1}{t^{\mu}}$$

  for $t_a \ll t$. The former condition correspond to the infinitely aged system, with $\mu \to \mu - 1$. Since $\mu > 2$, a stationary condition is reached, even it takes an infinite time to attain it. In the latter case, if $t_a < \infty$ we observe sojourn times larger than t_a, and the asymptotic exponent becomes μ. This effect is called *rejuvenation*.
- In the case $\mu < 2$

  $$\psi(t, t_a) \sim \frac{1}{t^{\mu-1}}$$

  In this case, no stationary condition is possible, and the system keeps aging forever.

In Fig. 4.1 the renewal aging effect is shown for the renewal process of Eq. (1) (Fig. 2.1). The age of the system is $t_a = 4000$. The non-aged curve (full line) is indicated by the symbol Ψ_0, while the aged curve (dashed line) is called Ψ_{ren}. As it is possible to see from the Figure, aging implies a slower decay of the SP, as predicted by the theory. In the next section, a comparison between the aging properties of renewal and modulation processes will be presented.

4.3. The Aging Experiment Technique

The surprising aging effect outlined in the previous section allows a further level of time series investigation. In this section we introduce a numerical algorithm, called *Aging Experiment* (AE), on which we shall base the analysis of the aging. The main tenet of the

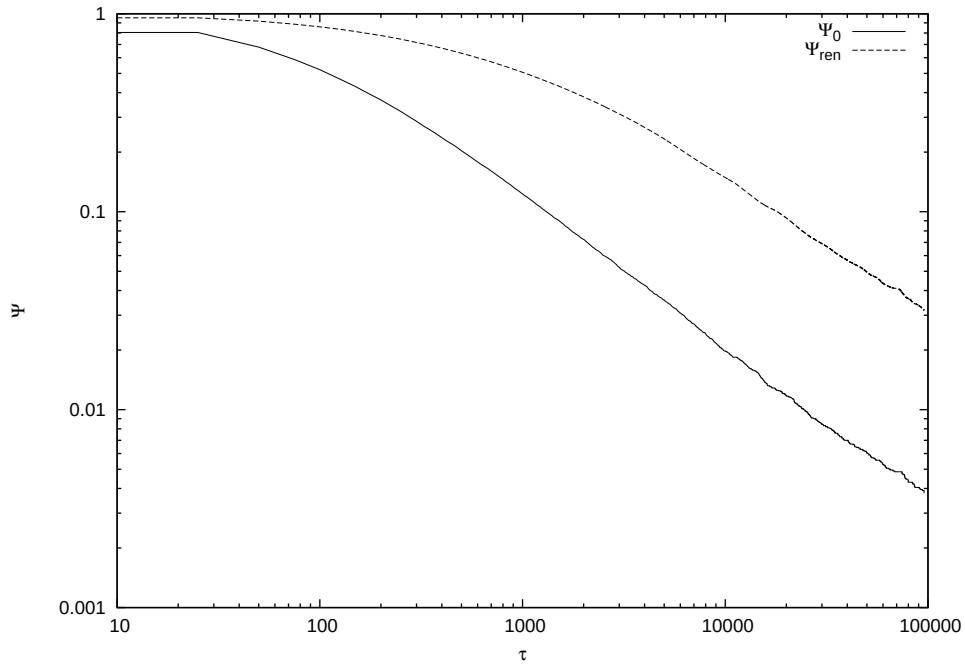

FIGURE 4.1. In this Figure the renewal aging effect is shown. The aged SP is obtained by applying Eq. (57), with $\Psi(\tau)$ coming from Eq. (1). The decay of the aged curve, indicated as Ψ_{ren}, is slower than the non-aged one, denoted by the symbol Ψ_0. $t_a = 4000$, $\mu = 1.8$.

AE is the conversion of a single sequence afforded by the experiment (or by the numerical simulation) into an ensemble of sequences with the same age. This is done as follows: Let us indicate the waiting time with the symbol τ, and the absolute time with t. The first sequence of the Gibbs ensemble is: τ_1^1, τ_2^1, τ_3^1, ..., the superscript indicating the sequence, the subscript chronological order of waiting times. The second sequence is obtained from the first by erasing the first waiting time, i.e. $\tau_1^2 \equiv \tau_2^1$, $\tau_2^2 \equiv \tau_3^1$, $\tau_3^2 \equiv \tau_4^1$ and so forth. The third is obtained from the second again by erasing the first waiting time, thus yielding $\tau_1^3 \equiv \tau_2^2$, $\tau_2^3 \equiv \tau_3^2$, $\tau_3^3 \equiv \tau_4^2$, ... In this way an ensemble of statistically equivalent trajectories is created, as the beginning of every trajectory corresponds to a jump. Note that $t_1^j = \tau_1^j$, $t_2^j = \tau_1^j + \tau_2^j$, and so on, t_i^j being the absolute time at which an event occurs.

To study the aging of the process it is necessary to fix the age t_a first. Then, for every trajectory, the first exit time, namely the quantity $\tau_i^j(t_a) = t_i^j - t_a$, is recorded. The first

exit time is nothing but a truncated part of the waiting time of the original time series. Iterating the procedure for all the sequences one can build a distribution density of waiting times, that we call $\psi_{exp}(\tau, t_a)$, from which we can obtain the correspondent SP, denoted as $\Psi_{exp}(\tau, t_a)$. Comparing the decay of this curve with the prediction of the renewal theory, computed through Eq. (98), it is possible to infer the aging properties of the process.

From the results of the previous section it is already known that, if a process is non-Poisson and renewal, its SP decays more slowly if the age increases. In the next section, I apply the numerical procedure introduced in this section to time series generated by a non-Poisson renewal and modulation processes.

4.4. Aging in Renewal and Modulation

In the previous chapters two different approaches to Complexity have been introduced, namely non-Poisson renewal and modulation. Both approaches can lead, given suitable choices of the parameters, to the inverse power law waiting times distribution density of Eq. (14). This implies that the mere analysis of the waiting time distribution is not enough to assess if a process is a non-Poisson renewal or modulation.

To solve this ambiguity it is useful to analyze the renewal aging properties of a modulation process. As already stated in section 3, in order to be classified as modulation, the time scale of the rate changing process must be much smaller than the time scale of the single Poisson process, that is, the number N_m of events extracted from the same exponential distribution must be very large. If $N_m = 1$, the process is indistinguishable from a non-Poisson renewal process, and therefore we expect a time series generated with the condition $N_m = 1$ to yield the same aging. Increasing N_m should reduce the aging effect, because a subtle form of correlation is introduced in the data, namely the number of events extracted from the same Poisson distribution increases. Let us prove this heuristic argument through a numerical experiment. Let us generate two time series, the first adopting the renewal model of Eq. (1), and the second using the modulation theory, with $N_m = 1, 10, 100$ [28, 6]. We choose the distributions to be an inverse power law with exponent $\mu = 1.8$. Let us then apply the AE

on the time series, for two different ages t_a. The results are plotted in Figs. 4.2, 4.3 and 4.4.

Our theoretical arguments predict that when $N_m = 1$ (Fig. 4.2), the modulation and the renewal processes should be identical. Therefore the aging they yield should be identical. This appears to be confirmed by the numerical simulations of Fig. 4.2. When we increase N_m, the aging of the modulation process (circles in Figs. 4.3 and 4.4) becomes smaller, and it is annihilated in the situation $N_m = 100$. This last case should be a situation of infinitely slow modulation, or Superstatistics.

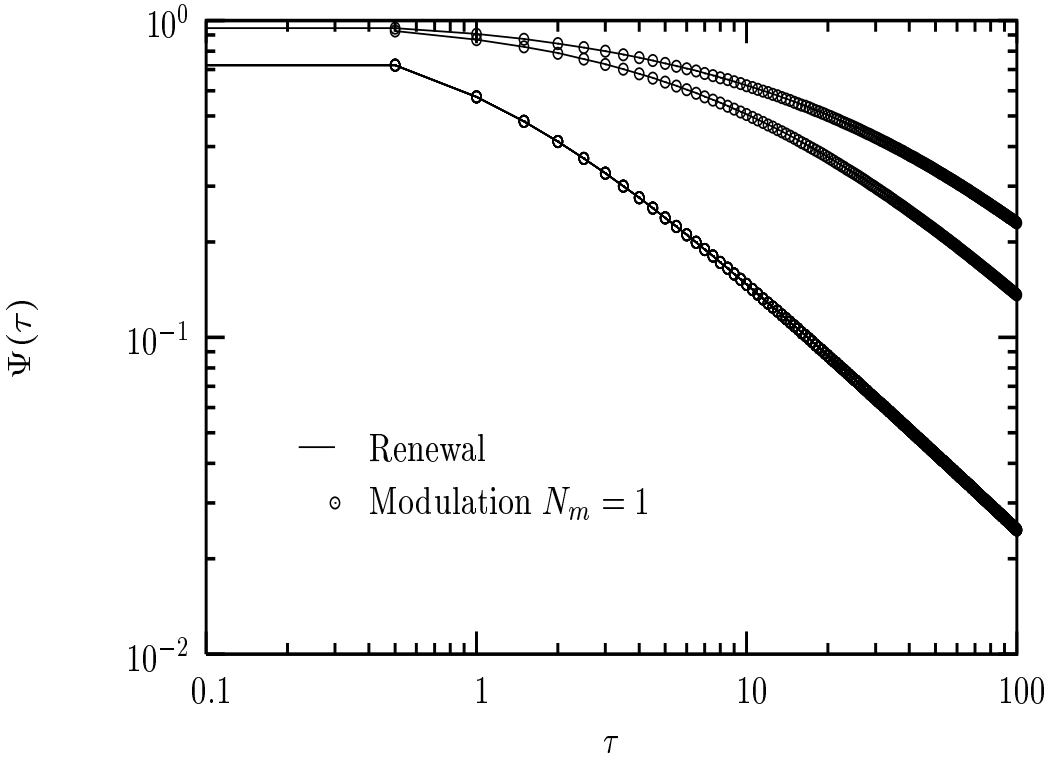

FIGURE 4.2. Comparison between the AE for a non-Poisson renewal process (full line) and for a modulation process with $N_m = 1$ (circles), for two different values of t_a. The result shows a perfect agreement between the aged histograms for both ages of the system. $\mu = 1.8$.

Summarizing, I have introduced a reliable way of distinguishing a non-Poisson renewal process from a modulation process by only adopting the informations already present in the

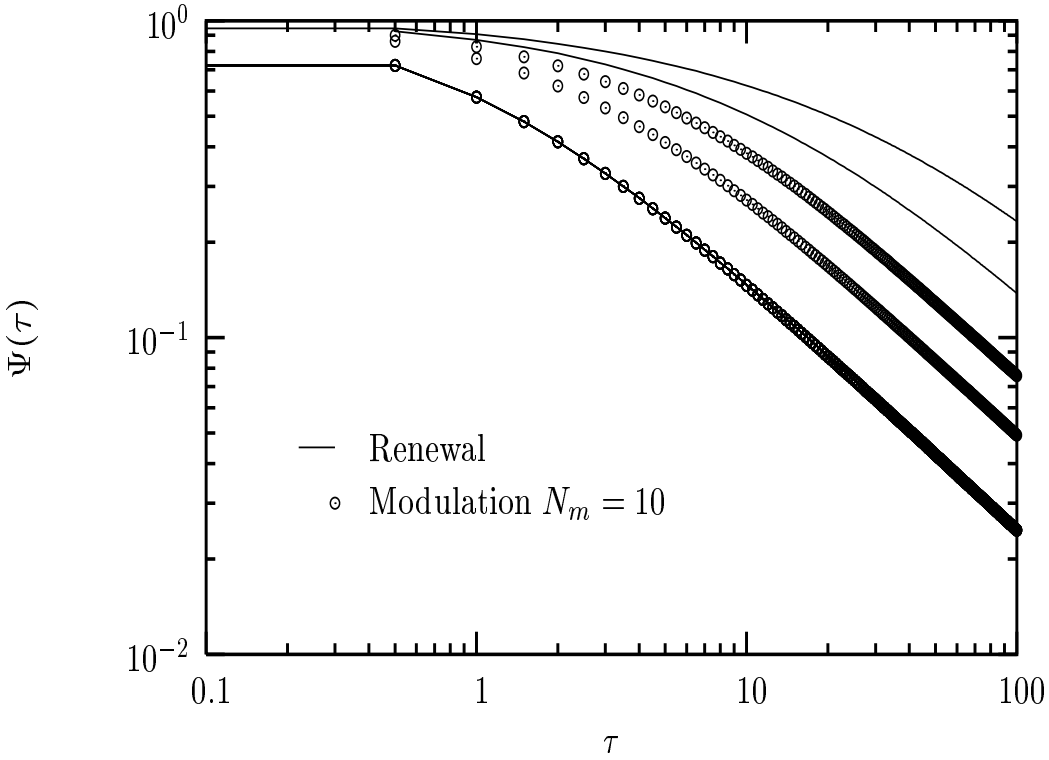

FIGURE 4.3. Comparison between the AE for a non-Poisson renewal process (full line) and for a modulation process with $N_m = 10$ (circles), for two different values of t_a. The result shows a reduced aging effect for the modulation process. $\mu = 1.8$.

time series. I apply this method on real time series in the next chapters, where real systems will be analyzed.

4.5. Further Considerations: The Generalized Master Equation vs. the Continuous-Time Random Walk

Before concluding this chapter, some considerations about the theoretical consequences of the aging effect in renewal systems should be addressed. An exhaustive review of this argument can be found in Ref. [55].

The equivalence between trajectory view and density view has been proved in the seventies, thanks to the work of Kenkre and co-workers [61]. The authors of [61] proved that a generalized master equation (GME) can be obtained from the continuous-time random

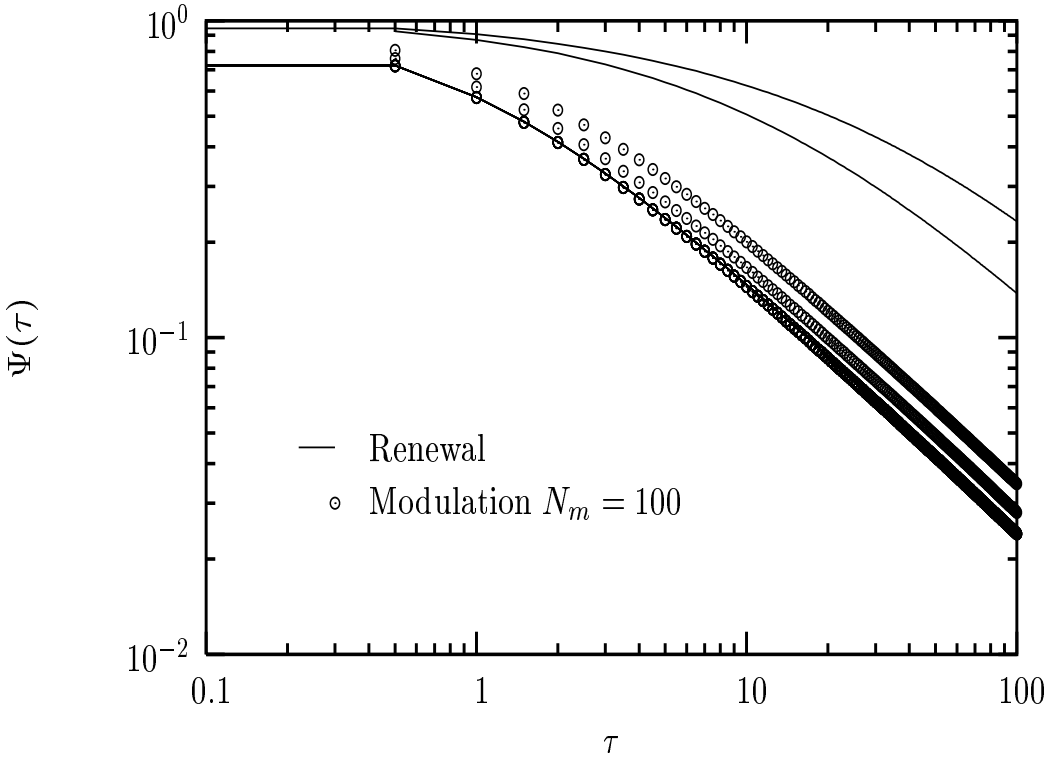

FIGURE 4.4. Comparison between the AE for a non-Poisson renewal process (full line) and for a modulation process with $N_m = 100$ (circles), for two different values of t_a. The aging effect is almost absent in this case. $\mu = 1.8$.

walk (CTRW) picture. The form of the master equation is identical to the one obtained through the classical Liouville approach. A connection between the trajectory (CTRW) and the density (GME) is explicitly obtained. In a recent paper [4], Aquino and co-workers have been studied the effect of renewal aging on the GME of renewal origin. As a consequence of the presence of renewal aging on the single trajectory, a GME of arbitrary age can be derived [4] through the application of the generalized Onsager principle. Let us imagine to build a GME of age t_a. According to the theoretical arguments of Ref. [4], this ME refers only to the specific age for which has been built. Instead the trajectories, through which the GME is built adopting a Gibbs ensemble view, will keep aging. Thus, while the trajectories evolve according to the renewal theory, that considers aging, the GME does not. This might imply a departure between the two pictures when the response of the system to external perturbations is studied. If we consider times $t > t_a$ the response of the trajectory may be

completely different with respect to the response of the density, given the age difference. This might have as a consequence the possibility of considering a departure from the ordinary linear response theory when dealing with renewal systems.

A clear picture taking into account these effects is still missing. However, recent works pointed out the need for a more general theory of response to perturbations. The new theory goes under the name of *Complexity Matching* and I shortly outline it later in this dissertation.

4.6. Conclusive remarks

In this chapter the formal aspects of the aging effect have been introduced. Aging in both renewal and modulation systems has been investigated. Numerical proofs of the presence of aging in both systems have been given. While non-Poisson renewal processes shows pronounced aging effects, modulation processes do not. This fact has been used to build an algorithmic procedure that allows to distinguish a non-Poisson renewal process from a modulation process. In the next chapter I present the first applications of this numerical test on real time series.

CHAPTER 5

RENEWAL AND MODULATION IN SINGLE MOLECULE SPECTROSCOPY

Single molecule spectroscopy plays a very important role in today's physics. Intermittent fluorescence properties of nanocrystals, of which Blinking Quantum Dots (BQD) are an important example, pose new challenges to both experimental and theoretical physicists. The theoretical interest in these materials is mainly due to the properties of their power spectrum. Recent papers [79, 38] proved the emergence of $1/f$ noise from macroscopic samples of BQD. Therefore the study of their properties could be a way of understanding the intriguing issue of the ubiquitous $1/f$ noise.

The macroscopic emission process is characterized by the presence of two states, indicated usually as *light on* (emission) and *light off* (no emission), or, more simply, *on* and *off*. Statistically, the two states are not equivalent: the measure of the waiting times between two successive *on* (*off*) regions allows us to build a waiting time distribution density, indicated as $\psi_{on}(\tau)$ ($\psi_{off}(\tau)$). Recent experimental and theoretical studies [72, 28] show that both $\psi_{on}(\tau)$ and $\psi_{off}(\tau)$ have the form of Eq. (14), with parameters $T_{on} \neq T_{off}$ and $\mu_{on} \neq \mu_{off}$. Moreover, μ_{on} and μ_{off} are smaller than 2, thereby implying that the processes involved are non-ergodic.

5.1. Blinking Quantum Dots

Blinking quantum dots are nanomaterials that, even under the steady influence of a laser field, emit intermittent fluorescence. The light emission $I(t)$ changes abruptly and randomly from a value $I \gg 0$ to $I \simeq 0$.

A typical BQD is a single nanocrystal, usually CdSe overcoated (*capped*) with ZnS. While the physical principle upon which the intermittency is produced is still argument of debate [72], it is well known that, statistically, BQD are characterized by inverse power law

distribution densities for the inter-events times [64, 65, 66]. The power indexes μ_{on} and μ_{off} are smaller than 2 and, in most cases, statistically different. The condition $\mu < 2$ implies a strong departure from ordinary Statistical physics, as it is a non-ergodic condition [75, 36]. The extension of the power law tail depends on the experimental setup, with exponential truncations in the long time regime in the *on* state depending on temperature and laser intensity.

Let us analyze in the next sections two physical models proposed to explain the fluorescence intermittency of BQD.

5.1.1. *Physical Models: Diffusion Model*

Some of the experimental observations of BQD can be explained through a simple diffusion model [72]. Consider the following simple controlled chemical reaction $A + B \rightleftharpoons AB$, where A is fixed in space. Let us assume, for simplicity, that the dots are uncapped, this implying an exponential decay for the *on* state [72]. In this case, once the dot is ionized, a charge is ejected, and its motion is assumed to be a random walk on a surface. This problem has been discussed in Refs. [60, 84], being it similar to the classical Onsager's problem of an ion escaping neutralization. The SP of the *off* state is known to decay as an inverse power law, with exponent 1/2. This has been observed experimentally in many recent experiments [64, 65, 66].

The case of diffusion for capped nanocrystals is very close to the trap model, discussed in the next section. The presence of traps all around the dot implies an equal return time for the trapped electron in both the *on* and *off* states. The physical reason for the blinking behavior is the presence of a different Auger non-radiative recombination for the *on* and *off* states [45]. As a consequence of this, the distribution of waiting times is an inverse power law, with the same power index for *on* and *off* times. Let us analyze the general features of the trap model.

5.1.2. *Physical Models: Trap Model*

This model was proposed by Bouchaud [35] along the lines of the kinetical treatment of Stillinger and Weber [90], based on the concept of *energy landscape*. According to the authors of Ref. [90], a system is characterized by a solid-like behavior if it spends most of its time at the bottom of the potential well. Its dynamics becomes instead diffusional if it spends most of the time at the top of the barrier. The relation between this kinetic scheme and thermodynamics is exemplified by a relation introduced by Adam and Gibbs [1], namely

$$\tau = \tau_0 \exp\left(\frac{A}{TS_c}\right), \tag{99}$$

where τ is a characteristic relaxation time, A and τ_0 are constants, T is the temperature, and S_c is the so-called configuration entropy of the system, stemming, in the original derivation, from the number of structural arrangements available to the liquid's constituent molecules [1].

The model of Bouchaud [35] introduces an energy landscape with the following distribution

$$p(E) = \beta_g e^{-\beta_g E}, \tag{100}$$

where $T_g \equiv 1/\beta_g$ is the glass transition temperature. Each barrier is described by the following Arrhenius-like prescription

$$t = t_0 e^{\beta E}, \tag{101}$$

where $T \equiv 1/\beta$ is the sample temperature, and t is the time necessary to overcome a barrier of intensity E by means of only thermal fluctuations. Let us now prove that the these times are distributed according to an inverse power law distribution density.

Imposing the conservation of the probability

$$\psi(t)dt = p(E)dE \tag{102}$$

immediately one obtains

$$\psi(t) = p(E)\left|\frac{dE}{dt}\right|. \tag{103}$$

Eq. (101) yields the following

$$\frac{dt}{dE} = \beta t, \tag{104}$$

and

$$E = \frac{1}{\beta} \log \left(\frac{t}{t_0} \right). \tag{105}$$

Combining the last two expressions with Eq. (103) one obtains

$$\psi(t) = \frac{\beta_g}{\beta} \exp \left\{ -\frac{\beta_g}{\beta} \log \left(\frac{t}{t_0} \right) \right\} = \tag{106}$$

$$= \frac{\beta_g}{\beta} \exp \left\{ \log \left(\frac{t}{t_0} \right)^{-\beta_g/\beta} \right\} = \tag{107}$$

$$= \frac{\beta_g}{\beta t} \frac{t_0^{\beta_b/\beta}}{t^{\beta_b/\beta}}. \tag{108}$$

By posing $\nu \equiv \beta_g/\beta$, the previous becomes

$$\psi(t) = \nu \left(\frac{t_0^{\nu}}{t^{1+\nu}} \right), \tag{109}$$

that is asymptotically an inverse power law. It is important to stress that the condition $\mu < 2$, common to both *on* and *off* BQD states, it is realized by $T < T_g$.

Adopting this simple scheme is possible to build a model for BQD. The authors of Ref. [93] propose a model where infinitely many traps are distributed around the fluorescent state, at different distances D. The probability that an electron is trapped after it leaves the fluorescent state is given by the expression

$$p(D) = ae^{-aD}, \tag{110}$$

and therefore the mean recovery time, i.e. the time that the particle spends in a trap, is

$$t = t_0 e^{bD}. \tag{111}$$

We can recognize the trap model of Bouchaud [35], with $a \equiv 1/T_g$ and $b = 1/T$. Proceeding as before, we obtain

$$\psi(t) = \alpha \left(\frac{t_0^\alpha}{t^{\alpha+1}} \right) \qquad \alpha \equiv \frac{a}{b} = \frac{T}{T_g} \tag{112}$$

Therefore, the trap model can be utilized to obtain a WT-PDF with an inverse power law form. Thus, it can be used to describe the BQD.

The model of Bouchaud, even though being very attractive, has the flaw of being analytically very difficult to treat. In a later paper, the perturbation of a trap model was studied (citare). The complication of the response formula makes it almost impossible to effectively use it for practical purposes. This is one of the reason why other models should be preferred, when equivalent results are achieved.

Can the trap model be ascribed to either renewal of modulation theory? According to the author of Ref. [28], the trap model is compatible with the renewal theory, provided that the particle resides in the trap only once. On the contrary, if the time the particle spends in a trap increases, through its residence for many times in the same trap, then the process becomes a modulation process.

5.1.3. *Aging in Blinking Quantum Dots: Renewal or Slow Modulation?*

In chapters 2 and 3 it was shown how two different approaches to complexity can generate the same distribution of waiting times. Statistically, BQD are systems characterized by a WT-PDF of the form of Eq. (14), with power indexes μ_{on} and μ_{off} smaller than 2 and different one another. This situation can be generated by the simple model of Eq. (1), of renewal nature, as well as by the trap model of Bouchaud, with long residence times, which is a modulated Poisson process.

In chapter 4 through a numerical algorithm it has been showed that it is possible to distinguish a renewal from a modulation process. The AE affords significant informations, otherwise hidden by the analysis of the shape of the WT-PDF. It seems therefore natural to apply the AE on the real time series of the BQD. 100 time series were kindly provided

by the group of Prof. M. Kuno, at Notre Dame University. Each of them consists of one hour of record, sampled every *ms*, for a total of 360000 data each. The experimental setup, described in details in Ref. [64, 65], records the fluorescent light emitted by the single QD. A typical sample of the BQD signal is shown in Fig. 5.1.

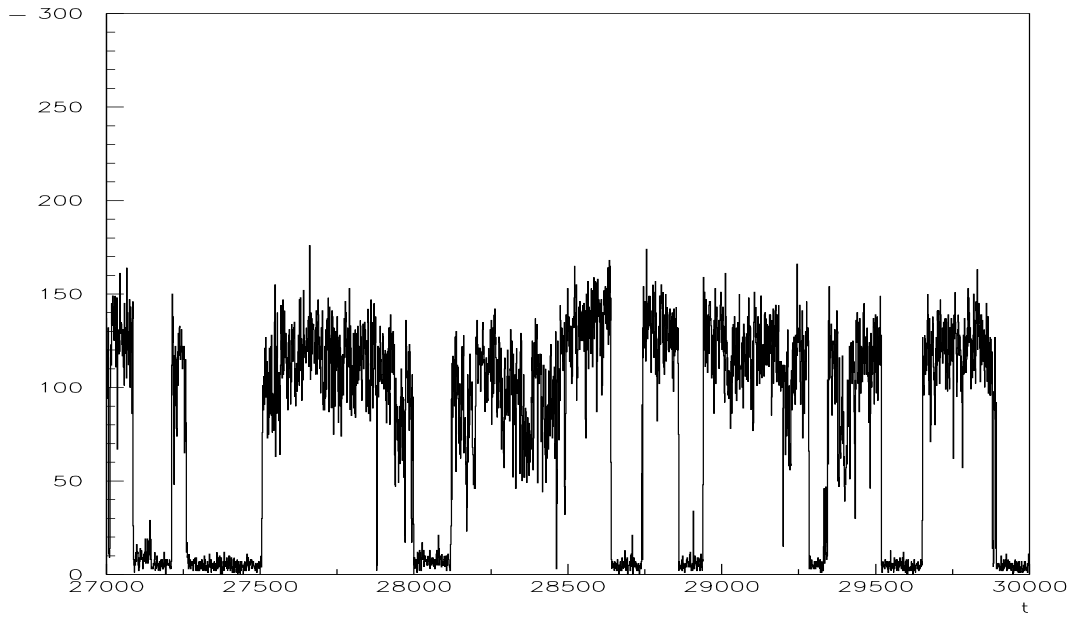

FIGURE 5.1. In this Figure an example of the BQD signal is shown.

Let us now apply the AE to the BQD sequences. Three curves will be compared: The *brand new* SP, denoted as Ψ_0, a SP corresponding to the numerical procedure described in chapter 4, called Ψ_{exp}, and the prediction of renewal theory, afforded by Eq. (98), that we call Ψ_{ren}. The coincidence between Ψ_{exp} and Ψ_{ren} is a sign of the renewal character of the process. An example of the results of our analysis is shown in Figs. 5.2 and 5.3.

In Fig. 5.2 the AE is applied to a sample time series of *on* residence times, for three different ages, $t_a = 20, 120, 220$. The continuous line is the SP for age 0, Ψ_0, the dotted line is the aged SP obtained with the AE technique, indicated as Ψ_{exp}, and the dashed line is the aged SP predicted by the renewal theory if the time series was generated by a renewal process, denoted as Ψ_{ren}. Aging is present in the time series, as revealed by the slower decay of the aged SP. Its comparison with the SP predicted by the renewal theory allows us to

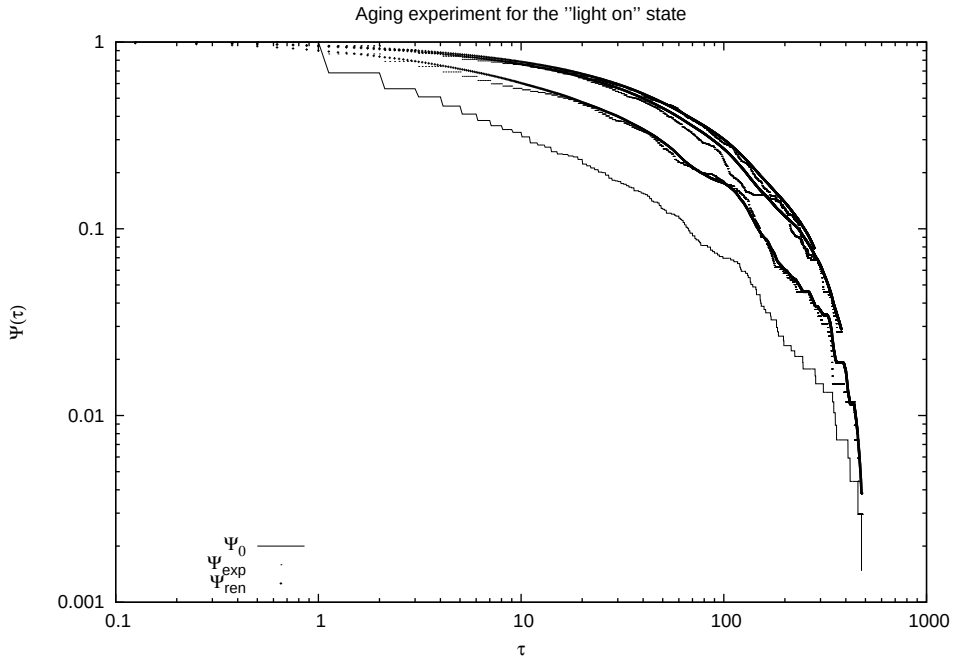

FIGURE 5.2. Results of the AE on a sample BQD time series of *on* residence times. The continuous line is the SP for age 0, Ψ_0, the dotted line is the SP obtained with the AE technique, indicated as Ψ_{exp}, and the dashed line is the SP predicted of the renewal theory, denoted as Ψ_{ren}. Aging is present and compatible with the renewal theory. $t_a = 20, 120, 220$, from the bottom to the top.

conclude that the process is renewal. Note that the inverse power law tail of Fig. 5.2 is not very extended, and an exponential cut-off emerges in the long-time region.

Also in the case of the *off* waiting times the AE signals the presence of strong aging, and this is shown in Fig. 5.3, for $t_a = 20, 120, 220$. The aging is again renewal, as can be inferred from the closeness of Ψ_{exp} and Ψ_{ren}, for all the considered ages. This numerical agreement has been proved in Ref. [28] through the introduction of a suitable indicator, called *aging intensity*, I_a, defined as

$$I_a = \frac{\Psi_{exp} - \Psi_0}{\Psi_{ren} - \Psi_0}. \tag{113}$$

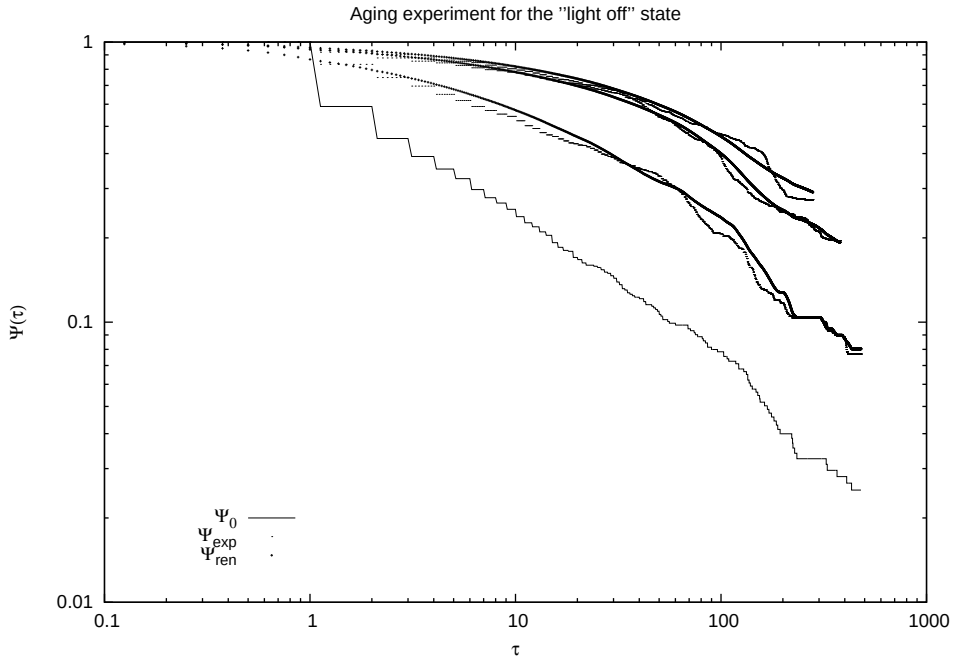

FIGURE 5.3. Results of the AE on a sample BQD time series of *off* residence times. The continuous line is the SP for age 0, Ψ_0, the dotted line is the aged SP obtained with the AE technique, indicated as Ψ_{exp}, and the dashed line is the aged SP predicted by the renewal theory, denoted as Ψ_{ren}. Also in this case, aging is present and compatible with the renewal theory. $t_a = 20, 120, 220$, from the bottom to the top.

The value of I_a ranges from 0 to 1: The former corresponds to the condition of no aging, since it implies $\Psi_{exp} \equiv \Psi_0$, while the latter should be indication of renewal aging, as it is realized by the condition $\Psi_{exp} \equiv \Psi_{ren}$. The analysis of the aging intensity allows in principle to assess the flowing important task: In the case $N_m = 1$ renewal and modulation coincide; if $N_m \gtrsim 1$, then it means that there are a few of what were called *pseudo-events*, events extracted from the same exponential waiting time distribution. In this case, at the light of the results of chapter 4, the aging effect is expected to be slightly reduced, therefore creating an intermediate condition. This property can be detected through the aging intensity I_a. In Fig. 5.4 is reported the value of the indicator I_a with respect to the number of events N_m extracted from the same Poisson process. The result is for simulated modulation process,

with parameter $\mu = 1.8$. Different ages are considered, ranging from $t_a = 20$ to $t_a = 220$. When $N_m = 1$ the value of the indicator approaches 1, this being a sign of aging compatible with the non-Poisson renewal theory. When the number of pseudo-events N_m increases, the value of I_a decreases. This allows to estimate the number of pseudo-events present in the real time series. For instance, $I_a = 0.1$ corresponds to approximatively 30 pseudo-events. It is worth noticing that the value of I_a coincides for all the considered ages. Also, note that I_a decays with N_m as an inverse power law, with power index $\alpha = 0.7$.

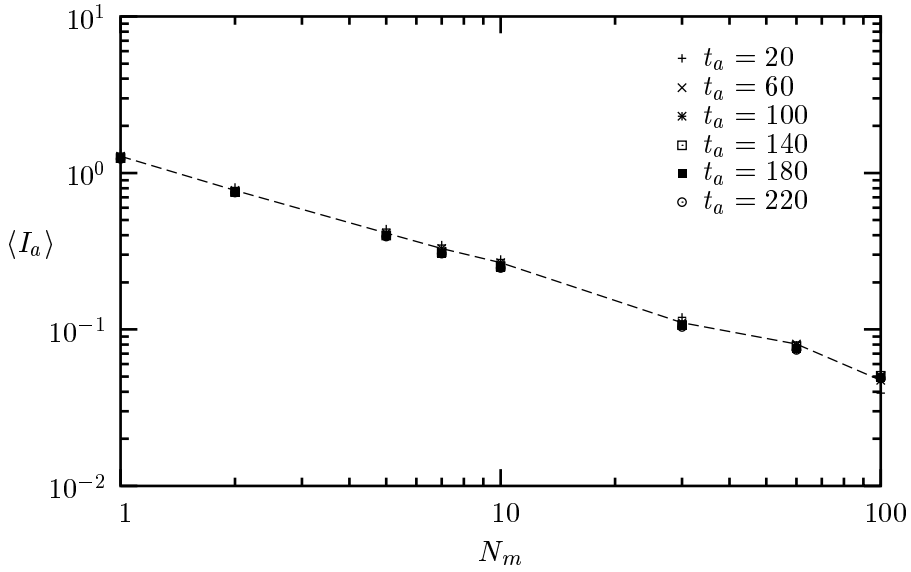

FIGURE 5.4. The value of the aging intensity I_a as a function of the number of pseudo-events N_m, for different ages t_a ranging from 20 to 220. The data set consists of simulated time series with $\mu = 1.8$. Increasing N_m implies an inverse power law decay of I_a, with power index $\alpha = 0.7$.

Let us summarize the results of this section. The BQD intermittent fluorescence has been studied. Even though the BQD behavior is, in principle, compatible with both renewal and modulation theory, the application of the AE technique introduced in the previous chapter proves that BQD are renewal systems.

In the next section I present a different kind of single system emitting intermittent fluorescence.

5.2. The Fluctuating Enzyme

In a recent paper [50] the intermittent fluorescence intensity of a single lipase molecule under the action of a laser field was investigated. As in BQD, also in this case random jumps are observed between an *on* and an *off* state. The waiting time distribution densities are in this case very different with respect to the BQD case. While the *off* state departs significantly from the Poisson prescription, being its waiting times distributed as a stretched exponential, the *on* state shows exponential decay. We shall therefore focus our attention only on the *off* state, and consider the *on* state just a flashing snapshot, of no interest from the point of view of complexity.

5.2.1. *Experimental Results*

The experimental setup [50] involves the stimulation, through a steady laser field, of a single lipase B molecule, *Candida Antarctica*. To highlight its activity, a fluorescence substrate is added to the molecule. The activity of the single molecule is compatible with a quasi-deterministic and quasi-periodic fluctuation of the environment, as shown by the chronological order of *off* waiting times (see Fig. 5(a) of Ref. [50]). The distribution density of the *on* state decays exponentially with time, while the *off* state shows anomalous behavior, according to the following

$$\psi(t) = \psi_0 e^{-\left(\frac{t}{t_0}\right)^{\alpha}}, \tag{114}$$

i.e. a stretched exponential with $\alpha = 0.15$.

In addition to the waiting times PDF, the two-states correlation function is computed from the experimental data. Note that, in this case, the correlation function coincide with

the relaxation function of the process. The experimental results show a stretched exponential decay, with exponent $\alpha = 0.085$ [50].

A recent paper [49] confirms statistically the results of Ref. [50] with the help of Monte Carlo simulations. The reliability of the numerical fitting of the stretched exponential PDF and relaxation function is proved in the considered case, against the criticism raised by the paper of Ref. [77].

5.2.2. *The Fluctuating Environment: A Slow Modulation Approach*

In a recent publication [29] a model explaining the emergence of a stretched exponential relaxation was proposed. According to the authors of Ref. [29], the single lipase conformational changes are compatible with a slow quasi-periodic and quasi-deterministic evolution of a time dependent rate, $q(t)$, thereby making the picture compatible with the NHPP of section 3.2. In order to get a quasi-periodic behavior, imagine the rate to increase from an initial value q_0 to a final, very large, value q_f, and then decrease until it gets again the value q_0.

Let us obtain the expressions for the time dependent rate $q(t)$ in the considered case. According to Eq. (38),

$$\psi(t) = \int_0^\infty \Pi(q) q e^{-qt} dq = \psi_0 e^{-\left(\frac{t}{t_0}\right)^\alpha}, \tag{115}$$

where $\psi_0 = \alpha/(t_0\Gamma(1/\alpha))$ is the normalization constant. From the previous, it comes that $\psi(t)$ is the Laplace transform of the function $f(q) = q\Pi(q)$. Thus, in the short time region, where the stretched exponential can be expanded

$$\psi(t) \sim \psi_0(1 - (t/t_0)^\alpha) \tag{116}$$

one gets, using the Tauberian theorem for $q \gg 1$ [48], the following asymptotic expression

$$\Pi(q) = Cq^{-q-2}. \tag{117}$$

where C is a constant. The general relation linking $\Pi(q)$ to $q(t)$ is given by Eq. (46). If Eq. (117) is plugged into Eq. (46), the following relation is obtained

$$\frac{dq}{dt} = \pm\frac{q^{\alpha+2}}{TC}. \tag{118}$$

In order to get the dynamical prescription for the rate, we need to integrate between 0 and $t < T$. From the integration two different dependences on time are obtained for the rate, namely

$$q_{inc}(t) = \frac{q_0}{(1 - t/T_{inc})^r} \tag{119}$$

$$q_{dec}(t) = \frac{q_0}{(1 + t/T_{dec})^r}. \tag{120}$$

The expressions in Eqs. (119) and (120) refer to the cases of increasing (+ sign in Eq. (117)) or decreasing (− sign in Eq. (117)) rate, respectively. It is worth pointing out that the switch between decreasing and increasing patterns of $q(t)$ is not exactly periodical, insofar as we decide not to cut the last waiting time, even though it stretches off the period length T. This implies the presence of some random events (i.e., *renewal*), whose presence will be revealed by the AE. The time scales T_{inc} and T_{dec} are given by the following expressions

$$T_{inc} = \frac{T}{1 - (q_0/q_f)^{\alpha+1}} \tag{121}$$

$$T_{dec} = \frac{T}{(q_f/q_0)^{\alpha+1} - 1}, \tag{122}$$

while the parameter r is linked to the exponent α of the stretched exponential by the following simple expression

$$r = \frac{1}{\alpha + 1}. \tag{123}$$

The prescriptions of Eqs. (119) and (120) are valid in the case of slow modulation, i.e., T very large, and are expected to yield a time series whose WT-PDF is a stretched exponential of the form of Eq. (115).

Let us now find how large the parameter T should be in order to produce results in qualitative agreement with the experimental observations of Ref. [50]. Let us run Eqs. (119) and (120) for parameters $\alpha = 0.2$, $q_0 = 10$ and $q_f = 10^3$. The numerical procedure that we adopt is different when dealing with increasing or decreasing rates. Let us first evaluate the waiting times corresponding to the increasing prescription of Eq. (119). Consider the following dynamical prescription

$$\dot{y} = q_{inc}(t) y \qquad y \in [0, 1]. \tag{124}$$

It is evident that Eq. (124) corresponds to generate a Poisson process with a rate given by $q_{inc}(t)$. It is possible, by inverting and solving the differential equation (124) to get the time that it takes to have an event, i.e., the waiting time for the Poisson process. With straightforward algebra,

$$\tau_n = -T_{inc} \left[\left(1 - \frac{t'_{n-1}}{T_{inc}} \right)^{1-r} + \frac{(1-r)}{q_0 T_{inc}} \log y_0 \right] - t'_{n-1} \tag{125}$$

where y_0 is random initial condition, uniformly drawn between 0 and 1, $t'_n = \sum_{i=0}^{n} \tau_i$ and $\tau_0 = 0$. In this way we build a sequence of waiting times that extends until $t'_n \geq T$. As already mentioned, when the first t'_n gets a value larger that T, we switch from the increasing to the decreasing rate.

In order to have the waiting times for the decreasing case, we adopt a general procedure [44] to obtain a NHPP from a homogenous Poisson process. The procedure is based on the following theorem (given here without proof):

THEOREM 5.1. *If $0 < t_1 < t_2 < \ldots$ is a homogenous Poisson process with unit rate on $[0, \infty)$, and if Q is an integrated rate function, then*

$$0 < Q^{-1}(t_1) < Q^{-1}(t_2) < \ldots \tag{126}$$

determines a NHPP with integrated rate function Q.

Adopting the procedure indicated by the previous theorem, we are able to build a NHPP with rate $q_{dec}(t)$. We first build a homogenous Poisson process, then, adopting the numerical procedure indicated by Eq. (126) we get the NHPP we need.

The results of our numerical experiment are in Fig. 5.5. The WT-PDFs are shown for $T = 0.1, 1, 100$. The full line indicates a numerical fit, through a data analysis program, with a stretched exponential. Just by visual inspection we realize that in the case $T = 0.1$ (Fig. 5.5(a)) the numerical procedure does not afford a good stretched exponential function. The reason for this is the fact that a small value of T implies a small number of exponential waiting times extracted from the same distribution, i.e. the slow modulation condition is not satisfied anymore. As we increase the value of T, we have a better agreement between the numerical experiment and the fit. In both the cases $T = 1$ and $T = 100$ the stretched exponential is well fitted through the entire time span.

In order to see which of the conditions $T = 1$ and $T = 100$ fits the experimental results of Ref. [50], we plot the waiting times in chronological order, i.e. the waiting times in the order they are extracted. Fig. 5.6 shows the chronological order of WT for different values of T. The left side of the Figure shows a fixed number of peaks, that is a fixed number of the enzyme's fluctuation, while on the right side the number of peaks per fixed number of WT is compared. By visual inspection, comparing Fig. 5.6 to Fig. 5(a) of Ref. [50] we see

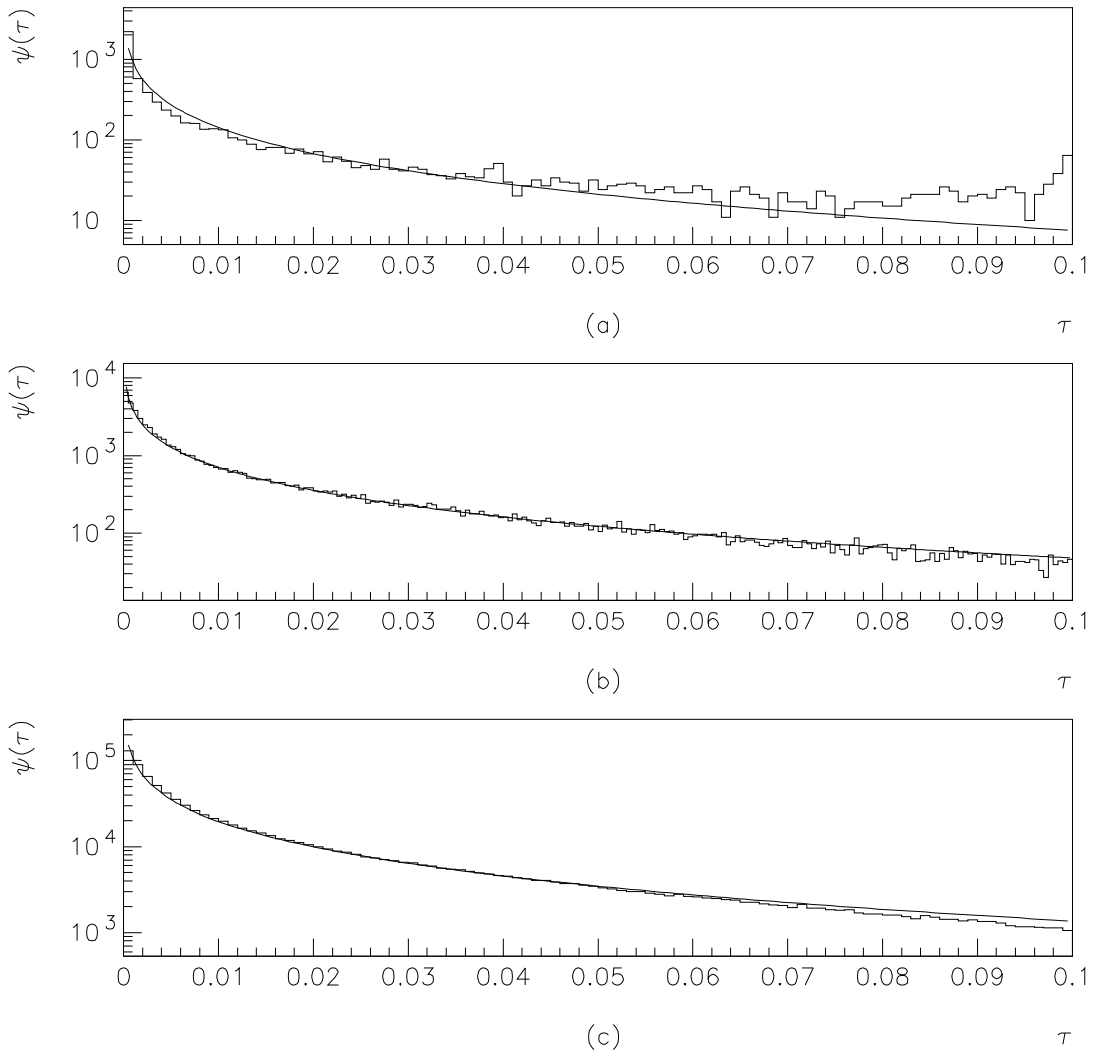

FIGURE 5.5. The WT-PDF $\psi(\tau)$ as a function of τ. (a) $T = 0.1$, (b) $T = 1$, and (c) $T = 100$. The full line is the stretched exponential, with $\alpha = 0.2$ and t_0 determined by a numerical fitting through a data analysis program yielding: (a) $t_0 = 3.1 \cdot 10^{-6}$, (b) $t_0 = 4.9 \cdot 10^{-6}$, and (c) $t_0 = 5.1 \cdot 10^{-6}$.

that the condition $T = 1$ seems the closest to the experimental results.

5.2.3. *Aging Experiment on Simulated Time Series*

To draw some conclusions on the physics driving the enzyme's fluctuation, the AE technique is applied to the artificial sequences. In this way, a prediction about the results of

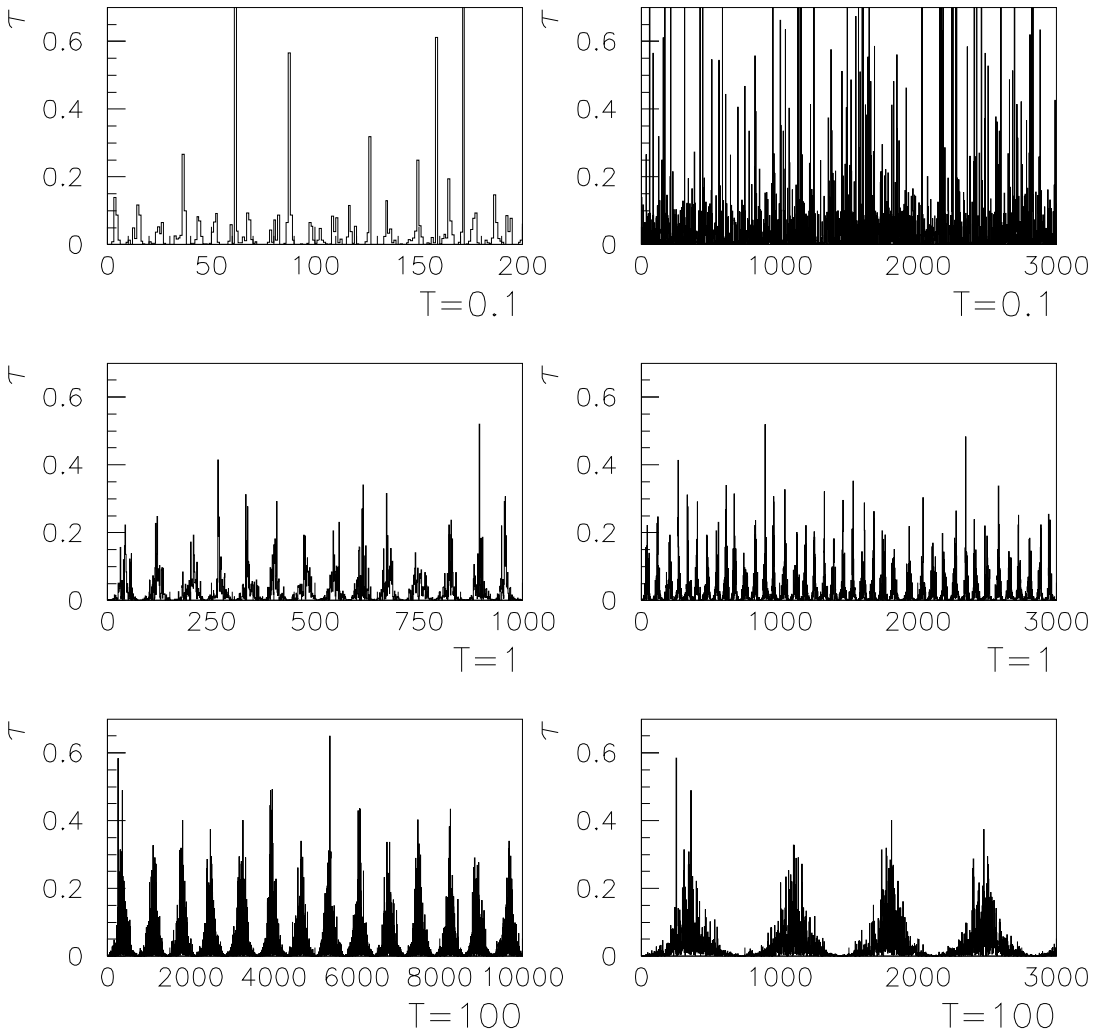

FIGURE 5.6. A comparison of the chronological order of WTs for different values of the parameter T. On the left side we arranged the same number of peaks (fixed number of enzyme fluctuations), while on the right side the number of peaks per fixed number of WTs (or system's jumps) is compared. We consider the values $T = 0.1, 1, 100$ from the top to the bottom.

the application of the method on real sequences can be done. The results are plotted in Figs. 5.7, 5.8, and 5.9. The non-aged SP (full line) is indicated with the symbol Ψ_0, the result of the numerical procedure (dashed line) with Ψ_{exp}, and the prediction of the renewal theory (dashed-crossed line) with Ψ_{ren}.

In Fig. 5.7, corresponding to the case $T = 0.1$, the slow modulation prescription is violated, as there is aging in the SP, and it is compatible with the renewal assumption. The aged curves, obtained for $t_a = 0.1$ and $t_a = 1.1$, for the real time series and the prediction of the renewal theory are very close one another. This, as discussed in chapter 4, is a sign of a renewal process. A worse agreement between the curves implies that the process is not exactly renewal, i.e., the number of events extracted from the same Poisson process is not 1, but might be slightly larger.

In the case $T = 1$, reported in Fig. 5.8, a faster decay of the aged SP corresponding to the experimental results with respect to the predictions of renewal theory is observed. The parameter t_a is equal to 0.1 and 6.1, from the bottom to the top. The aging effect is still present, and this is a sign that many renewal events may exist, but it is strongly reduced, for both the considered ages of the system.

Finally, in Fig. 5.9 the result of the experiment on the SP corresponding to the case $T = 100$ is reported. As this is a very slow modulation condition, an annihilation of the aging is expected, and this is indeed what appears from the analysis. The aged curves coincide with the non aged SP, for both $t_a = 1$ and $t_a = 10$.

Concluding, the adoption of the AE technique on the simulated time series affords useful indication about the results expected by analyzing the real time series. The process may be a NHPP, generated by the enzyme's conformation changes. The renewal aging experiment might be a crucial instrument to clarify this issue.

5.3. Conclusions

In this chapter the properties of the intermittent signal of two different nanosystems was analyzed. We have seen how both BQD and fluctuating enzymes yield a non exponential distribution of waiting times. We have also seen how, in spite of this similarity, the physics of the two systems is very different. BQD obey renewal theory [28], while the enzyme's fluctuation might be a sign of a NHPP [29]. This two approaches to complexity generate different aging properties, according to the renewal aging experiment proposed in Ref. [28],

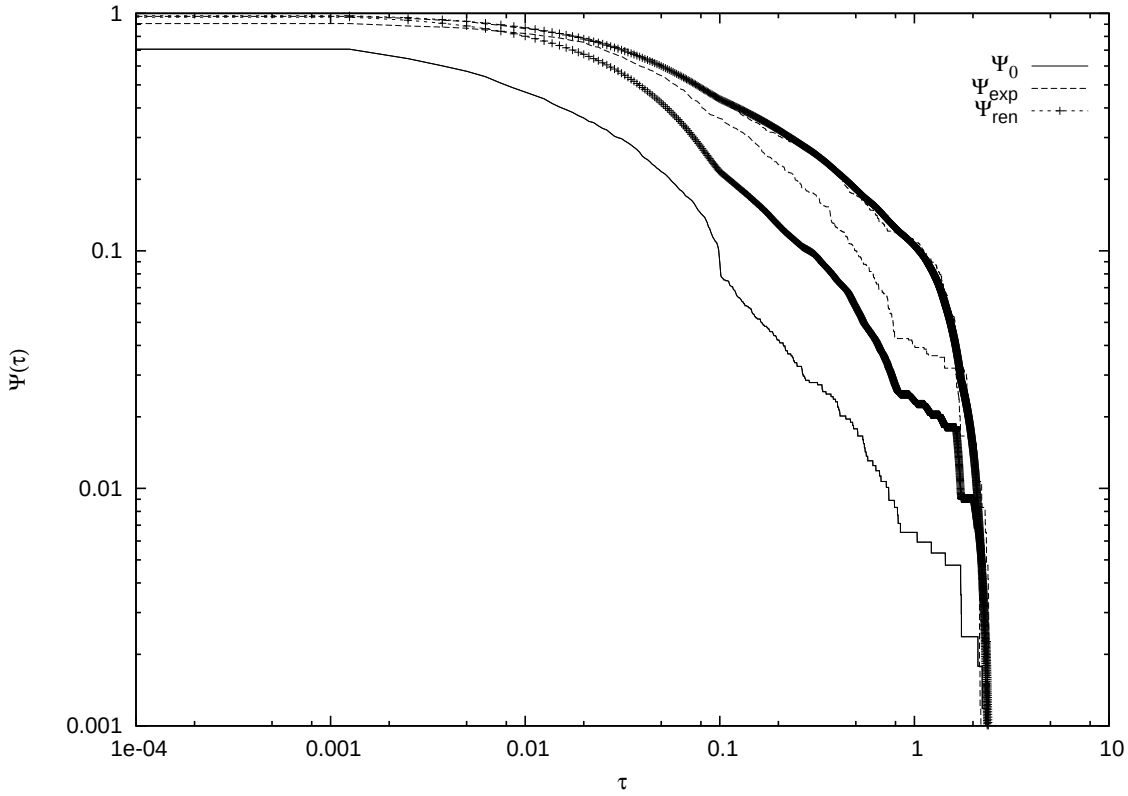

FIGURE 5.7. Result of the AE on the SP in the case $T = 0.1$, for $t_a = 0.1, 1.1$. The full line indicates the non-aged SP, called Ψ_0, the dashed line the aged SP, indicated as Ψ_{exp}, and the dashed-crossed line the prediction of the renewal theory, denoted by Ψ_{ren}. There is aging, compatible with the renewal assumption.

and described in chapter 4.

Finally, it is worth quoting the recent paper of Ref. [15], where a quasi-periodic behavior was found in a different intermittent fluorescence process. The NHPP discussed in this section may be useful to describe also this result.

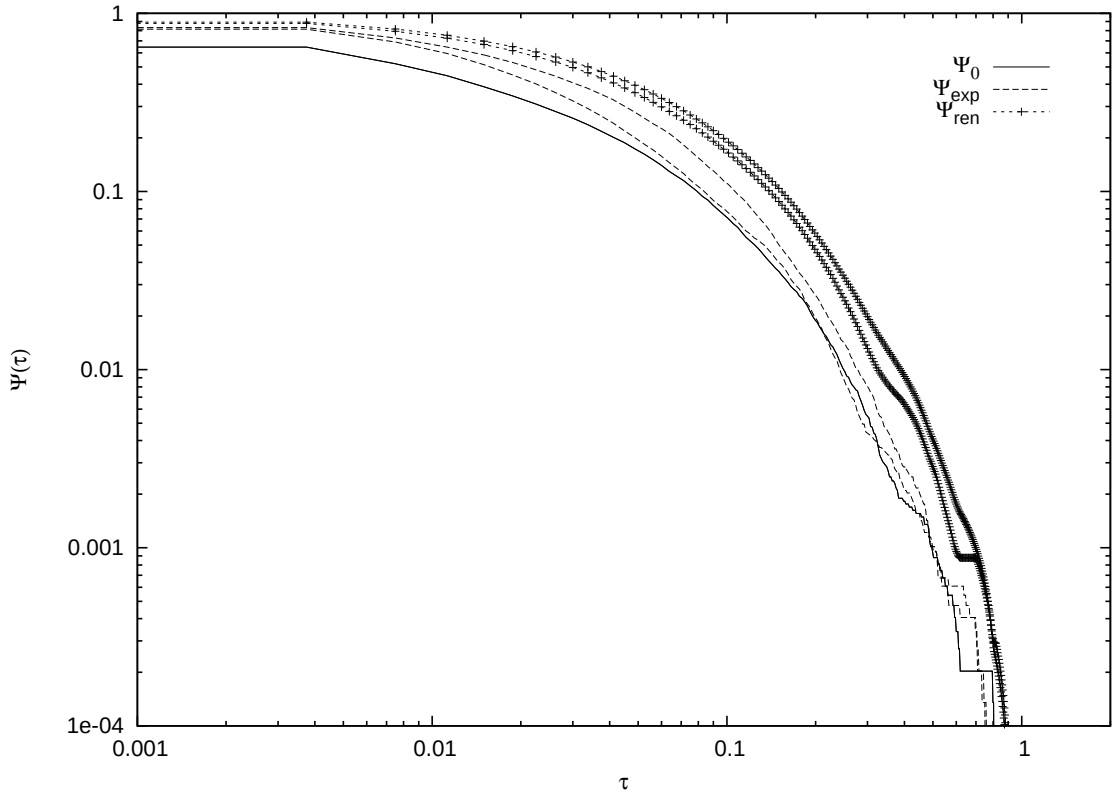

FIGURE 5.8. Result of the AE on the SP in the case $T = 1$, for $t_a = 0.1, 6.1$, from the bottom to the top. The full line indicates the non-aged SP, called Ψ_0, the dashed line the aged SP, indicated as Ψ_{exp}, and the dashed-crossed line the prediction of the renewal theory, denoted by Ψ_{ren}. There is aging, but it is reduced.

S

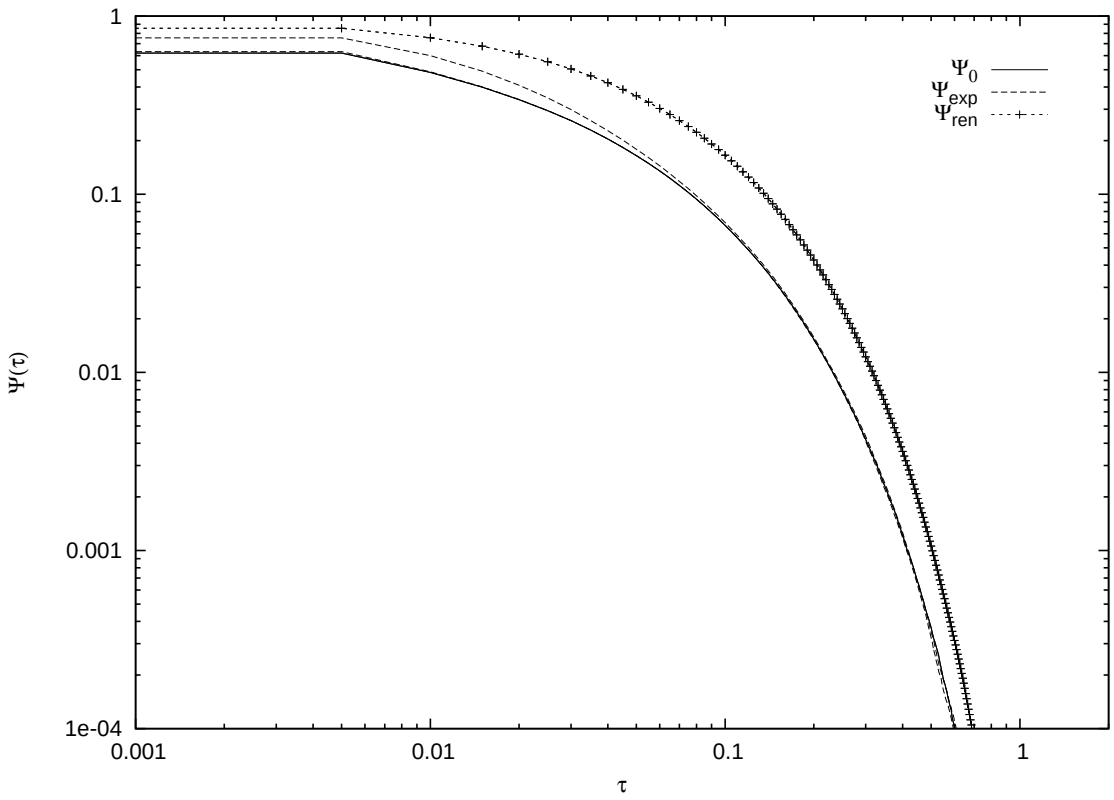

FIGURE 5.9. Result of the AE on the SP in the case $T = 100$, for $t_a = 1, 10$, from the bottom to the top. The full line indicates the non-aged SP, called Ψ_0, the dashed line the aged SP, indicated as Ψ_{exp}, and the dashed-crossed line the prediction of the renewal theory, denoted by Ψ_{ren}. The aging effect is annihilated in this case.

CHAPTER 6

THE COMPLEXITY OF THE BRAIN

6.1. Introduction

The study of neuronal systems through typical instruments of statistical physics has increased in the last few years. The challenges that this kind of analysis pose are triggered by the consideration that Poisson physics is inadequate to properly describe the complexity of these systems. Several models have been proposed by physicist to properly take into account the properties of experimental data. It is opinion of some neurophysiologists that single neurons are renewal [92] and non-Poissonian [12] systems, this result being suggested experimentally. However, a collection of neurons is usually thought to be Poissonian, this implying the strong statement that the human brain is a Poisson system.

The purpose of this chapter is to prove, through a new numerical technique based on the adoption of a popular instrument of graph theory, the Minimal Spanning Tree (MST), that the assumption that the human brain is a Poisson system is not correct. Also, the same technique, applied to complex sounds generated adopting a suitable computer apparatus, proves that music composition shares the same non-Poisson properties of the human brain, affording a possible way of explaining the effect of music on the brain activity.

The action of music on the brain is a well known phenomenon, but only recently it has attracted the interest of neurophysicists [10]. In a recent publication [25] the brain response of both musicians and non-musicians was studied, with the formers yielding a higher degree of the gamma band synchrony. This results suggests that a synchronization mechanism through which music exerts its influence on the brain might exist.

We shall see how the analysis of electroencephalograph (EEG) and complex sound time series using both the MST and AE technique show a statistical similarity between the two

systems. Both EEG and complex sound are proved to be non-Poisson renewal systems, living in the non-ergodic condition. The SPs of the properly build time series are found to be stretched exponentials, that the AE proves to be renewal. This important result can be therefore adopted to explain the impact of music on the brain. However, to generate this conclusion, a novel approach to synchronization is necessary, the ordinary one being unable to fit the non-Poisson renewal properties of the two systems. This new approach goes under the name of *complexity matchin* and it is shortly introduced at the end of this chapter.

6.2. Mittag-Leffler-Type Functions of Renewal Origin

In this section, a class of Mittag-Leffler-type (ML) functions is obtained from a particular class of stochastic processes. The result of the procedure is a renewal process with a SP of the ML form.

The ML function [76] is attracting the interest of a larger and larger number of scientists in the field of complexity [43]. Its main characteristics is that it establishes a compromise between the stretched exponential, a behavior that appears at short times, and the inverse power law, characteristics of the long time regime. The authors of Ref. [88, 68] argue that the SP of the returns in a financial time series can be fitted through a ML function. However, in a later paper [80] the difficulty in finding the inverse power law tail in the empirical data, due to poor statistics, was acknowledged. The authors of Ref. [27] used the AE to make the inverse power law tail distinctly appear from the noisy background, see chapter 7 for a more detailed discussion of this effect.

In this section an approach to ML function is proposed that can explain the emergence, in particular limiting conditions, only of the short time regime, namely the stretched exponential part.

Let us imagine a Poisson process driven by a rate $q \ll 1$. This condition makes a discrete representation indistinguishable from a continuous time picture. The distribution of waiting times between consecutive events, denoted by $\psi_P(n)$, in the natural time representation is exponential

(127) $$\psi_P(n) = qe^{-qn}.$$

The process of interest is generated through a subordination prescription [78], namely, the natural time n is converted into the continuous time $t(n)$, utilizing

(128) $$t(n+1) - t(n) = \tau_n.$$

According to the subordination theory [78], the time τ_n must be randomly drawn from a distribution density $\psi(\tau)$. The form of $\psi(\tau)$ must be suitably chosen in order to obtain the desired result. It is straightforward to prove that the adoption of an inverse power law as subordinating function yields as SP Mittag-Leffler of order α, namely

(129) $$\Psi_{SP}(t) \equiv E_\alpha(-(\gamma t)^\alpha) = \sum_{n=0}^{\infty}(-1)^n \frac{(\gamma t)^{\alpha n}}{\Gamma(\alpha n + 1)s},$$

if we assume the event production process to be renewal, and $q \ll 1$. The ML function admits the following asymptotic expressions [87], in the case $0 < \alpha < 1$

(130) $$E_\alpha(-(\gamma t)^\alpha) \sim \frac{1}{(\gamma t)^\alpha} \qquad t \to \infty \quad t > \frac{1}{\gamma},$$

that is an inverse power law, and

(131) $$E_\alpha(-(\gamma t)^\alpha) \sim \exp(-(\gamma t)^\alpha) \qquad t \to 0 \quad t < \frac{1}{\gamma},$$

that is a stretched exponential.

The power index μ of the subordinating function is linked to α by the following relation

(132) $$\alpha = \mu - 1.$$

Let us now prove the previous assertion. Let us consider a set of sequences $\xi(t)$, all of them prepared at time $t = 0$. In the continuous time scale the SP for the events generation process is given by

$$\Psi_{SP}(t) = \sum_{n=0}^{\infty} \int_0^t dt' \psi_n(t') \Psi(t - t') e^{-qn}. \tag{133}$$

Let us discuss the physical meaning of Eq. (133): $\Psi_{SP}(t)$ is, by definition, the probability that no event is produced up to the time t. In the natural time scale this probability, up to the $n-$th event, is expressed through $\exp(-qn)$. Thus, to have $\Psi_{SP}(t)$ we have to multiply $\exp(-qn)$ by $\psi_n(t')$, that implies than n drawings have been done from the function ψ up to the time t', and by $\Psi(t - t')$, that indicates that no drawing has been made between t and t'. The integration between 0 and t takes into account the fact that the last drawing can take place anywhere before t. If there are no drawings, $\Psi_{SP}(t) \equiv \Psi(t)$, where $\Psi(t)$ is the SP of $\psi(t)$. The function $\psi_n(t')$ indicates the probability that n drawings from $\psi(t)$ occurred, the last of which exactly at time t'. Since the process is renewal, the probability of having n collision is given by the convoluted structure of Eq. (64).

The Laplace transform of $\Psi_{SP}(t)$ is given by

$$\hat{\Psi}_{SP}(u) = \frac{1}{\left[1 - \hat{\psi}(u) exp(-q)\right]} \frac{1}{u} \left[1 - \hat{\psi}(u)\right]. \tag{134}$$

Note that still no hypothesis on the form of $\psi(t)$ has been done. If $\psi(t)$ is an exponential, then the subordination has no effect on the SP, as its form remains exponential. Let us imagine the subordination function to be not exponential. In general, Eq. (134) can be rewritten as

$$\hat{\Psi}_{SP}(u) = \frac{1}{u + q\hat{\Phi}(u)} \qquad \hat{\Phi}(u) = \frac{u\hat{\psi}(u)}{1 - \hat{\psi}(u)}, \tag{135}$$

that is the Laplace transform of

$$\frac{d}{dt}\Psi_{SP}(t) = -q\int_0^t \Psi_{SP}(t-t')\Phi(t')dt'. \tag{136}$$

$\Phi(t')$ is a memory kernel. Note that the assumption $q \ll 1$ was still not used. This last assumption is necessary to go to the continuous time regime, therefore justifying the form $\exp(-qn)$ for the SP, and it has also have the physical effect of making more extended the stretched exponential regime of the ML function. The case of ordinary exponential WT-PDF is recovered by imposing the memory kernel to be a delta of Dirac. Instead, let us assign to the memory kernel the following form in the Laplace space

$$\hat{\Phi}(u) = \chi(u+\Gamma)^{2-\mu} \qquad \chi \equiv \left[\Gamma(2-\mu)T^{\mu-1}\right]^{-1}. \tag{137}$$

Let us imagine the parameter μ to be smaller than 2. With this choice the SP becomes, in the Laplace space

$$\hat{\Psi}_{SP}(u) = \frac{1}{u+\gamma^{\alpha}(u+\Gamma)^{1-\alpha}}, \tag{138}$$

where

$$\alpha \equiv \mu - 1 \qquad \gamma \equiv (\chi q)^{1/\alpha}. \tag{139}$$

If $\Gamma = 0$, then Eq. (138) is the Laplace transform of a ML function of order α. The role of the parameter Γ is to taking into account the fact that the system is not infinite. Thus, the value of Γ is finite.

Let us first assume that $\Gamma > 0$ and $\Gamma \ll \gamma \ll 1$. The condition $\gamma \ll 1$ is guaranteed by $q \ll 1$. The condition $\Gamma < \gamma$ is necessary to realize a physical situation where the fat tail of the ML function does not appear. Let us see which form the SP gets in this case:

- In the short time limit, i.e. $\gamma \ll u \ll 1$, in the expression of the SP of Eq. (138) it is not possible to neglect the first term in the denominator. Therefore

$$\hat{\Psi}_{SP}(u) = \frac{1}{u + \gamma^{\alpha} u^{1-\alpha}}, \tag{140}$$

that is the Laplace transform of a stretched exponential;

- In the limit $\Gamma \ll u \ll \gamma$, it is possible to neglect the first term in the denominator of Eq. (138). Therefore

$$\hat{\Psi}_{SP}(u) = \frac{1}{\gamma^{\alpha} u^{1-\alpha}}, \tag{141}$$

that is the Laplace transform of an inverse power law, thanks to the Tauberian theorem [48].

In this regime, the inverse power law tail of the ML function appears. In the case of $\Gamma \leq \gamma$ the inverse power law regime cannot appear.

Let us now find the explicit form of the subordination function. So far, it was defined only indirectly through the memory kernel $\hat{\Phi}(u)$ of Eq. (135). Let us invert the relation linking the two quantities, namely

$$\hat{\psi}(u) = \frac{\hat{\Phi}(u)}{u + \hat{\Phi}(u)} = \frac{1}{1 + \frac{u}{\hat{\Phi}(u)}} = \frac{1}{1 + \frac{u}{\chi (u+\Gamma)^{2-\mu}}}. \tag{142}$$

Again, it is clear the importance of the parameter Γ:

- If $\Gamma \ll u \ll 1$, then

$$\hat{\psi}(u) \simeq 1 - \frac{1}{\chi} u^{\mu-1}, \tag{143}$$

that is the Laplace transform of an inverse power law WT-PDF;

- In the regime $u < \Gamma$,

$$\hat{\psi}(u) \simeq \frac{1}{1 + \frac{u}{\chi \Gamma^{2-\mu}}}, \tag{144}$$

that is the Laplace transform of an exponential WT-PDF.

Summarizing, the form of $\psi(t)$ is an inverse power law, truncated by an exponential in the long time limit.

Concluding, the adoption of a subordinating function with an inverse power law form, asymptotically truncated by an exponential, yields a SP with a stretched exponential form, depending on the choice of the parameter Γ we make. This assumption make it also possible for us to prove the important relation linking the parameter $\mu < 2$ of the subordinating function to the order α of the ML function, of which a stretched exponential of exponent $0 < \alpha < 1$ is a limit.

In the next section I introduce a method of analysis based on the minimal spanning tree.

6.3. The Minimal Spanning Tree as Event Selector

The analysis of real EEG time series is typically conducted on single sequences of data, afforded by one of the electrodes on the human scalp. A recent example of this kind of work is the paper of Ref. [37]. Our view of complexity requires the presence of critical events. On a single sequence, this means that we have to choose a threshold in the signal. When the signal exceeds the threshold, an event is recorded. This way of proceeding permits to obtain a time series from the original signal that can be analyzed, but it has the flaw to be threshold dependent, and this may lead to ambiguous results.

We propose a way of solving this issue by mapping the signal recorded by all the electrodes on the scalp in a network, through the Minimal Spanning Tree [40] (MST). To introduce the MST, we follow closely Ref. [70]

Consider a data set consisting of N columns. Each column indicates the signal recorded by an electrode. Taken two columns, say $\boldsymbol{x}$ and $\boldsymbol{y}$, define the correlation coefficient between $\boldsymbol{x}$ and $\boldsymbol{y}$ as

$$\rho_{\boldsymbol{xy}} = \frac{\sum_{k=0}^{t}(x_k - <\boldsymbol{x}>)(y_k - <\boldsymbol{y}>)}{\sigma_{\boldsymbol{x}}\sigma_{\boldsymbol{y}}}, \tag{145}$$

where the quantities $< \boldsymbol{x} >$ and $\sigma_{\boldsymbol{x}}$ are, respectively, the mean value and the standard deviation of the values of $\boldsymbol{x}$ in the interval $[0, t]$. Consider now the quantity

$$\tilde{\boldsymbol{x}} = \frac{\boldsymbol{x} - < \boldsymbol{x} >}{\sigma_{\boldsymbol{x}}} \tag{146}$$

and imagine that $\boldsymbol{x}$ gets the values $\tilde{x}_k, k = 1, \ldots, t$ in the interval $[0, t]$. The Euclidean distance between two columns over the time horizon t is expressed by

$$d^2_{\boldsymbol{xy}} = ||\tilde{\boldsymbol{x}} - \tilde{\boldsymbol{y}}|| = \sum_{k=1}^{t} (\tilde{x}_k - \tilde{y}_k)^2. \tag{147}$$

Note that $\sum_{k=1}^{t} \tilde{x}_k^2 = 1$. Therefore, Eq. (147) becomes

$$d^2_{\boldsymbol{xy}} = \sum_{k=1}^{t} (\tilde{x}_k^2 + \tilde{y}_k^2 - 2\tilde{x}_k\tilde{y}_k) = 2 - 2\sum_{k=1}^{t} \tilde{x}_k\tilde{y}_k. \tag{148}$$

The last sum on the right hand side of Eq. (148) is the correlation coefficient between $\boldsymbol{x}$ and $\boldsymbol{y}$ of Eq. (145) at the time t. The distance between the columns $\boldsymbol{x}$ and $\boldsymbol{y}$ can be defined as

$$d_{\boldsymbol{xy}} = \sqrt{2(1 - \rho_{\boldsymbol{xy}})}. \tag{149}$$

Since $-1 < \rho_{\boldsymbol{xy}} < 1$, $0 < d_{\boldsymbol{xy}} < 2$. Moreover $d_{\boldsymbol{xy}}$ fulfills the property of a distance, see thorough discussion in Ref. [70].

Adopting the distance $d_{\boldsymbol{xy}}(t)$ it is possible introduce the MST over the time horizon t. In a connected graph of N objects, weighted through the distances $d_{\boldsymbol{xy}}$, the MST is the tree with $N - 1$ links for which the total sum of the edges is minimum. In the literature there are many algorithms to create the MST, and here the method proposed by Kruskal [63] was selected. This method consists of the following steps: sort the distances in increasing order; select the shortest distance and draw an edge between the associated nodes; go to the next distance and draw edges; if an edge creates a loop, erase it; continue drawing links until all the N columns are represented.

In order to build a time series, the MST is used in a dynamical way. Divide the original time series in windows of size t. Then build the MST in every window and monitor the

topology, through the distribution of edges, of the MST in time. Whenever a change in the topology occurs, define an event. As a result of this, a time series of MST topological changes is obtained. The use of the MST as a dynamical variable is also common to Ref. [73], where the property in time of the MST for the US FX financial market were studied. However, in Ref. [73] the evolution of the number of links for a single node was observed.

It needs to be stressed that the MST conformation depends on the sign of the correlation. Particularly, negative and positive correlations are treated differently, with smaller distances induced by positive correlations, and larger distances associated to negative correlations. However, this is only relatively a problem, since the use it is made here of the MST only takes informations from the changes in correlation patterns.

In the next section, I describe the data set and the results of the MST method.

6.4. Analysis of the Experimental Data

The EEG data were collected utilizing a Scan LT-40 amplifier. The data were kindly afforded by Dr. Mark S. Rider and Dr. Mary J. Ross. The Scan LT-40 is an FDA approved medical device for the collection of digital EEG. Offline evaluation and the removal of artifacts from the EEG record and the conversion of the data to ASCII files were accomplished using a suitable software software. An electrode cap was used to provide standardized electrode placement. Digital EEG data was collected from 19 locations using the international 10-20 system of electrode placement. A reference electrode was placed on each earlobe to provide a linked ears montage for the physical reference of the scalp recordings. The impedance of the respective earlobe reference electrodes was maintained within 1 $K\Omega$ of each other. All other electrode impedances were maintained at 1 or 2 $K\Omega$ relative to amplifier input impedance with no more than 1 $K\Omega$ of variance between any of the electrode contacts. The EEG data was digitized at a rate of 250 samples per second. Before Analog to Digital conversion, anti-aliasing was achieved by a low-pass filter built in the software. The EEG was visually inspected online during acquisition to monitor for artifact. The number of human

subjects included in the study is 5, for a total of 20 sequences. The collected sequences correspond to 2 healthy subjects, 1 subject with chronical back pain, and 2 subjects with mental depression. Subjects were medication-free during the acquisition. The average number of data collected is $26,141$, corresponding to about 104 seconds of record. The minimum number of data for a single subject is $10,961$, corresponding to about 43 seconds of recording, for one of the healthy subjects, while the maximum number of data for a single subject is $56,544$, corresponding to about 226 seconds, for the subject with chronical back pain. Only two states were considered for the subjects, namely eyes open (EO) and eyes closed (EC). The acquisitions were made in the same conditions for all the subjects.

Performing the statistical analysis described in the previous section on the data affords a time series of MST topological changes. As in the previous chapters, we consider the SP associated to the time series. Fig. 6.1 shows a sample of the results. The time series corresponds to the subject with chronical back pain in the EO condition. The function is fitted through a stretched exponential distribution density, namely

$$\Psi(\tau) = e^{-(\gamma\tau)^{\alpha}} \qquad 0 < \alpha < 1, \tag{150}$$

with $\gamma = 0.205$ and $\alpha = 0.595$.

Similar results were obtained from the analysis of all the time series at out disposal. This important result allows to rule out the possibility that the human brain is a Poisson process.

However, as proved by the statistical analysis of chapter 4, the adoption of the AE gives useful informations about the dynamical process generating the time series. If the process is renewal, then the theoretical prescriptions of section 6.2 apply. This is the argument of the next section.

6.5. Aging Experiment on the Minimal Spanning Tree Time Series

In this section the AE analysis is applied to time series of MST topological changes. In Fig. 6.2 the result of the technique on the same time series of Fig. 6.1 is showed.

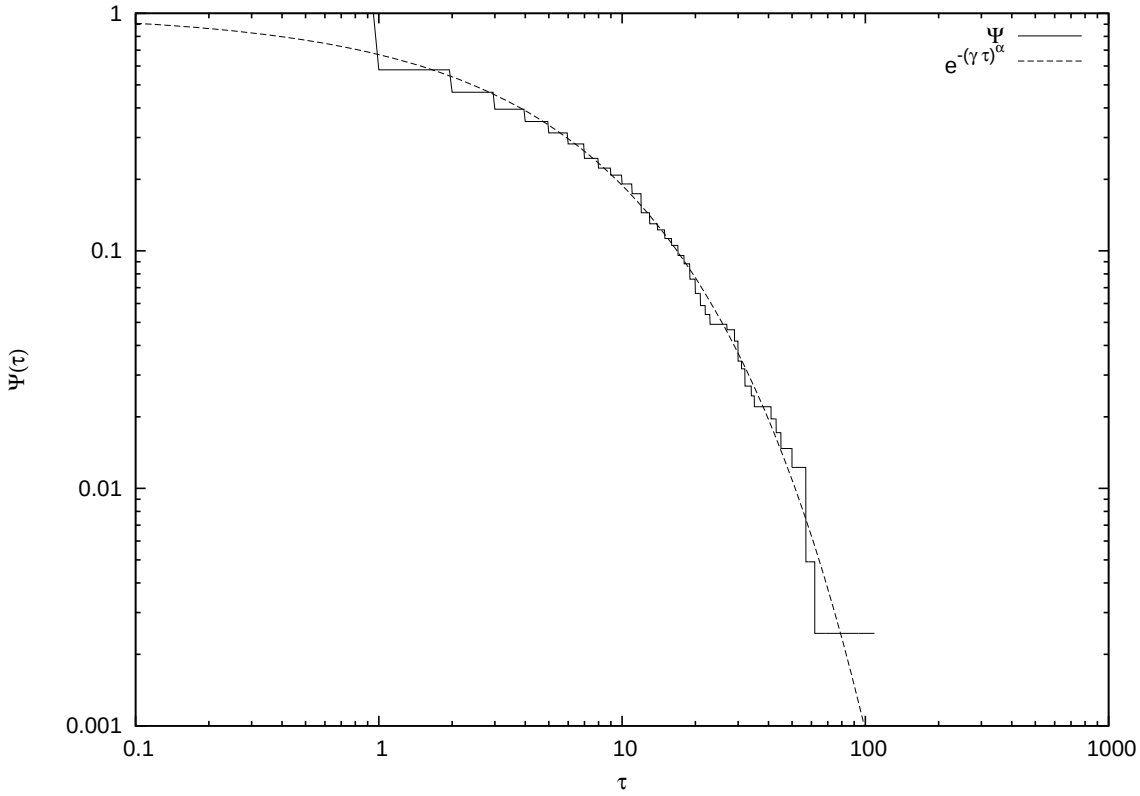

FIGURE 6.1. The SP of the MST topological changes (full line). The fitting function (dashed line) is a stretched exponential with index $\alpha = 0.595$ and time scale $\gamma = 0.205$.

Aging is present and very pronounced, and it is compatible with the predictions of the renewal theory. Similar results were obtained with all the time series at our disposal. This important result implies the validity of the prescriptions of section 6.2. Using Eq. (132) it is possible to find the parameter μ for the human brain. Since $\alpha < 1$ for all the time series, then $\mu < 2$, i.e., the human brain, as the BQD, is a system living in the non-ergodic condition. Table 6.1 reports the results of the analysis of this section, expressed in terms of the parameter μ, for both EC and EO conditions. Note that the μs for the EC are statistically smaller that the one generated by the EO condition. This is only a trend, given the small sample, but it is indeed a interesting effect, that should require more work to be proved.

How can we explain the emergence of the stretched exponential in the human brain? We

μ

Id	EC	EO
H1	1.730 (0.010)	1.800 (0.010)
H2	1.740 (0.012)	1.770 (0.013)
BP	1.595 (0.005)	1.746 (0.018)
D1	1.748 (0.013)	1.787 (0.014)
D2	1.960 (0.023)	1.974 (0.024)

TABLE 6.1. This Table shows a sample of the results of the analysis on our group of individuals in the EO (left side of the Table) and EC (right side of the Table) conditions. Results show a larger value of μ for EC condition. In parenthesis the standard deviation is reported. The symbol H indicates a healthy individual, BP the individual with back pain, D the subjects with mental depression.

can imagine [57] that the global behavior of the human brain is the result of the interaction of many synchronized units [26]. As a consequence of this, a correlated noise appears in the human brain, and this is detected by the MST. The changes in the MST are a consequence of the abrupt modification of the structure of the noise in the brain.

Let us also notice that it may exists a dominant tree and that the MST can appear in its conformation with a probability depending on the distance from the dominant structure. This process, being an indipendent process, might mimic a non-Poisson renewal process. However, if there is an alternance between short and long times, this process is essentially compatible with the a Non-Homogeneous Poisson Process (NHPP) of chapter 3, used to describe the fluctuating environment. We have already seen that the a NHPP is compatible with a renewal process only if the change between short and long times is fast, as confirmed by the results of the AE.

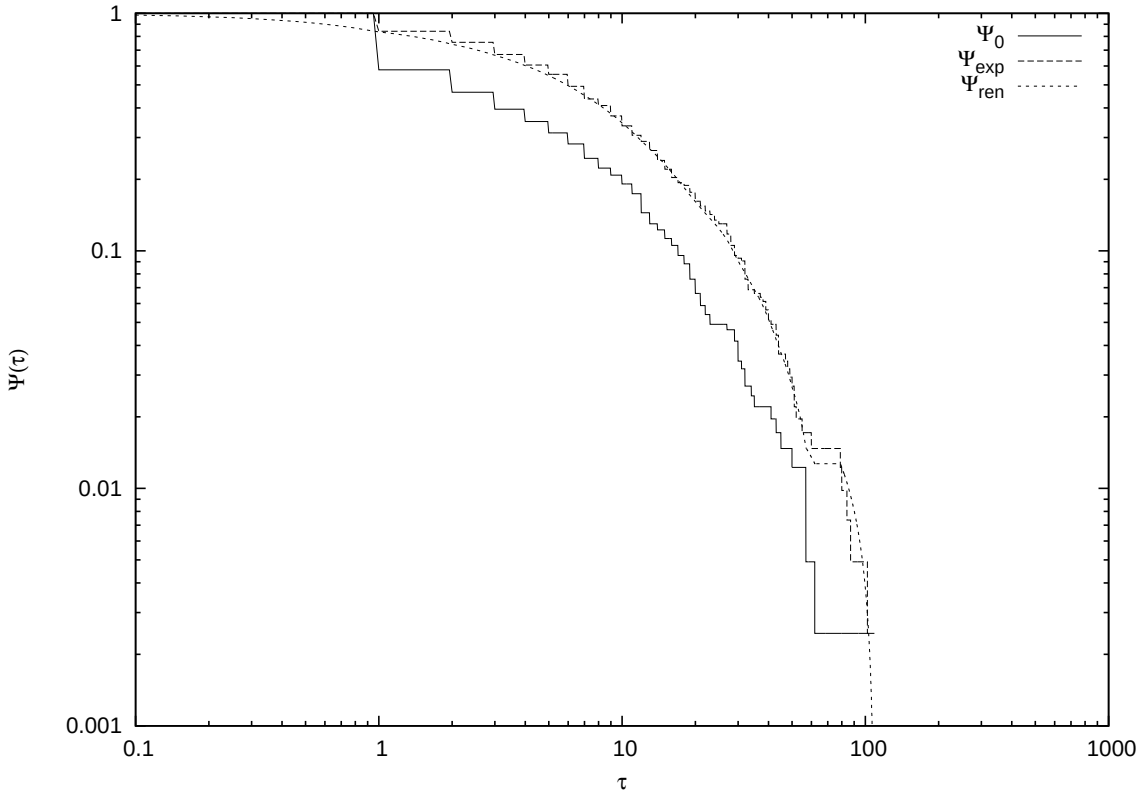

FIGURE 6.2. The AE on the SP of Fig. 6.1. The non-aged SP (full line) is indicated with the symbol Ψ_0, the aged SP (dashed line) with the symbol Ψ_{exp}, and the prediction of the renewal theory (dotted line) with Ψ_{ren}. Renewal aging effect is present, confirming the predictions of section 6.2. $t_a = 30$.

6.6. Analysis of Music Composition

In this section we analyze complex sound data afforded by means of a virtual instrument (software synthesizer) suitably designed [99, 98] to produce physiological effects [101, 103]. Data were kindly afforded by Prof. P. Winsor. The instrument can generate abstract sonic textures that are free from cultural influences. Moreover, through the use of Presets, a record can be kept of all parameters of consequence in the generation of the musical material. This feature is important for purposes of correlating the output sonic textures with, for instance, biological data from EEG recordings. In this way, researchers can precisely pinpoint areas of interest in biological data for analysis of and comparison with the generative parameters of the sound structures. Designed to allow control over the redundancy of time-point and

pitch/frequency patterns in a hierarchical framework, the virtual instrument sonic textures can be gradually morphed between constant states (stable) regimes and chaotic (complex) regimes via controls built into the graphical user interface. Moreover, precise measurement and recording of all generative schemes is possible, as well as synchronization with the EEG data time series. An important characteristic of the instrument is that vertical sonic textures are flexibly configurable with respect to the degree of vertical and horizontal redundancy of pitch- and time-space organization within the ongoing sonic flow. Various degrees of complexity can be introduced via Presets prior to and during the transmission of audio data to the test subject. For instance, microtonal controls are built into the instrument, so that the researcher can regulate the content of the sonic texture at any given point to create a relative harmonicity shift of the composite sonic data stream. In other words, there is maximum control over the degree of complexity via overlapping, phase-modulated patterning of melodic, harmonic, rhythmic, and texture-density data.

The instrument produces a vector $V(t)$, with 7 components, namely pitch onset time (in milliseconds), note frequency (in Hertz), waveform type, amplitude, articulation, preset number, and oscillator number. All these components are filed and assumed to afford informations about the signal. We therefore adopt for the music composition the same procedure applied before for the EEG signal, building also in this case a time series of MST topological changes. The resulting SP for a sample record is plotted in Fig. 6.3.

From the figure it also comes in this case that the distribution of topological changes produces a non-exponential SP, namely a stretched exponential with parameters $\gamma = 0.430$ and $\alpha = 0.600$. As in the previous section, a further test is needed to prove that the process is renewal. The results of the AE are plotted in Fig. 6.4.

Also in this case the application of the AE suggests that the process is renewal. Since the form of the distribution is, again, a stretched exponential, we can apply the theory of section 6.2, and conclude that complex sound shares the same properties as the EEG signal analyzed in the previous section. This suggests that both human brain and music

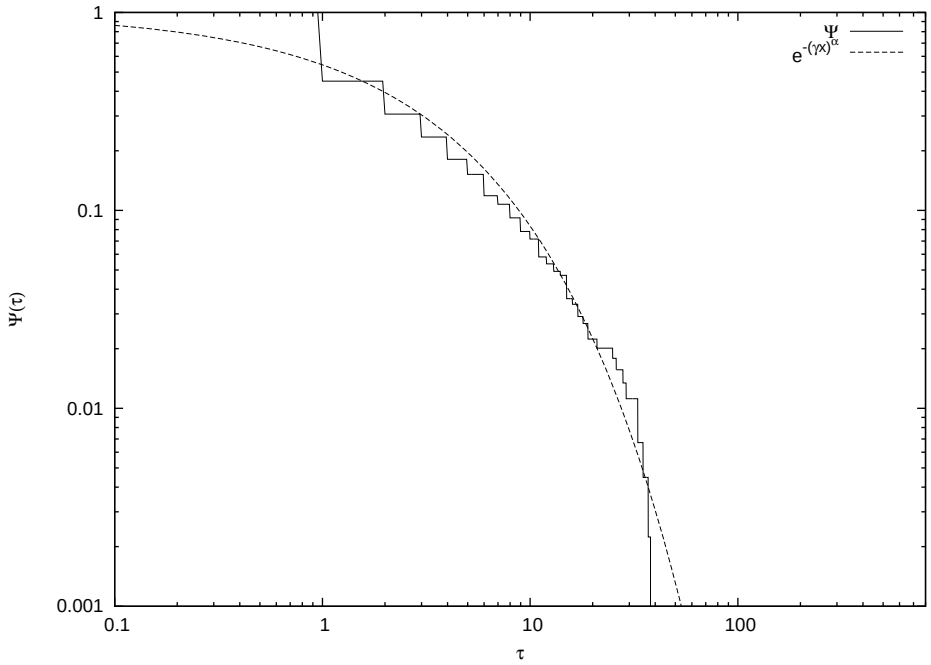

FIGURE 6.3. The SP of MST topological changes obtained from the music composition (full line). The curve is fitted by a stretched exponential function (dashed line) with $\gamma = 0.430$ and $\alpha = 0.600$. $t_a = 100$.

composition, sharing the condition $\mu < 2$, are complex systems that, in the absence of the exponential truncation, violate the ergodic condition.

6.7. Complexity Matching

How to interpret the results of the previous sections? The authors of Refs. [19, 5], have developed a new linear response theory for non-Poisson renewal processes. This new theory emerges in consideration of the fact that non-Poisson renewal systems do not respond to ordinary perturbations. The new form for the linear response reads

$$\langle \xi_S(t) \rangle = \epsilon \int_0^t dt' \chi(t,t') \xi_P(t'), \tag{151}$$

where $\xi_S(t)$ denotes the signal produced by the system of interest, $\chi(t,t')$ is the linear response function and $\xi_P(t)$ is the external perturbation. In the case of the human brain the

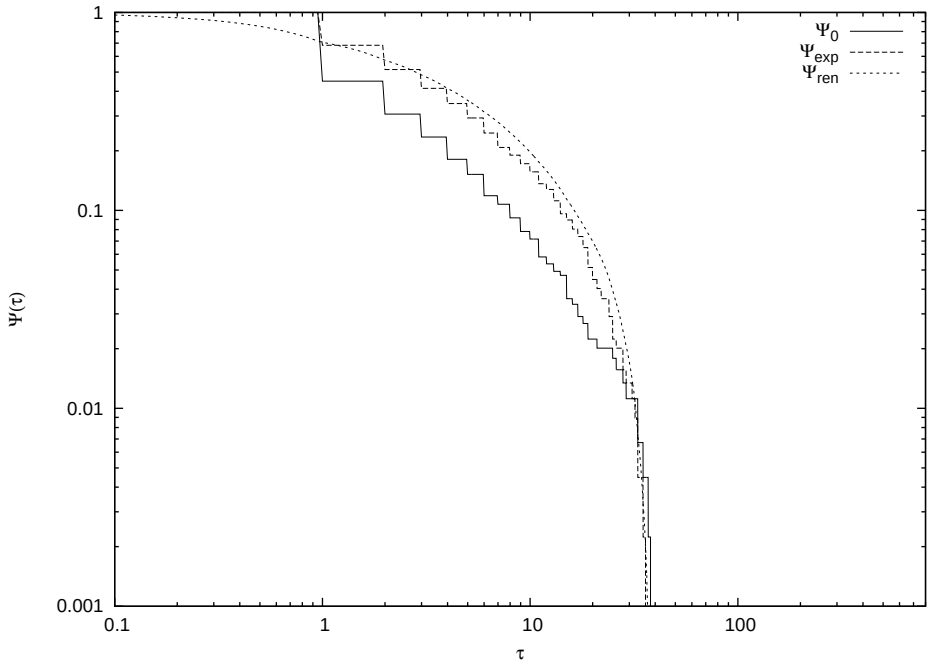

FIGURE 6.4. The AE on the time series of Fig. 6.3. The non-aged SP (full line) is indicated with the symbol Ψ_0, the aged SP (dashed line) with the symbol Ψ_{exp}, and the prediction of the renewal theory (dotted line) with Ψ_{ren}. Aging is present, and compatible with the predictions of renewal theory.

signal $\xi_S(t)$ is a global property emerging from the synchronization of different brain areas, roughly corresponding to the superposition of the signals detected by the electrodes fixed on the patient's scalp. In the absence of perturbation this global signal is characterized by the non-Poisson renewal events revealed by the method described in section 6.4. To transform these data into $\xi_S(t)$, we assign alternate signs to the quiescent time regions between two consecutive events. The complexity of this signal is denoted by means of the power index $\mu_S < 2$, emerging from the analysis of section 6.4.

If the perturbation function $\xi_p(t)$ is harmonic the system does not respond [19]. This is a clear sign of complexity, insofar as a non-Poisson renewal signal cannot be interpreted as the superposition of infinitely many independent processes. The individual constituents of a set of neurons responsible for any cognitive action are expected to be strictly cooperating with all the others' constituents. As a consequence, a harmonic perturbation triggers a cascade

of different time scales, thereby violating the prescriptions of ordinary stochastic resonance processes [19]. Thus, we are led to make the conjecture that the transmission of information from the perturbing signal to the human brain is determined by the interaction between the renewal events of the perturbing signal and the renewal events of the perturbed system. If the perturbing signal does not have any renewal events, as in the case of a harmonic perturbation, there is no response to a weak perturbation.

More recently the authors of Refs. [7, 8] have proved that this conjecture is correct, and that in the case where $\xi_P(t)$ is a signal derived from another non-Poisson renewal system with index $\mu_P < 2$, the system responds, and the intensity of the response is maximum when the matching condition $\mu_S = \mu_P$ [7] holds. The authors of Refs. [7, 8] have denoted this effect with the name of complexity matching, and they proved that when $\mu_P < \mu_S$ the perturbed system inherits the perturbation power index. In the previous section it has been proved that music composition is actually a complex signal with $\mu_P < 2$. Thus, the existence of the complexity matching effect leads to conjecture that the reason why the brain is sensitive to music lies on the fact that both the brain and music are non-Poisson renewal systems living in the non-ergodic region.

6.8. Conclusions

In this chapter the important result that the human brain is a non-Poisson renewal system living in the non-ergodic condition has been attained. The SP has been shown to be compatible with a stretched exponential. This result is essentially due to the cooperation among the single units, in this case the electrodes on the scalp.

Moreover, theoretical arguments, based on subordination theory, suggest that the stretched exponential of renewal origin might be the first part of a Mittag-Leffler function. It has been proved that, in particular limiting conditions, the inverse power law tail of the ML function may not appear. Still, the renewal properties of the process should be detected through the AE. This appears to be the case, as shown in the previous sections. Moreover, a new instrument of time series analysis, based on the MST, has been introduced. The analysis

of complex sound reveals non-Poisson renewal events as well, detected by the AE. As a consequence of this, and through the application of the complexity matching, the influence of music composition on the human brain can be explained. Of course, the applications of this new theory are not limited to the results of this chapter, but can be extended to many different fileds, where renewal events appear.

In the next chapter the important task of finding a suitable model that takes into account the results of this chapter is accomplished.

CHAPTER 7

A POSSIBLE MODEL FOR BLINKING QUANTUM DOTS AND THE HUMAN BRAIN

7.1. Introduction

In the last two chapters, three very different systems have been analyzed. Among these, two of them have been proved to be renewal, while numerical simulations suggest that one of them is a modulation process. Both BQD and the human brain share the feature of being non-Poisson renewal processes, and their properties are generated by the cooperation of many sub-units. In this chapter a model to explain the emergence of non-Poisson renewal processes from the cooperation of many independent units is discussed. The physical paradigm used in order to attain this scope is the *complex network*.

7.2. Random Networks

Historically, the birth of the graph theory is placed in 1736, in Könisberg, a flowering town of the old Prussia. Not so far from Könisberg in the city of St. Petersburg resided the famous Swiss mathematician L. Euler. Solving a problem that was puzzling the inhabitants of the city of Könisberg, Euler generated graph theory [16]. The city of Könisberg was built partially on an island in the middle of the river Bregel. Seven bridges connected the island to the main land. The puzzling question for the inhabitants of the town was if it were possible to cross all the bridges, without crossing the same twice. A schematic representation of the problem is in Fig. 7.1.

To solve the problem, Euler noticed that the crossing path will have a departure point P, which can be any of the four nodes of the graph. The arrival point, P', will be again one of the four nodes. He also noticed that P must have an odd number of links. One is the departure link, the other links are used to come back and leave again. The same condition applies to P', if $P \neq P'$. An even number of links is used to get to P' and leave it before

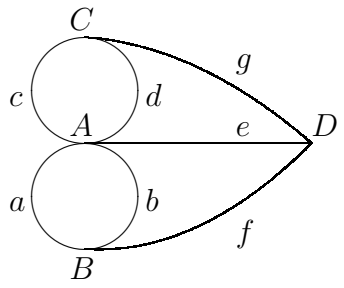

FIGURE 7.1. Schematic conformation of the Könisberg problem. A is the island, B,C, and D indicate the main land (*nodes*), a, b, c, d, e, f, and g the bridges (*links*).

the final arrival. On the contrary, if $P = P'$, then P must have an even number of links.

In the case $P \neq P'$, all the nodes but two must have an even number of links, as the intermediate nodes are used to transit, and this implies the same number of departures and arrivals. For the same reason, in the case of $P = P'$ all the nodes but one must have an even number of links. In Fig. 7.1 we see that A has five links, while B, C, and D have three links. Thus, it is impossible to go through the seven links without crossing the same link twice.

The problem solved by Euler is the first example of graph theory. A graph is a pair of sets $G = \{P, E\}$, where P is a set of N *nodes* or *vertices*, and E is a set of *edges* or *links*, that connect two elements of P. A very important concept of graph theory is the concept of *random graph*, introduced originally by P. Erdös and A. Rényi. A review of the work of Erdös and Rényi can be found in Ref. [2]. In order to generate a random graph, let us adopt the following algorithm: Consider an interval $I = [0, 1]$, and divide the interval into two parts of size $p \ll 1$ and $q = 1 - p$. Let us now take a set of N nodes and choose randomly two of them. Draw a number from I. If the number lies between $1 - p$ and 1 we draw a link between the two nodes. Vice-versa, no link is created.

If p is very small, then it is straightforward to prove that

$$\Psi(t) = \exp(-pt). \tag{152}$$

The probability of not creating any link is

$$\Psi(E_{max}) = \exp(-pE_{max}), \tag{153}$$

where $E_{max} = N(N-1)/2$ is the maximum possible number of links. Thus,

$$p = \frac{1}{E_{max}} \log \frac{1}{\Psi}. \tag{154}$$

In this way it is possible to estimate the value of p corresponding to a graph with no links. Already the value $p = 0.1$ [2] is large enough to violate this condition, and realize links among the nodes.

The random graph theory, even though being an attractive perspective, is linked to ordinary statistical physics. In fact, the Poisson distribution emerges from random graphs. To show this it is enough to point out that the probability for a node to have k links (*degree* k) with the other $N-1$ nodes is described by a Binomial distribution

$$p_k = \binom{N-1}{k} p^k (1-p)^{N-1-k} \tag{155}$$

as can be easily proved by probabilistic considerations. The Poisson distribution is the well known limit of the Binomial distribution for N very large. Therefore, the adoption of random graph theory does not provide the right physical description of the complexity of the process we are studying. This limitation can be overcome by adopting the concept of complex network, introduced in the next section.

7.3. Scale-Free Networks

The picture afforded by the theory of random networks of Erdös and Rényi is not enough to reproduce the characteristics of the complex systems we observe in nature. Its adoption to describe, for instance, the human brain would lead to conclude that it is a Poisson system. This naive assumption would certainly be questionable in many ways, one of those being the results of chapter 6. Thus, a different approach must be used. Let us describe a type of networks, called *complex* or *scale-free* networks, originally introduces by A.-L. Barabasi and R. Albert in the paper of Ref. [18]. On this perspective we shall base our representation of the results of chapters 5 and 6.

The difference between the approach of Erdös and Rényi and the one of Barabasi and Albert lies on the way the network grows. While in the case of random networks a new connection is established in a totally random way, in the case of complex networks a preferential order is chosen. Let us imagine that at $t = 0$ there are m_0 points with no connections. At later times, new connections are established on the nodes, each of them yielding m new links. Of course, $m \leq m_0$. The choice of the new m points is done randomly. However, from the arrival of the first node on, the choice of the new connections is no longer random, but is proportional to the number of links already present in the network. This is the now famous principle of the *rich gets richer*: The nodes with more edges attract even more edges. In this way it is possible to prove [18] that the distribution of edges follows an inverse power law $P(k) \sim 1/k^{\mu}$, with $\mu = 3$. Different values of μ are obtained assuming more complicated features for the growing of the network. However, the important thing to stress here is the difference between complex and random networks as a consequence of the preferential attachment.

7.4. A Model for Blinking Quantum Dots and the Human Brain

Using the idea of Barabasi and Albert, a complex network is built in the following way: Consider N nodes, all-to-all coupled, this meaning that every node has $N - 1$ connections with the other nodes of the network. Imagine that the nodes can be found in two states.

This characteristics makes the nodes compatible with the view of Winfree [97]. According to Winfree, every biological system can be schematically represented through a oscillator, a clock, whose oscillations rule the fundamental biological processes. In our view, the clocks oscillate only between two positions, two phases $\Phi = 0$ and $\Phi = \pi$. The model proposed here is similar to the one proposed by the authors of Ref. [100]. In the case of Ref. [100], three states are accessible to the single unit instead of two. Moreover, the clocks are distributed on a $d-$dimensional lattice, therefore having $2d - 1$ nearest neighborhoods. In the mean field approximation, i.e. the condition $d \to \infty$, a phase transition occurs when the coupling among the clocks increases. This behavior is found to be universal when the dimension of the lattice becomes finite.

Let us focus now to our case. Let us call $|1>$ and $|2>$ the two states available to the clocks. Consider the interval $I = [0, 1]$ and divide it into two parts, I_1 of size $g_{12(21)}$, and I_2 of size $1 - g_{12(21)}$. The size of the interval depends on whether the clock is in the state $|1> (g_{12})$ or $|2> (g_{21})$. For each clock, numbers are uniformly extracted from the interval I. Whether a number is found in I_1 or I_2, a transition occurs.

The all-to-all coupling is established through the following condition for the transition rate

$$g_{12(21)} = g \exp[K(\pi_{2(1)} - \pi_{1(2)})], \tag{156}$$

where K is the coupling constant, g is the unperturbed rate of transition, and π_i is the fraction of the total number of clocks in the state i, that is N_i/N.

In the mean field approximation, that is, when we let $N \to \infty$, the dynamics of the single clock is determined by the following two-states master equation

$$\begin{cases} \frac{d}{dt}P_1 = -g_{12}(t)P_1(t) + g_{21}(t)P_2(t) \\ \frac{d}{dt}P_2 = -g_{21}(t)P_2(t) + g_{12}(t)P_1(t) \end{cases}. \tag{157}$$

where P_1 and P_2 represent the probabilities of finding a clock in the state 1 and 2, respectively.

Let us define the quantity $\Pi(t) = P_1(t) - P_2(t)$. From Eq. (157), with straightforward algebra, and using the normalization condition for the probability, $P_1 + P_2 = 1$, we obtain the following time evolution for $\Pi(t)$

$$\frac{d}{dt}\Pi(t) = -2g\cosh(K\Pi)\Pi + 2g\sinh(K\Pi) = -\frac{\partial}{\partial\Pi}V(\Pi). \tag{158}$$

The problem of Eq. (158) is formally equivalent to the problem of a particle in a potential. The formal solution is an over-damped motion in a double well potential, depicted in Fig. (7.2), for three values of the coupling constant K, and unperturbed rate $g = 0.01$.

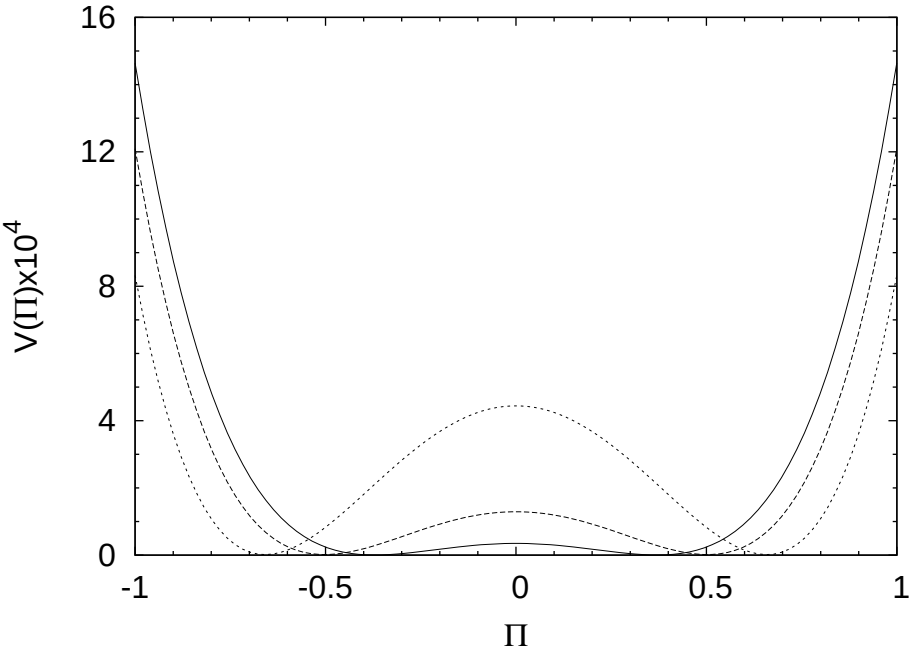

FIGURE 7.2. The shape of the potential $V(\Pi)$ obtained from the integration of Eq. (158), for three values of the coupling K. From the bottom to the top, $K = 1.05$ (full line), $K = 1.1$ (dashed line), and $K = 1.2$ (dotted line). The unperturbed value of the rate is $g = 0.01$.

The potential is symmetric and the value of the minima depends only on the coupling K. Moreover, a critical value for the coupling constant is found

$$K = K_c = 1. \tag{159}$$

Two different behavior are observed depending on K: If $K < K_c$, then only a minimum is observed, in $\Pi = 0$; If, on the contrary, $K > K_c$ two minima are present, and the larger is K, the higher the potential barrier. The barrier is centered in $\Pi = 0$.

As a consequence of the shape of the potential, the time evolution of Π is determined by K. Fig. 7.3 shows Π as a function of K, for $N = 10000$. In particular, if $K < K_c$, $\Pi \simeq 0$, being it slightly positive if the initial condition was positive, and vice-versa. If $K > K_c$, a clear phase transition occurs: $\Pi(t)$ evolves towards an asymptotic value, $\Pi_\infty = \pm 1$, depending on the sign of the initial conditions, when $K \to \infty$. This result indicates that the single clock prefers a state instead on the other, when starting from a given initial condition. This is a consequence of the fact that the transition rates are different when $K > K_c$.

The same result can be viewed through the analysis of a single clock. In Fig. 7.4 the time evolution of two clocks is reported, for $g = 0.01$ and $K = 1.05$: The clock starting from the state $|1>$ (top part of Fig. 7.4) spends on average more time in the same state, while the other clock (bottom part of Fig. 7.4) starts from the state $|2>$, where it spends, on average, most of its time. The WT-PDF for the clocks in the two states is an exponential, with different mean times.

Let us now consider the variable

$$\xi(t) = \frac{\sum_{j=1}^{N} \exp(i\Phi_j(t))}{N} = \frac{N_1(t) - N_2(t)}{N}, \tag{160}$$

where $\Phi_j(t)$ is the phase of the j-th clock at the time t and $N_l(t)$ is the number of clocks in the state l at the time t. The quantity ξ represents a global variable (global clock) of a system of N clocks under the all-to-all coupling condition [100]. If we are in the mean field

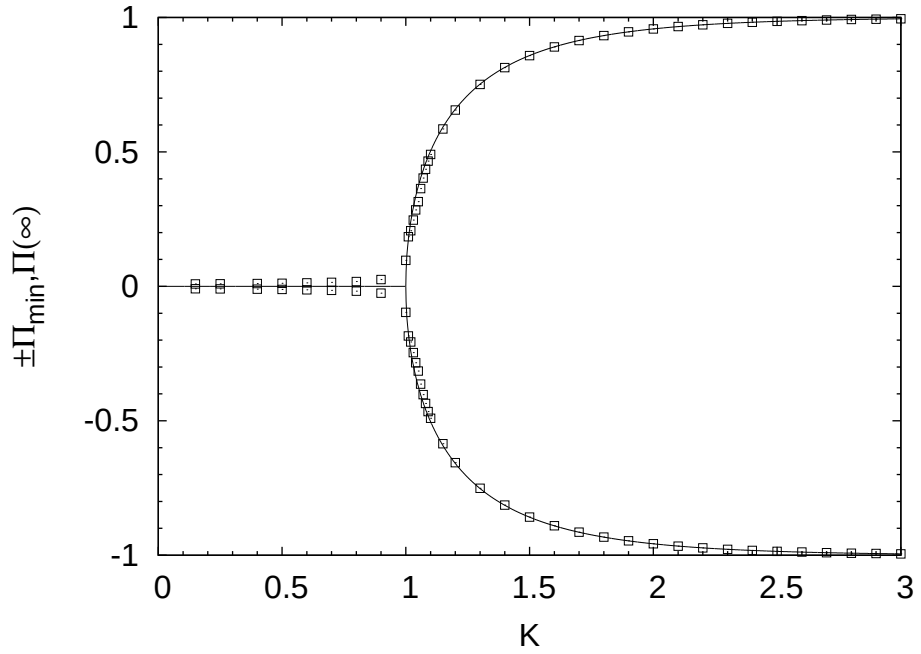

FIGURE 7.3. The evolution of the quantity Π as a function of the coupling K. A clear phase transition occurs at $K = K_c = 1$. The full line is the theoretical prediction obtained solving $\frac{\partial V(\Pi)}{\partial \Pi} = 0$ and $\frac{\partial^2 V(\Pi)}{\partial \Pi^2} > 0$. The squares represent the numerical evaluation of Π for a Gibbs ensemble of a system with $N = 10000$ units.

approximation, the time evolution of ξ coincide with the time evolution of Π, as the two quantities are identical. In fact, by definition of probability

$$P_i = \lim_{N\to\infty} \frac{N_i}{N}, \tag{161}$$

and substituting in Eq. (160), we get $\xi \equiv \Pi$.

Let us now abandon the mean field condition, and let us study the time evolution of the global clock $\xi(t)$. In this case, Eq. (161) does not hold anymore. From the definition of transition rate, we get

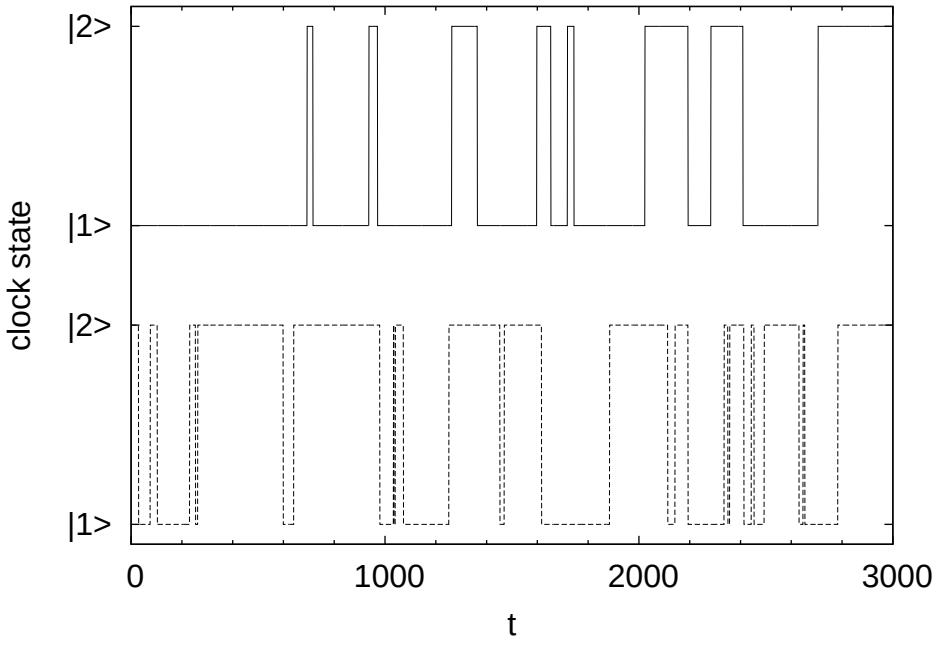

FIGURE 7.4. Time evolution of a clock starting from the state $|1>$ (top part of the figure) and $|2>$ (bottom part of the figure). On average the clocks prefer to stay in the state they started from. $N = 10000$, $g = 0.01$, and $K = 1.05$.

$$\begin{cases} g_{12}P_1 = \lim\limits_{N\to\infty} \dfrac{N_{1\mapsto 2}}{N} \\ g_{21}P_2 = \lim\limits_{N\to\infty} \dfrac{N_{2\mapsto 1}}{N} \end{cases}, \tag{162}$$

where $N_{1\mapsto 2}$ ($N_{2\mapsto 1}$) is the number of clocks that undergo a transition from state $|1>$ ($|2>$) to state $|2>$ ($|1>$) per unit of time, and N is the number of clocks of the system. Using the law of large numbers, we get that, for any N fitting the condition $\infty > N \gg 1$,

$$\begin{cases} \dfrac{N_{1\mapsto 2}}{N} = g_{12}P_1 + \varepsilon_{12}P_1 \\ \dfrac{N_{2\mapsto 1}}{N} = g_{21}P_2 + \varepsilon_{21}P_2 \end{cases}, \tag{163}$$

where ϵ_{12} and ϵ_{21} are fluctuating variables whose intensities are $\propto 1/\sqrt{(}N)$.

From Eqs. (162) and (163), we conclude that the master equation of a system with a

finite number of clocks is equivalent to the master equation of a system with an infinite number of clocks whose transition rates fluctuate, namely

$$\begin{cases} \frac{d}{dt}P_1 = -(g_{12}+\varepsilon_{12})P_1 + (g_{21}+\varepsilon_{21})P_2 \\ \frac{d}{dt}P_2 = -(g_{21}+\varepsilon_{21})P_2 + (g_{12}+\varepsilon_{12})P_1 \end{cases}. \tag{164}$$

If $\infty > N \gg 1$, we can still consider the mean field approximation to be valid. Using the master equation of Eq. (164) and the normalization condition $P_1 + P_2 = 1$, we get for Π the following equation of motion

$$\frac{d\Pi(t)}{dt} = -\frac{\partial V(\Pi)}{\partial \Pi} - \eta(t)\Pi(t) + \theta(t). \tag{165}$$

The presence of the fluctuations $\eta = \epsilon_{12} + \epsilon_{21}$ and $\theta = \epsilon_{12} - \epsilon_{21}$ in Eq. (165) has the effect of triggering transitions from one well to the other of the potential $V(\Pi)$ of Fig. 7.2. Thus, for a system with a finite number of clocks the phase synchronization of is not stable. This intuition is confirmed by the numerical simulation of Fig. 7.5.

Random transitions occur from one state to the other, and the process becomes essentially dichotomous. The time evolution of the variable $\xi(t)$ at the onset of synchronization resembles the time evolution of the fluctuation intensity for blinking quantum dots, see Fig. 5.1. The WT-PDF of ξ changes is the same for both the states, since the potential is symmetric, and follows an inverse power law, with power index $\mu = 1.5$. In the long time regime an exponential cutoff appears.

How to explain the power law fat tail of Fig. 7.6? If he coupling constant K is close to the critical value, the intensity of the potential barrier is small compared to the intensity of the fluctuations. In this case, as discussed by the authors of Ref. [71], an inverse power law PDF emerges, with power index $\mu = 1.5$ for an extended region of times, and this is exactly what happens in Fig. 7.6. In the long time regime, the intensity of the barrier will become much larger than the intensity of the fluctuations, therefore recovering the well known exponential

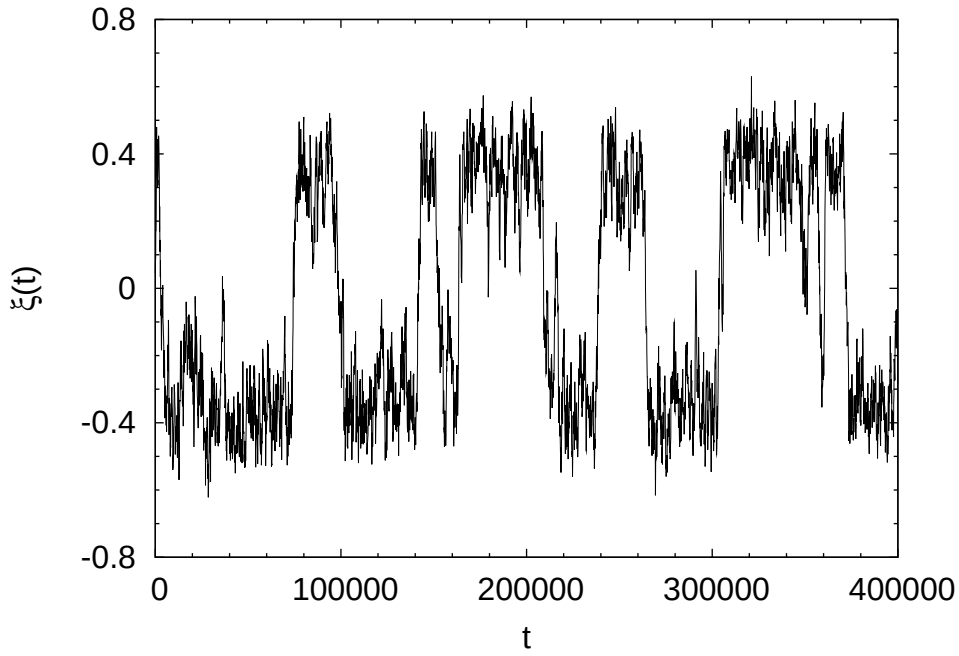

FIGURE 7.5. Time evolution of the global clock ξ. A dichotomous behavior appears at the onset of synchronization. $N = 1000$, $g = 0.01$, and $K = 1.05$.

behavior predicted by the Kramers theory [62].

Let us apply the AE on the time series of state changes of the global clock ξ. The result is plotted in Fig. 7.6, for age $t_a = 500$. Aging is present in the SP, and it is compatible with the predictions of renewal theory, as the curve obtained by the numerical simulation (thick line) almost coincides with the curve predicted by the renewal theory (dashed line). In the asymptotic regime, when the exponential cutoff becomes evident, the aging disappears, compatibly with the theoretical arguments of section 4.2.1.

7.5. Conclusions

In this chapter the important task of finding a model for both BQD and brain activity has been accomplished. The model is based on a complex network of N all-to-all coupled two-states stochastic clocks. In the mean field approximation ($N \to \infty$), when synchronization is established, a phase transition occurs. If the number of units becomes finite, the global

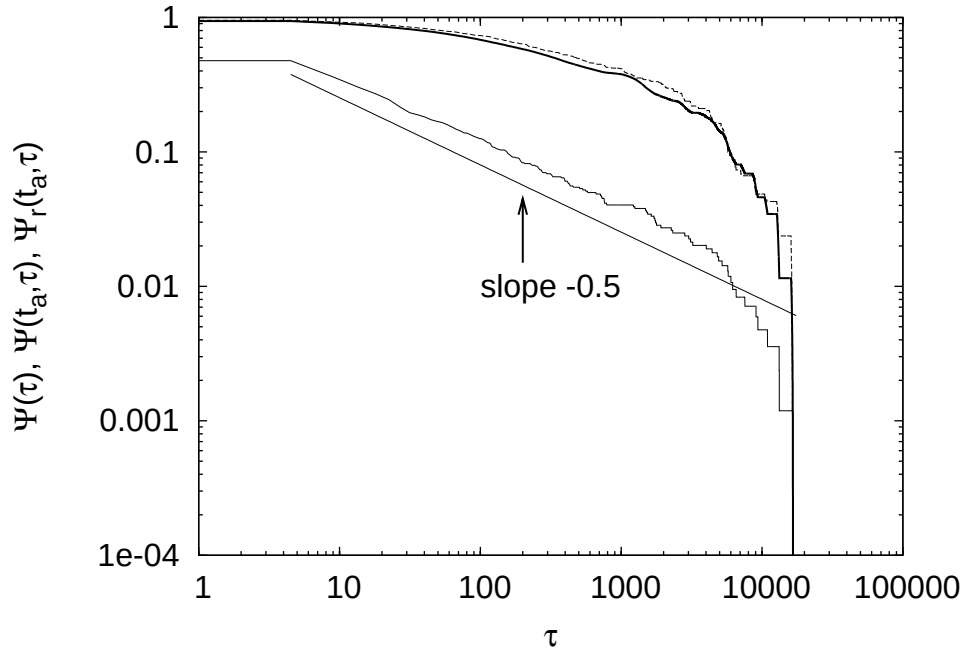

FIGURE 7.6. Result of the AE on the time series of global clock changes. The non-aged SP is the full line, the aged SP is the thick line, while the prediction of renewal theory is the dotted line. Pronounced aging is present, and compatible with the renewal theory. The non-aged curve decays as $1/\tau^{0.5}$.

variable shows random jumps from one state to the other. The WT-PDF decays as an inverse power law, with $\mu = 1.5$. The AE proves that the transitions obey renewal theory. This model can be used to explain the emergence of non-Poisson renewal behavior from the cooperation of many sub-units, at the onset of synchronization. Thus, the model introduced in this chapter can be applied to both BQD and human brain.

CHAPTER 8

FURTHER EXAMPLES

The presence of renewal events is still under investigation in other systems. In this chapter the statistical analysis of time series from two very different physical processes is proposed: The dynamics of financial returns and seismic fluctuations.

8.1. Physics and Finance: Econophysics

While the interest of the physical community in the analysis of seismic fluctuations is old and widespread, the adoption of methods of statistical physics to financial time series is new and just recently became a mainstream subject of investigation. This is mainly due to the consideration that the financial market is not a typical physical system. A very naive definition of a physical system might state that, to be physically meaningful, it should be possible to measure it, with a defined uncertainty. This very general assumption fails when dealing with financial time series, as the indicator, the stock price, is errorless. This difficulty can be overcome by introducing the concept of *volatility*. The definition of volatility depends on the mathematical model involved in the study of the price dynamics. Generally, the volatility is defined as the variance of the price evaluated on a time horizon, e.g. hourly, daily, etc. . The study of volatility is nowadays one of the most important topic of this new science, called *Econophysics*.

In the next section basics concepts about the stock price dynamics will be given.

8.1.1. *A Model for the Stock Price Dynamics*

8.1.1.1. *Basic Concepts: The Efficient Market Hypothesis.* The main feature of the financial market is that it should be a fair game. This means that, in principle, it should be impossible to gain without risking. The risk is also homogenous among the components of

the market, as all the subject involved (*agents*) have the same probability of winning.

From the point of view of the information present in the market, this means that all the agents have the same informations. The presence of private informations, available only to a part of the community playing in the market in that particular moment creates possibilities of gaining without risk. This phenomenon goes under the name of *arbitrage*.

The presence of arbitrage in the market violates one of the cornerstones of financial markets, the *Efficient Market Hypothesis* (EMI). According to this principle, a market is efficient when the following three conditions apply:

- The market reacts instaneously to the immission of new informations, correcting the prices; it is therefore always in equilibrium;
- agents are homogenous in their behavior when new informations are inserted in the market;
- agents are homogeneous in their scopes.

The previous may appear a very abstract definition, but is has a very important practical consequence: Every inhomogeneity in the price is instantaneously corrected. This implies a strict choice for a model describing the stock price dynamics. I introduce in the next section the most common and simplest model for the price dynamics, naturally satisfying the EMH.

8.1.1.2. *Geometric Brownian Motion.* A very simple model for the dynamics of the price in a financial market is the *geometric Brownian motion*. According to this model, the price $P(t)$ follows a random walk with drift, driven by a Wiener process with a given probability of realization. In other words

$$P(t) = P_0 e^{X(t)} \qquad P_0 \equiv P(0) > 0, \tag{166}$$

where

$$X(t) = \sigma B(t) + \mu t \tag{167}$$

is the Browian motion with drift, $B(t)$ is the Wiener process and P_0 is the inital value of the price. If we take the logarithms of both terms of Eq. (166) we get

$$X(t) = \log(P(t)/P_0) = \log(P(t)) - \log(P_0) \rightarrow \log(P(t)) = \log(P_0) + X(t) \tag{168}$$

that implies that $P(t)$ is a lognormal variable, i.e. its logarithmic value is distributed according to a Normal distribution.

Let us consider now for $0 < t_1 < \ldots < t_n = t$, the quantities $L_i \equiv P(t_i)/(P(t_{i-1})$, $0 < i < n$. They are independent random variable, distributed according to a lognormal distribution. This means that the percentual variations of the prices are independent, not the prices themselves. Let us prove this point.

Consider the quantities

$$L_1 \equiv \frac{P_1}{P_0} = e^{X(t_1)} \tag{169}$$

$$L_2 \equiv \frac{P_2}{P_1} = e^{X(t_2)-X(t_1)}. \tag{170}$$

$X(t_1)$ and $(X(t_2) - X(t_1)$ are independent and Gaussian variables. Therefore also L_1 and L_2 are independent and lognormal. Let us now write the quantity

$$P(t) = P_0 L_1 L_2 \ldots L_n. \tag{171}$$

Let us take as time horizon 1 day, and, as a consequence of this, take $t_i = i$. In this way the daily percentual variation is $L_i = P(i)/P(i-1)$. If we evaluate now the product of Eq. (171), we note that L_i are identically distributed, as $t_i - t_{i-1} = i - (i-1) = 1 \quad \forall i$. Thus, $\log(L_i)$ are Gaussian with mean value μ and variance σ^2.

The adoption of this model to describe the price dynamics is justifyied by the basic principles of Economics, as the EMH: Heuristically speaking, according to this model, there is no possibility to gain just by observing the prices time series, as it is impossible to predict

the future value of the price. It must be stressed that the Brownian motion is not the only model for the price dynamics, but it is indeed the simplest.

8.1.2. *Returns and Deviation from the Brownian Motion Model*

The usual indicator in the quantitative analysis of financial time series is the *return*, defined as follows

$$r(t) = \log P(t + \Delta t) - \log P(t). \tag{172}$$

The previous definition is not univocous [70], and it is suitable for high-frequency data, i.e., sampled, on average, every second. According to the Brownian model introduced in the previous section, $r(t)$ is distributed as a Gaussian distribution. This is just approximatively true, as it has been proved that the distribution of returns is strongly leptokurtic [70], with fat tails [69]. It has been suggested that $r(t)$ is distributed according to a symmetric truncated Lévy flight [70]. In Fig. 8.1 the distribution of 1 minute returns for the Italian futures market, called FIB30, is plotted. The dashed curve represents the Gaussian distribution. The difference between the two curves points out in a striking way the approximation that is done when the the Normal hypothesis is made for the returns.

Another way of assessing the validity of the Brownian motion model for the returns is through the evaluation of serial correlations in the time series. This kind of study is relatively new with high-frequency data. Recent papers on the subject [32, 30] quantitatively proved the presence of serial correlations in the time series of returns in several markets. Even though this may represent a deviation from the EMH, economic argument allow to support the validity of this principle in the considered markets, see throughout discussion in [32, 31, 30, 33].

Adopting the AE is a further investigation tool to assess the validity of the general hypothesis in the time series. Before approaching the problem from this point of view, a more general model must be introduced. This will be the argument of the next section.

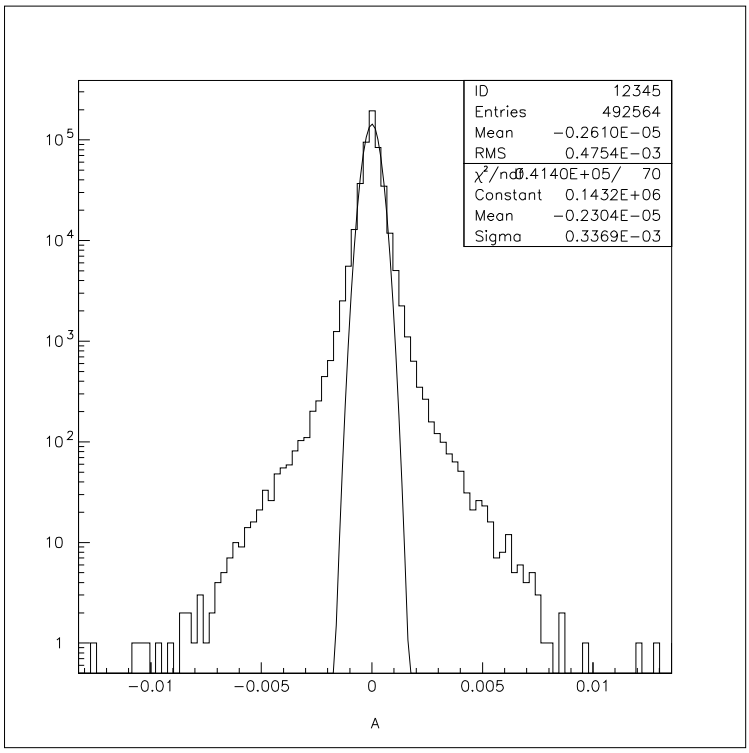

FIGURE 8.1. The Figure shows the distribution of returns for the Italian futures market (full curve), compared to the Gaussian distribution (dashed curve).

8.1.3. *Continuous-Time Random Walk for the Returns*

In a recent publication [88], Scalas and co-workers propose a continuous-time random walk (CTRW) view of the returns. They imagine both the value of the returns and the time at which this value is attained to be random variable. They define an event when the value of the return from positive becomes negative and vice-versa. Adopting the formalism of CTRW [78], they establish the SP of these events and find it to be a Mittag-Leffler function. In a later publication [68], this assumption has been tested analyzing the data from a real financial market and proved to be reliable for the considered data sets. However, the authors of Ref. [80] make the hypothesis that the SP is a stretched exponential, a limiting condition of ML function (see sec. 6.2), supporting their statements with time series analysis from other markets. The interested reader can also consult the review of Ref. [87].

In this section the analysis of the SP of high-frequency returns is performed, keeping in

mind the results of Refs. [68, 80, 88]. Two markets are under study: The Italian futures market, MIB30, and the US futures on the stock index, S&P500. A future is a standardized contract that rules the exchange of a good at a later time after its opening, called *maturity*. The futures belongs to a larger category of contracts, called *derivatives*. The interest in this kind of contracts is mainly due to the fact that the transactions involving derivatived represent almost 90% of the total number of transactions. Thus, they are the best proxy for the market dynamics.

Let us study first the *tick-by-tick* (transaction by transaction) dynamics of the two markets. All the transactions are considered. The sign of the return is not taken into account at this point. The event in this case is just the jump (*transaction*) of the walker (*return*). In Figs. 8.2 and 8.3 the SPs of the two markets are plotted. In the case of the Italian market, the SP (full line) is fitted by a stretched exponential (Eq. (131)), (dashed line) with $\gamma = 0.4$ and $\alpha = 0.49$, confirming the results of Ref. [80]. The inverse power law tail of the ML relaxation function is not present in this case. In the case of US stock index, an inverse power law with power index $\alpha = 2.3$ clearly appears. No stretched exponential decay is present in the first part. The absence of the stretched exponential part is not enough to rule out the possibility that the SP has been generated by a CRTW process. In order to assess this point, on the time series of Figs. 8.2 and 8.3 the AE technique is applied. Figs. 8.4 and 8.5 show the results.

In the case of the Italian futures returns, a clear aging affect emerges in the long time regime. The age considered is $t' = 1000$. The non-aged SP is denoted as Ψ_0, the aged SP by Ψ_{exp}, while the prediction of renewal theory is indicated as Ψ_{ren}. While partially reduced in the first part, the aging of the last part of the curve is compatible with the renewal assumption for the dynamics of the futures. It is worth noticing that the fat tail of the final part of Fig. 8.4 might be a sign of a hidden ML function. By construction, the AE enhances the tails of the SPs. In this case, a possible explanation of this effect might be that the ML tail is present in the data, but masked by low frequency noise, and through the AE it

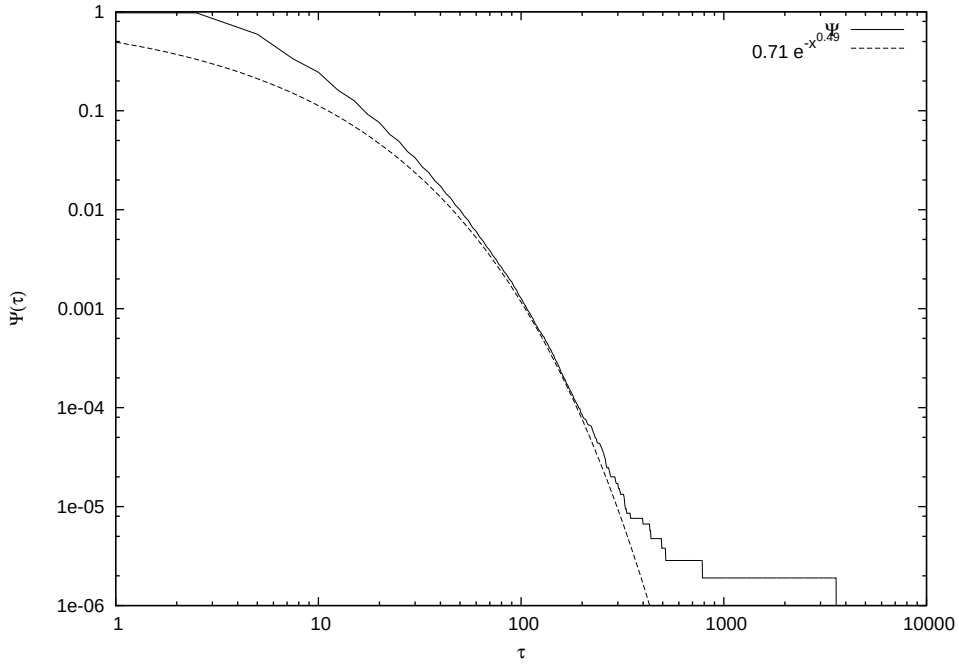

FIGURE 8.2. The SP of the *tick-by-tick* dynamics of the Italian futures market, MIB30 (full line). The curve is fitted by a stretched exponential (dashed line), with parameters $\gamma = 0.4$ and $\alpha = 0.49$.

emerges clearly.

On the contrary, the AE applied on the US futures SP does not produce and significant aging effect (Fig. 8.5). The aging is strongly reduced, therefore implying the failure of the CTRW hypothesis in this case.

How to explain the results of Figs. 8.4 and 8.5 in the framework of economic theories? From the analysis of slow modulation processes, it emerged that aging effects are strongly suppresses when correlations are present in the time series. In the case of financial time series, the presence of market microstructure effects is responsible for the failure of the CTRW hypothesis. Such effects, as the bid-ask spread, are sources of high-frequency serial correlations in the time series, see Ref. [32, 30], but they do not represent real inhomogeneities of the market. They are artifacts due to the presence of high-frequency interactions among agents.

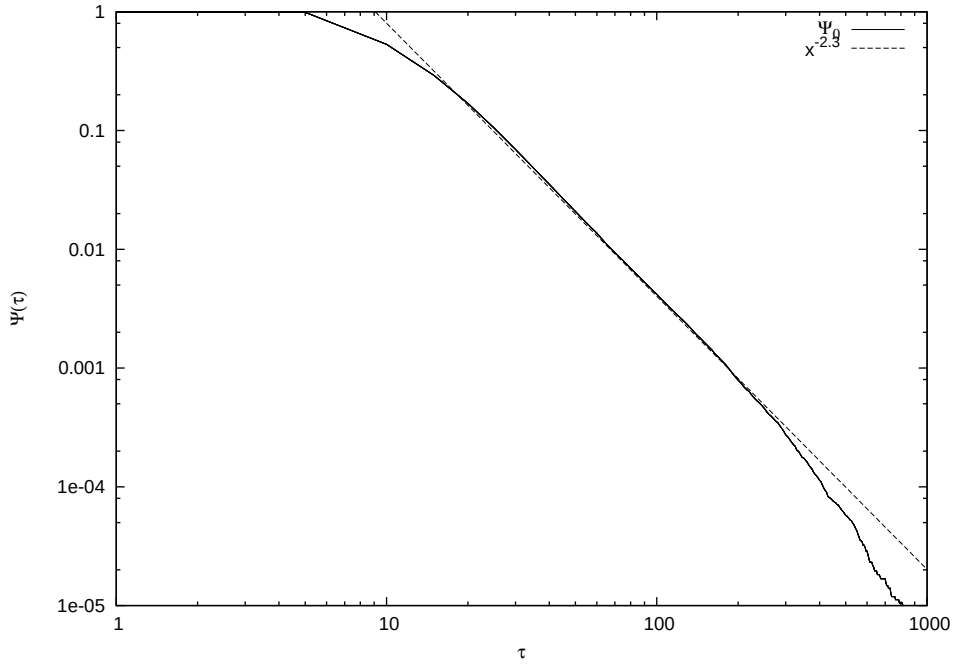

FIGURE 8.3. The SP of the *tick-by-tick* dynamics of the US futures on the stock index, S&P500 (full line). The curve is fitted by an inverse power law (dashed line), with power index $\beta = 2.3$.

Let us now consider a different point of view: Let us take into account the sign of the return, and consider the sign change of the return as an event. Therefore now the waiting time is determined by the distance between two subsequent sign changes. The AE analysis is performed also in this case. The results are sketched in Figs. 8.6 and 8.7.

As in the case of the *tick-by-tick* returns, aging is present in the Italian futures market (Fig. 8.6). Again, the effect is reduced in the first part, thereby suggesting the presence of serial correlations in the high-frequency region. On the contrary, the aging of the last part of the plot seems to be in agreement with the prediction of the renewal theory. An inverse power law tail distinctly appears, this being a sign of a hidden ML function. The age of the system is $t_a = 1000$.

The US futures time series shows no aging effects, for $t_a = 1000$. Again, we may impute this result to the presence of microstructure effects in the time series, and therefore to the presence of unwanted serial correlation patterns.

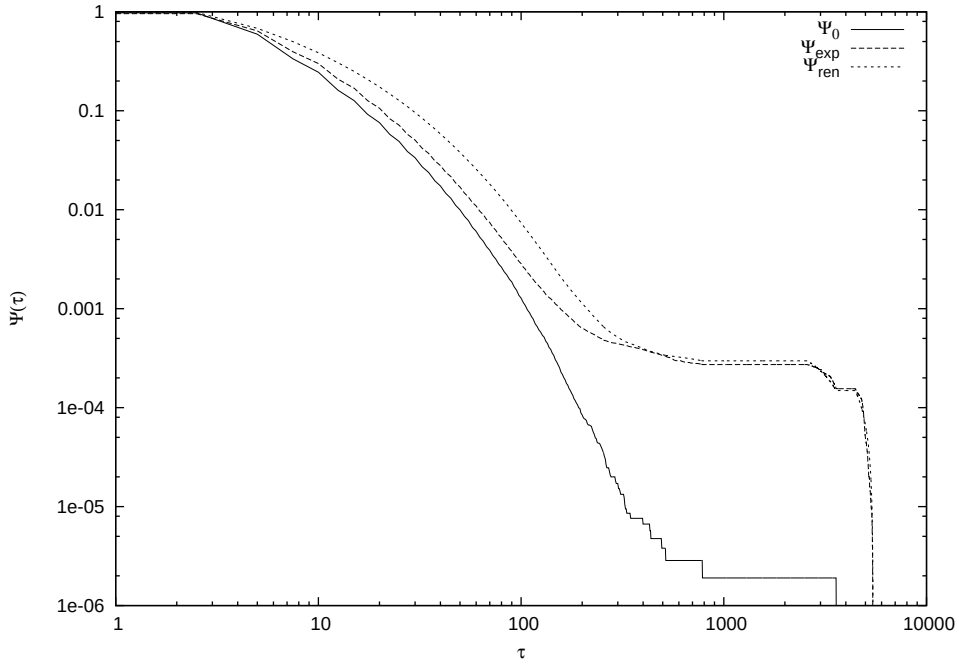

FIGURE 8.4. The result of the AE on the SP of Italian futures on the stock index. Aging is present in the last part of the plot, and compatible with the renewal hypothesis. Reduced aging effect is present in the first part of the plot. $t_a = 1000$.

It is important to stress that, in the case where the sign change of the walker is a fair coin tossing, the asymptotic power of the new time series keeps the same power as the original one, as already proved in section 4.2.2. In this case, the similarities between Figs. 8.2 and 8.6, as well as Figs. 8.3 and 8.7 confirm this aspect, implying the fact that the sign change in the market is a process with no or short correlation, the latter being responsible for the reduced aging condition of the first part of Fig. 8.2, which is, in fact, even less evident in Fig. 8.6.

8.1.4. *Serial Correlation in the Markets*

In the previous subsection we have seen how the presence of serial correlations in the returns time series and sign changes time series do not allow, or only limits, the CTRW assumption for the market. The AE suggests, at least for the Italian market, that the CTRW theory might hold. Memory effects might instead be responsible for the failure of

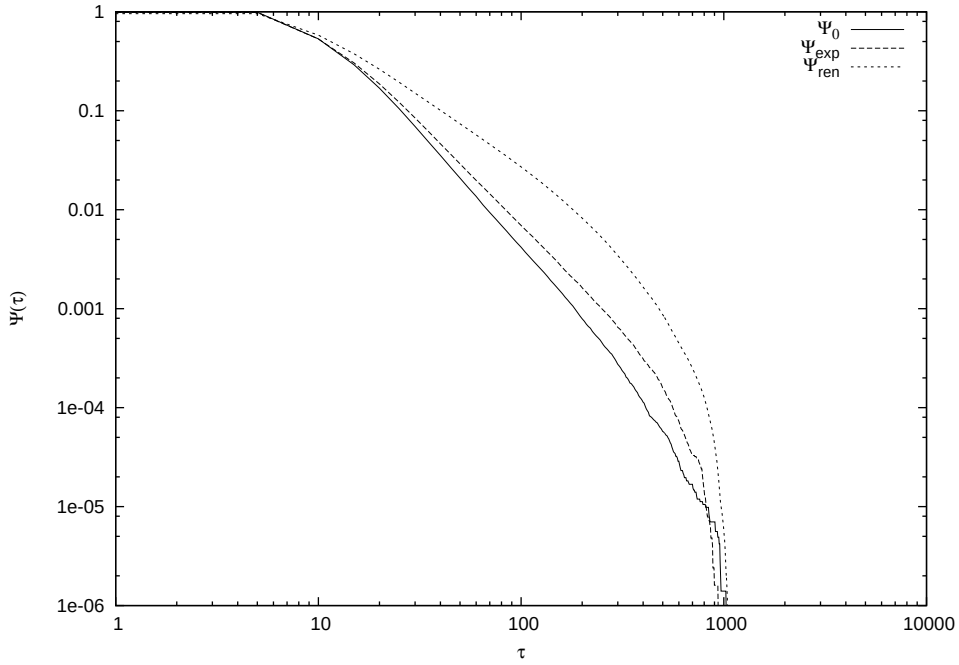

FIGURE 8.5. The result of the AE on the SP of US futures on the stock index. Aging is very reduced and very different from the renewal predictions. $t_a = 1000$.

this hypothesis in the US market. A more significant analysis might require a coarse graining procedure on the raw data. Following Refs. [32, 30], a previous tick interpolation procedure is applied. Let us consider a time window $[0, T]$, with $T = 1$ trading day, that is 495 minutes. We then build a grid of $T/\Delta t + 1$ points, Δt being a grid spacing. At every point the value of the return is defined as the value immediately preceding that point. Notice that different interpolation choices, as linear interpolation, might introduce spurious correlation effects [22]. Particular care should be taken when choosing the spacing Δt: If too large, the statistics might be affected, while a too short interval might not be enough to get rid of the microstructure effects. In order to properly assess this aspect, the integrated variance of the returns time series is plotted in Figs. 8.8 and 8.9. If the process is described by a stochastic differential equation with no drift, then the integrated variance over the time T must be equivalent to its expected value, for any Δt [21].

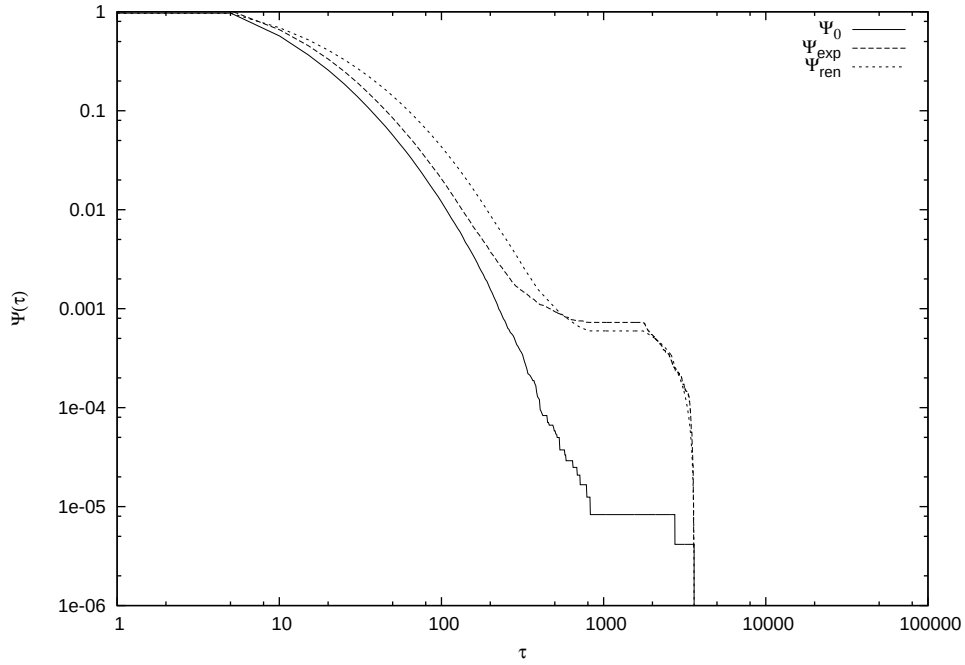

FIGURE 8.6. The AE applied to the sign changes time series, obtained from the Italian futures market. Aging is present, compatible with the prediction of the renewal theory in the tail, while reduced in the first part. $t_a = 1000$.

As we can see from Figs. 8.8 and 8.9, in line with previous remarks, if the spacing decreases, the variance increases. This effect, more evident on the Italian market, is well known and can be imputed to the presence of microstructure effects [82]. We use as spacing values $\Delta t = 60$s and $\Delta t = 240$s for the Italian and US market, respectively. Indeed, the percentage of empty intervals has been computed to be, respectively, of 1% and 3%.

Utilizing the coarse graining procedure should allow us to confirm the impression that the weakening of the aging effect is due to serial correlations in the time series. We repeat that the aging is reduced when correlated events (*pseudo-events*) are present. The coarse graining procedure has the effect of reducing the number of pseudo-events, thereby disclosing the true dynamics of the process.

Figs. 8.10 and 8.11 show the application of the AE on the new time series, obtained after the application of the coarse graining.

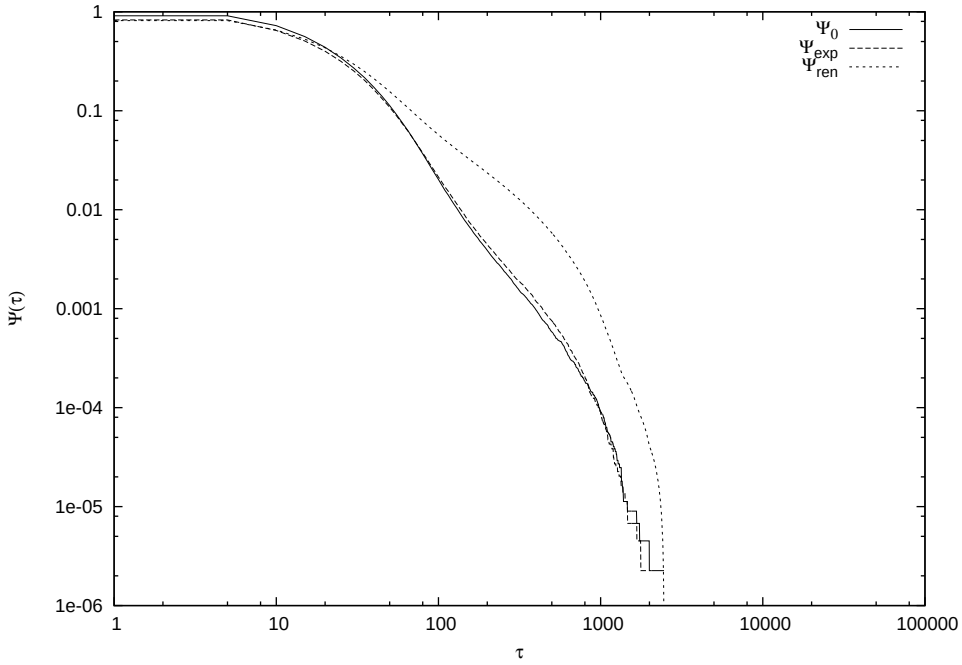

FIGURE 8.7. The AE applied to the sign changes time series, obtained from the US futures on the stock index. No aging is present in this case. $t_a = 1000$.

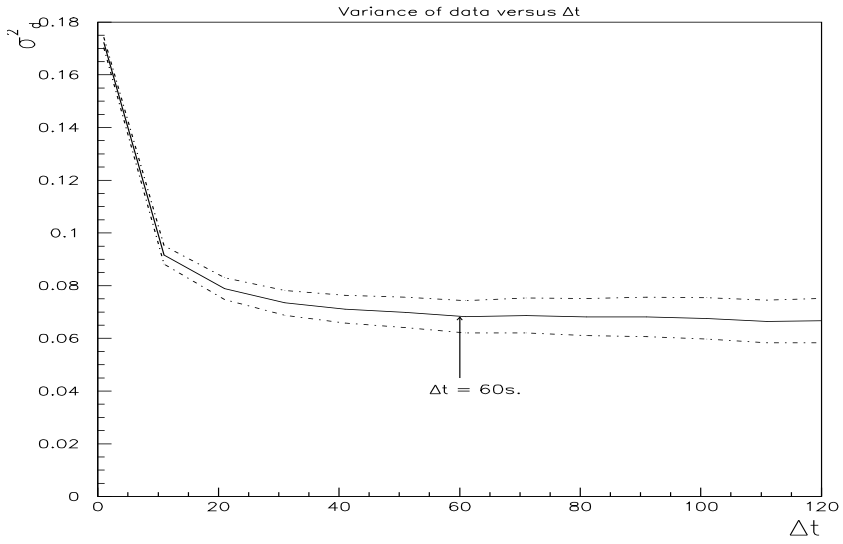

FIGURE 8.8. The integrated variance of the returns time series extracted from the Italian futures market as a function of the spacing Δt.

In both cases, the AE reveals hidden tails, and both seem compatible with the renewal assumption for the dynamics of the returns. It is important to notice that, in the case of Fig. 8.10, the AE makes the tail of a ML function distinctly appear. The ML function is

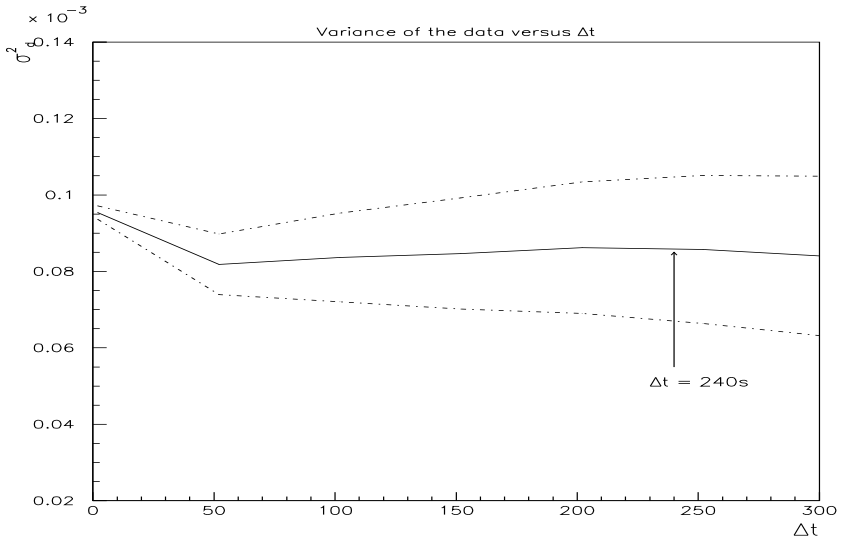

FIGURE 8.9. The integrated variance of the returns time series extracted from the US futures market as a function of the spacing Δt.

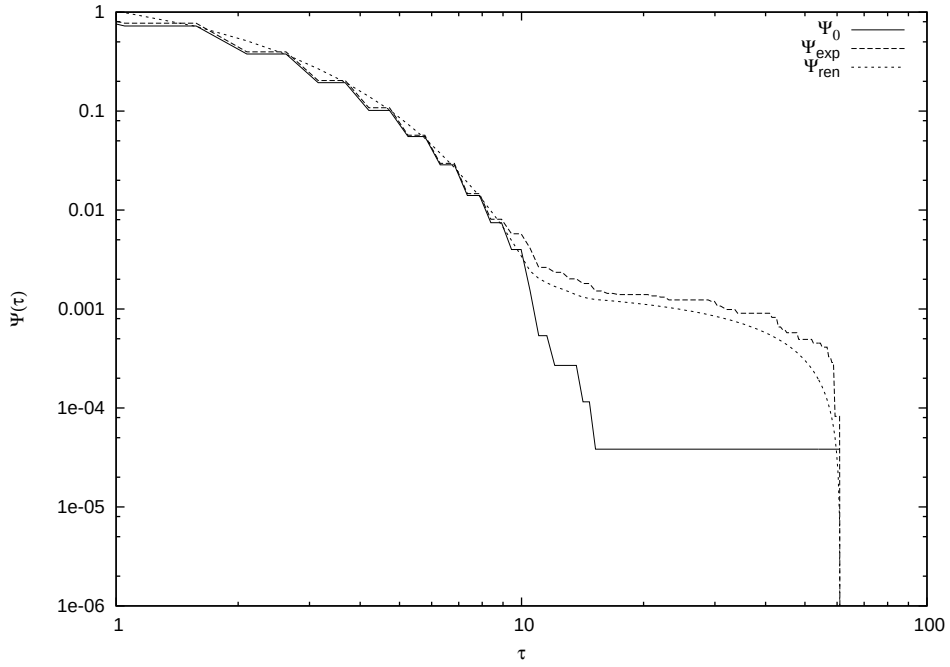

FIGURE 8.10. Result of the AE on the Italian futures returns SP after the coarse graining procedure. Strong aging is present in the tail of the distribution. $t_a = 1000$.

characterized by index $\alpha = 0.95$ and time scale $\gamma = 0.5$. This important result seems to confirm the impression that a ML-type function is a proper representation of the SP for the

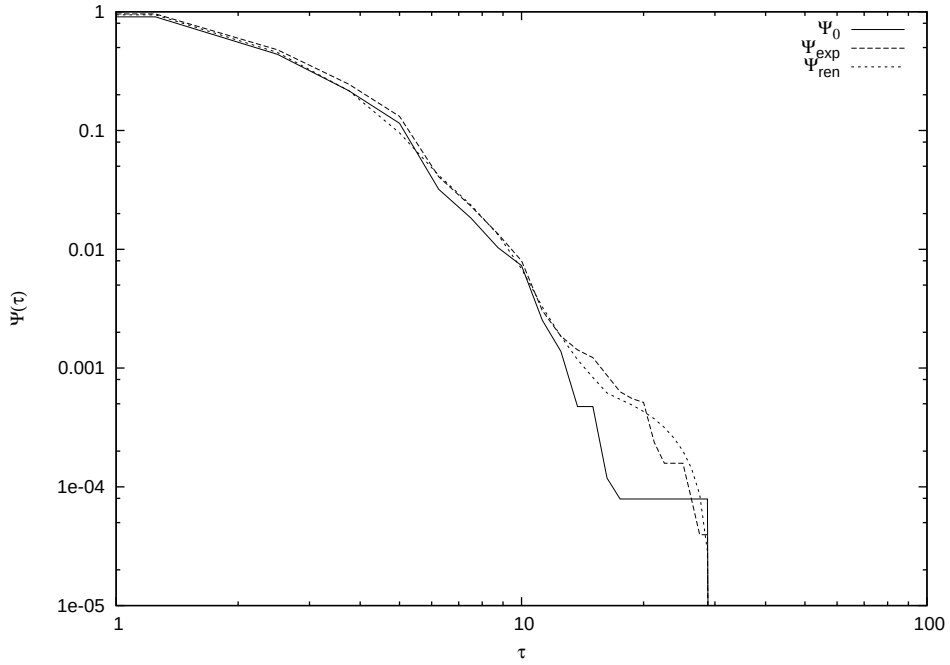

FIGURE 8.11. Result of the AE on the US futures returns SP after the coarse graining procedure. Weak aging effects are present in the tail of the distribution. $t_a = 1000$.

dynamics of high-frequency returns, at least for the Italian market. In the case of the US market, the aging is present only in the tail, but no ML function can be fitted this time. However, it is impossible to rule out completely the theory of Ref. [88] at this time, as the stretched exponential regime might be more extended than in the case of the Italian market. Also, as mentioned in Refs. [32, 30], the coarse graining procedure might be not enough to get totally rid of microstructure phenomena. To solve this problem, might be useful to increase the spacing interval. However, in this case, instead of 1 trading day, a different time horizon should be considered in order to have a sufficient statistics. The AE analysis might be used to settle this problem, as the transition from the non-renewal to the renewal condition is a sign of absence of serial correlations. However, the limited dimension of the data set under study does not allow to solve this problem at this time. Further work is required in this direction.

8.1.5. *Mittag-Leffler Function in the Financial Market*

To conclude this section dedicated to the analysis of financial time series with methods from statistical physics, a link with the model of section 6.2 is drawn.

As explained in section 6.2, a family of ML-type functions of renewal origin can be obtained. A proper subordination procedure is applied to a Poisson process with very large time scale. As a result of that, in particular limiting conditions, either a stretched exponential, an entire ML function, or an inverse power law can be perceived as SP. Thus, the theory of section 6.2 can be used to explain the results of this section. However, the results of the aging experiment are subtly different in the case of the brain and in the case of the financial market. While in the case of the brain, the AE confirms the renewal nature of the stretched exponential obtained from the MST topological changes, while it excludes the presence of power law tails, in this case the opposite holds. The stretched exponential part shows reduced or no aging, suggesting the presence of serial correlations in the short time regime. However, in our opinion, this does not imply that the theory of section 6.2 cannot be applied in this case. But it is our conviction that, while in the case of the brain the emerging tip of the ML function appears, in this case the tail is generated through the process sketched in section 6.2. A different mechanism might be more appropriate to describe the short time stretched exponential of the SP of the Italian futures market. However, the conclusions of the last section must be taken into account, and therefore a more exhaustive analysis should be performed.

We think, however, that the model of section 6.2 can be used as a fair representation of the results of this section, and therefore we can safely confirm the CTRW hypothesis for the Italian futures market.

8.2. Earthquakes Dynamics

The study of seismic fluctuations is a very important topic in the physical community. The number of works about the properties of main shocks and aftershocks has exponentially increased in the last few years. While some aspects are very well assessed and their validity

is accepted by the vast majority of scientists today, other features of earthquakes are still argument of debate. Among the first, we remember the famous Omori's law for aftershocks: The occurrence of a main shock triggers a cascade of aftershocks, whose rate decreases in time as

$$q(t) \sim \frac{1}{t^{\rho}} \tag{173}$$

with $\rho \approx 1$. The value of the parameter ρ depends on the magnitude of the main shock.

An example of the second kind of arguments is indeed the distribution of main shocks. However, detecting crucial events is a rather challenging task, still far from being settled. The authors of a recent paper [74] use the diffusion entropy analysis [85, 56] to investigate the scaling properties of the Southern California seismic fluctuations. The main features of the diffusion entropy technique is its scarce sensitivity to predictable events, such as the Omori's cascade. The result of their analysis suggests that the main shocks WT-PDF decays as an inverse power law, with power index $\mu = 2.06$. The presence of fat tails in the distribution of main shocks does not conflict with the assumption that it is impossible to predict them [53], since the renewal model of Eq. (1) can generate inverse power law distributions, with no correlations whatsoever among the times. However, some of the recent works have questioned this assumption [81, 86, 67], by discussing models, compatible with the observations according to the authors, that assume memory [67] or long range correlation [86] in the main shocks occurence.

Among the most recent works it is worth mentioning Refs. [59, 89, 83], which focus on the distribution of aftershocks, while other investigate the applications of models derived by particular theories, as Self Organized Criticality, to explain the features of the time series [42, 102].

How useful in this case may be adopting the instrument of analysis introduced in this dissertation? The AE technique applied to the seismic fluctuations catalog might detect the presence of crucial events, that are not necessarily events with largest magnitude, that are

responsible for the results of Ref. [74] and, at the same time, can be of renewal origin. Thus, the AE may become a way of settling this long-lasting struggle.

Let us consider the time series of seismic fluctuations in Southern California. The collected data are publicly available, and cover the period from 1930 to the present day. However, before January, 1st 1982 the database is strongly incomplete, due to the approximation of the recording instruments. The statistical analysis will be therefore limited to the period where seismic data were collected through computer.

Let us apply the AE on the time series of all the sesmic fluctuations. Let us consider no magnitude threshold, that is, let us analyze the data set in its entirity. The results are reported in Fig. 8.12, for $t_a = 30000$. Pronounced aging effects are present in the last part of the plot. An inverse power law tail seems to appear in this part of the plot, and the aged curve, indicated as Ψ_{exp} seems to decay accordingly to the renewal prediction, denoted as Ψ_{ren}. Very small aging appears instead in the first part of the plot. The decay of the tail of the WT-PDF is compatible with an inverse power law, with power index $\mu = 2.06$. The aging experiment correctly detects a slower decay, namely $\mu_{aged} = 1.06$. This effect is reported in Fig. 8.12, taking into account that the SP is plotted instead of the WT-PDF.

Note that the first part of the SP does not age. This observation implies the presence of pseudo-events in the time series. Taking into account the deterministic Omori decay should explain the absence of aging effects. However, the Omori cascade is not enough to generate the aging of the last part of the plot. Another effect should be consider in oder to correctly explain, and therefore reproduce, the result of Fig. 8.12. We shall see in the next section a model that may be used to describe the results of the AE analysis.

8.2.1. *A Model for Earthquakes*

In the last few years a large number of models have been proposed for seismic fluctuations. However, apart from the model proposed in Ref. [74], no paper in the recent literature discusses the renewal nature of the main shocks. Also, the application of the AE can be useful to infer important information about the short time regime, as it was for the financial time

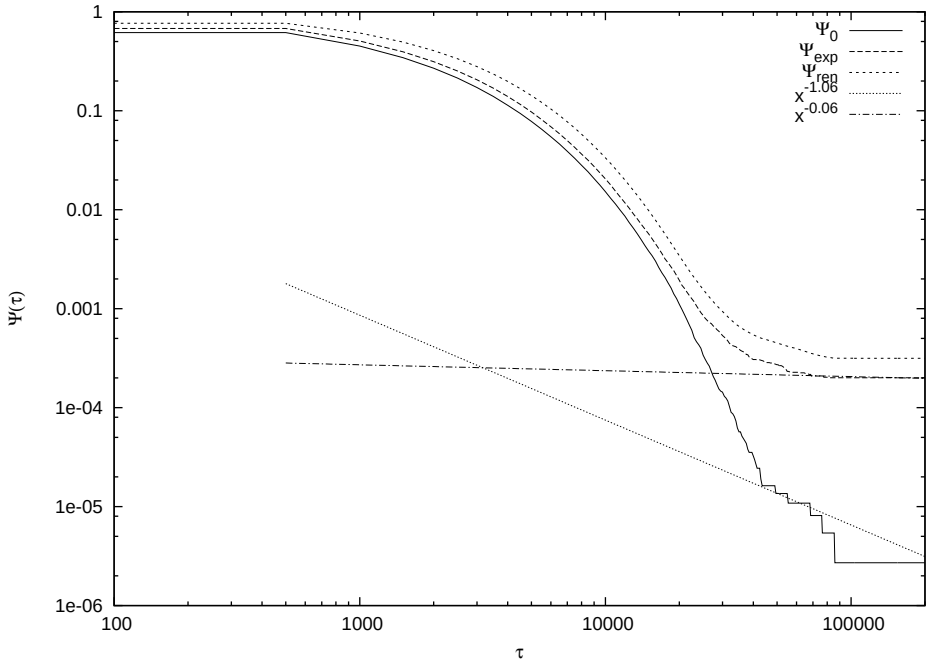

FIGURE 8.12. AE on the time series of all the seismic fluctuations in Southern California. Aging is present in the last part of the plot, where an inverse power law tail seems to appear. $t_a = 30000$.

series. This regime is well known to be dominated by the Omori's law, whose quantitative law is expressed by Eq. (173).

In a recent paper [89] the Omori's law is modeled through a non-homogeneous Poisson process. The form of the rate is

$$q(t) = \frac{q_0}{(1 + q_1 t)^p} \tag{174}$$

with $p = 1.2$. No hypothesis has been made on the main shocks. In the paper of Ref. [74] the distribution of main shocks is estimated to be an inverse power law of the form of Eq. (14), with $\mu = 2.06$. This conclusion has been reached by the authors by indirect measure of the scaling coeffcient through the diffusion entropy analysis.

Let us imagine the following situation: Consider the NHPP of Eq. (174). This process is supposed to mimic the Omori cascade. Let us extract a waiting time from the distribution of Eq. (14), τ_{ms}. This WT is considered to be a time distance between two subsequent main shocks. The parameter T is assumed to be very large, in order to have very large waiting times. The algorithmic procedure I am going to use is the following: Imagine to have a main shock at time $t = 0$; at this time the Omori cascade begins, according to Eq. (174). The Omori cascade stops when the absolute time becomes larger than τ_{ms}, where a new main shock occurs. At that moment, before creating a new cascade, a quiescent period T_w is considered. T_w is chosen to be much larger than the average after-shock inter-occurrence time. In this region no after-shocks occur. After this period, a new cascade begins, and another waiting time is extracted from the Nutting law to mimic a main shock. The adoption of the quiescent region T_w has the effect of truncating the Omori cascade. This effect is visible in the data, as the Omori cascade can exhaust itself, and a very long time passes before a new shock.

Numerical simulations are performed according to the previous procedure. The parameters are $q_0 = 0.1$, $q_1 = 1.16 \cdot 10^{-5}$, obtained from Ref. [89], $\mu = 2.06$ from Ref. [74], the time scale of Eq. (14) is $T = 10^5$, and the quiescent region is long $T_w = 10^6$. All the times and time scales are expressed in seconds. Also, another constraint is considered: It is impossible to have waiting times for the main shocks smaller than a give T^*. This assumption is justified by the fact that it is very unlikely to have two main shocks separated by a small waiting time. The result of the simulation is plotted in Fig. 8.13.

The SP obtained by the simulation, indicated in Fig. 8.13 as Ψ_0, is quite similar, apart from a scale factor, to the result of the analysis of real seismic fluctuations. There is a slow decay, compatible with the Omori's law, while in the tail an inverse power law seems to appear. Applying the AE techinque has the effect of enhancing the tail of the distribution, thereby forcing the inverse power law tail to emerge from the noise. Eventually, as in the real data, the distribution becomes flat, and this is a sign that only a few events appear at

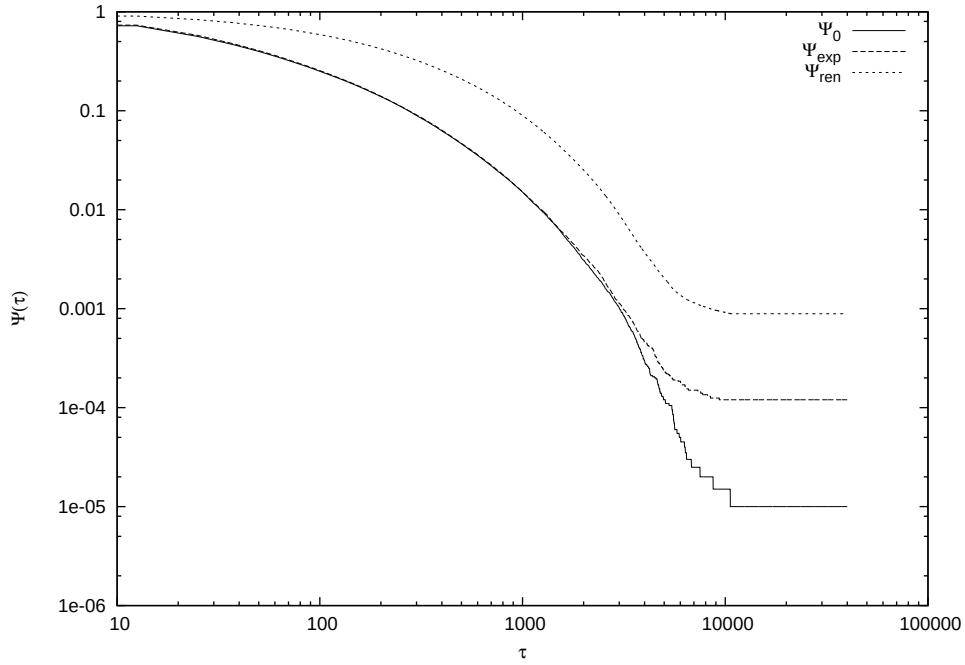

FIGURE 8.13. The results of the AE on the simulated time series for seismic fluctuations. The first part of the plot shows no aging, as Ψ_{exp} coincides with the non-aged SP, Ψ_0. A pronounced aging effect is present in the tail of the distribution. $t_a = 30000$.

very large waiting times. Also this behavior is present in the real data.

Moreover, the aged curve, indicated as Ψ_{exp} does not age in the first part, this being a consequence of the NHPP used to reproduce the Omori cascade. The prediction of renewal theory, through the SP Ψ_{ren}, implies a departure from the renewal picture in the first part, as expected, while there is aging in the tail. The difference in the decay of the tail for the aged curves is larger than the one observed in the real data. At the level of preliminary results, this difference is not very important. Some work is still needed to confirm the intuitions that this model affords. However, the comparison of the results of Figs. 8.12 and 8.13 is a good indication that this is the right direction. Particularly, this model would highly benefit from the application of the diffusion entropy technique on the simulated data, in order to prove that the resulting scaling is compatible with the results of Ref. [74].

8.3. Conclusions

In this chapter I have described some preliminary results of the analysis introduced in this dissertation on financial returns and seismic fluctuations time series. In the former case, the adoption of the AE has allowed to partially confirm the CTRW picture proposed by recent literature, even if this result is limited to only one of the considered markets. Moreover, the aging analysis supports the hypothesis that the financial returns SP is a Mittag-Leffler function.

In the case of seismic fluctuation, using the AE I have suggested that the conjecture made by the authors of Ref. [74] about the inverse power law distribution of large earthquakes may be correct. A numerical simulation involving this conjecture and the use of a NHPP to mimic the Omori's law shows a striking similarity with the real data. Moreover, the qualitative comparison of the aging effects of both simulated and real time series suggests that the model effectively reproduce the properties of seismic fluctuations. However more work is still necessary following the directions indicated in this chapter.

CHAPTER 9

CONCLUSIONS

In this dissertation the emergence of non-Poisson renewal processes has been investigated. Starting from simple models, I have described the basic features of these class of processes. I have used a property of non-Poisson renewal system, namely renewal aging, to build a technique of time series analysis. This techinique has been used to prove if a system obeys renewal theory. Particularly, I have proved how a different physical class of processes, called modulation, can generate a distribution density of waiting times identical to the outcome of a simple non-Poisson renewal process. The application of the aging experiment leads to different conclusions for the two processes: While renewal processes show aging, modulation processes do not, provide that the modulation is slow. To this purpose, the importance of the number of events extracted from the same Poisson distribution, called pseudo-events, has been acknowledged. The numerical technique allows also to estimate the number of pseudo-events present in the time series.

After posing the theoretical basis, I have investigated several physical systems. Blinking quantum dots are an example of systems following non-Poisson renewal theory, as proved by the application of the aging experiment. The analysis of (simulated) fluorescence data from the spectroscopy of a single lipase molecule suggests instead a physical mechanism compatible with the theory of modulation. I discussed in this case a non-homogenous Poisson process, determined by a quasi-periodic and quasi-deterministic evolution of a time dependent rate. The results of the aging analysis are compatible with the outlined theoretical framework.

The human brain is probably the most complex system anybody can think of. The analysis of the electric potential of the brain has been argument of an important section of this dissertation. Introducing a suitable method of data analysis, based on the minimal spanning tree, I have been able to produce a time series, whose properties I have investigated with

the help of the aging experiment. The resutls show that the human brain is a non-Poisson renewal system living in the non-ergodic regime. Similar results have been obtained by the data analysis of complex sound signal. This important feature can be interpreted in the framework of a new approach to synchronization, called complexity matching. Through complexity matching the challenging issue of explaining the influence of music on the brain can be clarified.

At the light of these results, I have proposed a model for blinking quantun dots and the human brain, through a complex network of interacting sub-units. The main features of blinking quantum dots and human brain are recovered when synchronization is established, this implying that the signal analyzed from both systems is the result of the cooperation of many sub-units, strongly interacting among themselves.

Finally, I have shown preliminary results about financial time series and seismic fluctuations. While the former are an example of renewal system, thereby confirming the theoretical prescription of the recent literature, the nature of the latter is a mix between non-homogeneous Poisson process, responsible for the Omori cascade, and the non-Poisson renewal process, invoked for the main shocks. The time series analysis suggests this interpretation to be correct.

This dissertation represents, at the best of my knowledge, the first attempt at discussing an encompassing model for Complexity: The emergence of non-Poisson renewal processes is linked indissolubly to Complexity. Moreover, the theory of complexity matching is an important consequence of this results. The importance of renewal events in a proper model for Complexity is stressed throughout this work. I hope this dissertation will trigger new lines of research in this important field of theoretical Physics.

BIBLIOGRAPHY

[1] G. Adam and J. H. Gibbs, J. Chem. Phys. 43 (1965), 139.

[2] R. Albert and A.-L. Barabasi, Rev. Mod. Phys. 74 (2002), 47.

[3] P. Allegrini, G. Aquino, P. Grigolini, L. Palatella, and A. Rosa, Phys. Rev. E 68 (2003), 056123.

[4] P. Allegrini, G. Aquino, P. Grigolini, L. Palatella, A. Rosa, and B. J. West, Phys. Rev. E 71 (2005), 066109.

[5] P. Allegrini, G. Ascolani, M. Bologna, and P. Grigolini, submitted to Phys. Rev. E; http://arxiv.org/abs/cond-mat/0602281 .

[6] P. Allegrini, F. Barbi, P. Grigolini, and P. Paradisi, Phys. Rev. E 73 (2006), 046136.

[7] P. Allegrini, M. Bologna, P. Grigolini, and M. Lukovic, submitted to Phys. Rev. Lett.; http://arxiv.org/abs/cond-mat/0608341.

[8] P. Allegrini, M. Bologna, P. Grigolini, and B. J. West, submitted to Phys. Rev. Lett.; http://arxiv.org/abs/cond-mat/0612303.

[9] P. Allegrini, P. Grigolini, and A. Rocco, Phys. Lett. A 233 (1997), 309.

[10] P. E. Andrade and J. Bhattcharya, J. of the Royal Soc. of Medicine 96 (2003), 284.

[11] G. Aquino, M. Bologna, P. Grigolini, and B. J. West, Phys. Rev. E 70 (2004), 036105.

[12] R. Baddeley, L. F. Abbott, M. C. A. Booth, F. Sengpiel, T. Freeman, E. A. Wakeman, and E. T. Rolls, vol. 264, Biological Sciences, no. 1389, Royal Society of London, 1997.

[13] M. Baiesi, M. Paczuski, and A. L. Stella, Phys. Rev. Lett. 96 (2006), 051103.

[14] P. Bak, C. Tang, and K. Wiesenfeld, Phys. Rev. Lett. 59 (1987), 381.

[15] G. Baldini, F. Cannone, and G. Chirico, Science 309 (2005), 1096.

[16] A.-L. Barabasi, *Linked: The new science of networks*, Perseus Publishing, 2002.

[17] A.-L Barabasi, Physics Today (July 2001), 33.

[18] A.-L. Barabasi and R. Albert, Science 286 (1999), 509.

[19] F. Barbi, M. Bologna, and P. Grigolini, Phys. Rev. Lett. 95 (2005), 220601.

[20] E. Barkai, Phys. Rev. Lett. 90 (2003), 104101.

[21] O. E. Barndorff-Nielsen and N. Shephard, J. Roy. Stat. Soc. Ser. B 64 (2002), 253.

[22] E. Barucci and R. Renò, Econ. Lett. 74 (2002), 371.

[23] C. Beck, Phys. Rev. Lett. 87 (2001), 180601.

[24] C. Beck and E. G. D. Cohen, Physica A 322 (2003), 267.

[25] J. Bhattcharya and H. Petsche, Phys. Rev. E 64 (2001), 012902.

[26] S. Bianco, E. Geneston, P. Grigolini, and M. Ignaccolo, submitted to Phys. Rev. Lett.; http://arxiv.org/abs/cond-mat/0611035.

[27] S. Bianco and P. Grigolini, forthcoming in Chaos, Solitons and Fractals.

[28] S. Bianco, P. Grigolini, and P. Paradisi, J. Chem. Phys. 123 (2005), 174704.

[29] ———, forthcoming in Chem. Phys. Lett. . (2007).

[30] S. Bianco and R. Renò, submitted to Quant. Fin.; http://arxiv.org/abs/physics/0610023.

[31] ———, Noise and Fluctuations in Econophysics and Finance (D. Abbott, J.-P. Bouchaud, X. Gabaix, and J. L. McCauley, eds.), vol. 5848, SPIE, 2005, p. 318.

[32] ———, J. Fut. Mark. 26 (2006), 61.

[33] ———, forthcoming, Proceedings of SPIE, 2007.

[34] M. Bologna, P. Grigolini, and B. J. West, Chem. Phys. 284 (2002), 115.

[35] J. P. Bouchaud, J. Phys. I France 2 (1992), 1705.

[36] X. Brokmann, J. P. Hermier, G. Messin, P. Desbiolles, J.-P. Bouchaud, and M. Dahan, Phys. Rev. Lett. 90 (2003), 120601.

[37] M. Buiatti, D. Papo, P.-M. Baudonniére, and C. van Vreeswijk, forthcoming in Neuroscience (2007).

[38] I. Chung and M. G. Bawendi, Phys. Rev. B 70 (2004), 165304.

[39] E. G. D. Cohen, Physica D 193 (2004), 35.

[40] T. H. Cormen, C. E. Leiserson, R. L. Rivest, and C. Stein, *Introduction to algorithms*, 2nd ed., MIT press and McGraw-Hill, 2001.

[41] D. R. Cox, *Renewal theory*, Chapman and Hall, London, 1962.

[42] J. Davidsen and M. Paczuski, Phys. Rev. Lett. 94 (2005), 048501.

[43] J.-L. Déjardin and J. Jadzyn, J. Chem. Phys. 123 (2005), 174502.

[44] L. Devroye, *Non-uniform random variate generation*, Springer-Verlag, 1986.

[45] A. L. Efros and M. Rosen, Phys. Rev. Lett. 78 (1997), 1110.

[46] M. W. Evans, P. Grigolini, and G. Pastori Parravicini (eds.), Adv. Chem. Phys., vol. 62, Wiley & Sons, 1985.

[47] R. Failla, P. Grigolini, M. Ignaccolo, and A. Schwettmann, Phys. Rev. E 70 (2004), 010101(R).

[48] W. Feller, *An introduction to probability theory and its applications*, vol. 2, Wiley & Sons, 1966.

[49] O. Flomenbom, J. Hofkens, K. Velonia, F. C. de Schyver, A. E. Rowan, R. J. M. Nolte, J. Klafter, and R. J. Silbey, Chem. Phys. Lett. 432 (2006), 371.

[50] O. Flomenbom, K. Velonia, D. Loos, S. Masuo, M. Cotlet, Y. Engelborghs, J. Hofkens, A. E. Rowan, R. J. M. Nolte, M. van der Auweraer, F. C. de Schyver, and J. Klafter, Proc. Nat. Acad. Sci. 102 (2005), 2368.

[51] L. Gammaitoni, P. Hänggi, P. Jung, and F. Marchesoni, Rev. Mod. Phys. 70 (1998), 223.

[52] M. Gell-Mann and C. Tsallis (eds.), *Nonextensive entropy: Interdisciplinary applications*, Oxford University Press, 2004.

[53] R. J. *et al* Geller, Science 275 (1997), 1616.

[54] G. Godréche and J. M. Luck, J. Stat. Phys. 104 (2001), 489.

[55] P. Grigolini, vol. 133, Adv. Chem. Phys., no. A, ch. 5, Wiley & Sons, 2006.

[56] P. Grigolini, L. Palatella, and G. Raffaelli, Fractals 9 (2001), 439.

[57] H. Haken, Journal of Psychophysiology 60 (2006), 110.

[58] U. Harder and M. Paczuski, Physica A 361 (2006), 329.

[59] A. Helmstetter, Phys. Rev. Lett. 91 (2003), 058501.

[60] K. M. Hong and J. Noolandi, J. Chem. Phys. 78 (1978), 5163.

[61] V. M. Kenkre, E. W. Montroll, and M. F. Shlesinger, J. Stat. Phys. 9 (1973), 45.

[62] H. A. Kramers, Physica 7 (1940), 284.

[63] J. B. Kruskal, Proc. Am. Math. Soc. 7 (1956), 48.

[64] M. Kuno, D. P. Fromm, H. F. Hamann, A. Gallagher, and D. J. Nesbitt, J. Chem. Phys. 112 (2000), 3117.

[65] ———, J. Chem. Phys. 115 (2001), 1028.

[66] M. Kuno, D. P. Fromm, H. F. Hamann, A. Gallagher, D. J. Nesbitt, O. J. Micic, and A. J. Nozik, Nano Letters 1 (2001), 557.

[67] V. N. Levina, S. Havlin, and A. Bunde, Phys. Rev. Lett. 95 (2005), 208501.

[68] F. Mainardi, M. Raberto, R. Gorenflo, and E. Scalas, Physica A 287 (2000), 468.

[69] R. N. Mantegna and H. E. Stanley, Phys. Rev. Lett. 73 (1994), 2946.

[70] R. N. Mantegna and H. E. Stanley, *An introduction to econophysics: Correlation and complexity in finance*, Cambridge University Press, 2000.

[71] G. Margolin and E. Barkai, Phys. Rev. E 72 (2005), 025101(R).

[72] G. Margolin, V. Protasenko, M. Kuno, and E. Barkai, *Power law blinking quantum dots: Stochastic and physical models*, vol. 133, Adv. Chem. Phys., no. A, ch. 4, Wiley & Sons, 2006.

[73] M. McDonald, O. Suleman, S. Williams, S. Howison, and N. F. Johnson, Phys. Rev. E 72 (2005), 046106.

[74] M. S. Mega, P. Allegrini, P. Grigolini, V. Latora, L. Palatella, A. Rapisarda, and S. Vinciguerra, Phys. Rev. Lett. 90 (2003), 188501.

[75] G. Messin, J. P. Hermier, E. Giacobino, P. Desbiolles, and M. Dahan, Optics Letters 26 (2001), 1891.

[76] G. M. Mittag-Leffler, C. R. Acad. Sci. Paris 137 (1903), 554.

[77] A. Molski, Chem. Phys. Lett. 428 (2006), 196.

[78] E. W. Montroll and G. E. Weiss, J. Math. Phys. 6 (1965), 167.

[79] M. Pelton, D. G. Grier, and P. Guyot-Sionnest, Appl. Phys. Lett. 85 (2004), 819.

[80] M. Raberto, E. Scalas, and F. Mainardi, Physica A 314 (2002), 749.

[81] O. Ramos, E. Altshuler, and K. J. Måløy, Phys. Rev. Lett. 96 (2006), 098501.

[82] R. Roll, J. of Finance 39 (1984), 1127.

[83] A. Saichev and D. Sornette, Phys. Rev. Lett. 97 (2006), 078501.

[84] H. Sano and M. Tachiya, J. Chem. Phys. 71 (1979), 1276.

[85] N. Scafetta, P. Hamilton, and P. Grigolini, Fractals 9 (2001), 193.

[86] N. Scafetta and B. J. West, Phys. Rev. Lett. 92 (2004), 138501.

[87] E. Scalas, Physica A 362 (2006), 225.

[88] E. Scalas, R. Gorenflo, and F. Mainardi, Physica A 284 (2000), 376.

[89] R. Shcherbakov, G. Yakovlev, D. L. Turcotte, and J. B. Rundle, Phys. Rev. Lett. 95 (2005), 218501.

[90] F. H. Stillinger and T. A. Weber, Phys. Rev. A 25 (1982), 978.

[91] C. Tsallis, J. Stat. Phys. 52 (1988), 479.

[92] C. van Vreeswijk, Neurocomputing 38 (2001), 417.

[93] R. Verberk, A. M. van Oijen, and M. Orrit, Phys. Rev. B 66 (2002), 233202.

[94] B. Vogelstein, D. Lane, and A. J. Levine, Nature 408 (2000), 307.

[95] B. West, M. Bologna, and P. Grigolini, *Physics of fractal operators*, Institute for Nonlinear Science, Springer, 2002.

[96] B. J. West, *Where medicine west wrong: Rediscovery the path to complexity*, Studies of Nonlinear Phenomena in Life Science, vol. 11, World Scientific Publishing Company, 2006.

[97] A. Winfree, *The geometry of biological time*, Springer-Verlag, New York, 2001.

[98] P. Winsor, *Automated music composition*, University of North Texas Press, Denton, Tx, 1992.

[99] ———, Chaos, Solitons and Fractals 20 (2004), 45.

[100] K. Wood, C. Van der Broeck, R. Kawai, and K. Lindenberg, Phys. Rev. Lett. 96 (2006), 145701.

[101] I. Xenakis, *Formalized music: Thought and mathematics in composition*, Pendragon Press, Stuyvesant, NY, 1992.

[102] X. Yan, S. Du, and J. Ma, Phys. Rev. Lett. 92 (2004), 228501.

[103] R. Zatorre, Nature 434 (2005), 312.